

**RECOMMENDED GUIDELINES FOR LIQUEFACTION EVALUATIONS
USING GROUND MOTIONS FROM
PROBABILISTIC SEISMIC HAZARD ANALYSES**

Report to the Oregon Department of Transportation
June, 2005

Prepared by
Stephen Dickenson
Associate Professor
Geotechnical Engineering Group
Department of Civil, Construction and Environmental Engineering
Oregon State University

ABSTRACT

The assessment of liquefaction hazards for bridge sites requires thorough geotechnical site characterization and credible estimates of the ground motions anticipated for the exposure interval of interest. The ODOT Bridge Design and Drafting Manual specifies that the ground motions used for evaluation of liquefaction hazards must be obtained from probabilistic seismic hazard analyses (PSHA). This ground motion data is routinely obtained from the U.S. Geological Survey Seismic Hazard Mapping program, through its interactive web site and associated publications. The use of ground motion parameters derived from a PSHA for evaluations of liquefaction susceptibility and ground failure potential requires that the ground motion values that are indicated for the site are correlated to a specific earthquake magnitude. The individual seismic sources that contribute to the cumulative seismic hazard must therefore be accounted for individually. The process of hazard *de-aggregation* has been applied in PSHA to highlight the relative contributions of the various regional seismic sources to the ground motion parameter of interest.

The use of de-aggregation procedures in PSHA is beneficial for liquefaction investigations because the contribution of each magnitude-distance pair on the overall seismic hazard can be readily determined. The difficulty in applying de-aggregated seismic hazard results for liquefaction studies is that the practitioner is confronted with numerous magnitude-distance pairs, each of which may yield different liquefaction hazard results. This situation is especially true in regions, such as the entire western portion of Oregon, where the cumulative seismic hazard is due to multiple sources having a wide range of magnitudes and source-to-site distances.

The most thorough method of evaluation for liquefaction hazards at bridge sites would be to utilize the results of the PSHA in a probabilistic liquefaction susceptibility and ground failure analysis. Truly probabilistic liquefaction hazards studies such as this have been performed for critical structures; however, this level of analysis is not routinely performed in practice. A consensus for the application of de-aggregated ground motion values from PSHA for more routine bridge projects has not been adopted.

This report provides an introduction to the process of hazard de-aggregation, pertinent considerations for the use of de-aggregated ground motion data in liquefaction hazard evaluations, and applications for two design examples. The results of seismic hazard de-aggregation using the interactive USGS Seismic Hazard Mapping web site for four sites in Oregon are presented. Finally, recommendations are provided for directly utilizing the results of the USGS PSHA de-aggregations in the simplified liquefaction susceptibility evaluations routinely performed in practice.

INTRODUCTION

The loss of soil stiffness and strength in loose- to medium-dense, saturated sandy soils due to liquefaction has been the leading cause of damage to bridge foundations during earthquakes. Soil liquefaction can result in a variety of failure modes that compromise the integrity of bridge components. Specific examples include; (a) loss of foundation stability due to reduced bearing capacity, (b) deep-seated instability and damage to deep foundations, (c) increased lateral earth pressures on earth retention structures, (c) loss of passive soil resistance against walls, anchors, and laterally loaded piles, (d) reduction of axial capacity of piles, and (e) post-liquefaction settlement of soils. Bridge foundations in soil are particularly vulnerable to liquefaction hazards at waterfront sites where the ground slopes to the body of water, or a free-face condition exists allowing the soil to move in response to static, driving shear stresses. Liquefaction damage to bridge foundations and appurtenant structures such as abutments, connector ramps and viaducts, and approach embankments has been well documented in the technical literature. A comprehensive review of case studies has been prepared for the Oregon Department of Transportation (ODOT) by Dickenson and others (2002). These field cases clearly demonstrate the influence of ground motion characteristics, most notably the intensity and duration of the motions, on the seismic performance of bridge foundations, approach abutments, and related components.

Soil Resistance to Liquefaction

Soil liquefaction is a fatigue mode of failure wherein undrained cyclic loading leads to a progressive increase in excess pore pressure in the soil. The increase in pore pressure is accompanied by an equal decrease in the effective confining stress, reducing the shear resistance of the soil. In order to assess the likelihood of liquefaction at a site the cyclic resistance of the soil and the nature of the design-level earthquake ground motions must be established. The factor of safety against the triggering of liquefaction is simply the ratio of the cyclic resistance of the soil to the cyclic loading induced by the earthquake of interest. In engineering practice the cyclic resistance of the soil to the generation of excess pore pressures is routinely estimated using empirical procedures based on soil density and stiffness. The results of in situ testing methods such as the Standard Penetration Test, Cone Penetration Test, and Shear Wave Velocity measurements are used for this purpose. These procedures have been thoroughly presented in several recent publications and they will not be addressed herein. It is recommended that geotechnical and bridge engineers should be familiar with the following important papers on the subject; Youd and others (2001), Robertson and Wride (1997), Seed and others (2003), Andrus and Stokoe (2004), Idriss and Boulanger (2004). Dickenson and his co-workers (2002) have summarized much of this work and presented it with a comprehensive analysis for a site along the Columbia River in Portland.

Cyclic Loading of Soil during Earthquakes

The cyclic loading of the soil during an earthquake represents the demand on the material, and this is requisite information for any evaluation of liquefaction and potential ground failure. The ground motions used to represent the cyclic loading are applied for

the initial liquefaction hazard assessment and, if necessary, in the design of mitigation strategies involving ground treatment. Fundamentally, the best measure of cyclic demand would account for the intensity, duration, and to a lesser extent the frequency content of the input motions. These three aspects of loading are explicitly accounted for using energy-based concepts, wherein the cyclic energy per unit volume of soil can be calculated from time-histories of particle motion or stress-strain plots. Although energy methods have been successfully applied to laboratory data and field case studies (Sunisakul 2004) these methods have not been widely adopted in engineering practice. Instead, the most commonly employed methods of analysis relate the intensity of shaking to either the horizontal acceleration or cyclic stress in the soil layer of interest, and the duration of the motions through simple, empirical magnitude-dependent scaling factors (Youd et al 2001, Seed et al 2003, Idriss and Boulanger, 2004). The characteristics of the horizontal ground motions within the soil column (i.e. acceleration, stress, strain time histories) are often computed using dynamic soil response models such as SHAKE (Schnabel et al 1972), ProShake 2004, DESRA (Lee and Finn 1978) and SUMDES (Li et al 2000). The input, or bedrock, ground motions required for these numerical models are selected on the basis of their similarity to target motions established using empirical ground motion relationships that account for factors such as the style of faulting, earthquake magnitude, source-to-site distance, and rock stiffness. Recorded ground motions can be easily obtained from on-line catalogs (web sites for CGS, COSMOS, MCEER, PEER, and USGS ground motion catalogs are provided in the reference list under *Strong Motion Databases*).

The characteristics of the bedrock, or firm soil, motions at a specific site will depend on several geologic and geographic variables. These include the regional tectonic environment, the seismicity of the region, the proximity of the site to active faults, and on the exposure interval of interest in design (e.g. 500, 1,000, or 2,500 year motions). A complete seismic hazard evaluation for ground motions at a site must address both the spatial and temporal occurrence of earthquakes. In Oregon, the primary seismic sources are associated with the Cascadia Subduction Zone (interface or “mega-thrust,” and intra-plate or intra-slab earthquakes), shallow crustal events, and to a lesser degree seismicity related to volcanic activity. The locations of each of these earthquake sources have been determined, or in some cases estimated, using an array of geologic and geophysical methods of field investigation, in situ imaging, and numerical modeling. The faults have been mapped (Geomatrix 1995, USGS 2004b, c) using the latest input and consensus from the geoscience community. The geoscience community acknowledges that the current understanding of seismicity rates in Oregon is incomplete due to factors such as the short historic record of earthquakes, the relatively long recurrence interval between events, and environmental controls that obliterate the geomorphic expression of most faults. To account for this source of uncertainty most seismic hazard analyses incorporate spatially random, “areal sources” to the collective hazard in the region. Once the locations of all of the regional sources have been established the occurrence of earthquakes as a function of time and magnitude (i.e. the *rate of seismicity*) is required.

The full characterization of source locations and the rate of occurrence of earthquakes is the basis of the seismic hazard evaluation. These primary factors, along with the location

of the site relative to the faults, are used to estimate the characteristics of the ground motions utilized in analysis. The temporal occurrence of earthquakes along a specific fault defines the rate of seismicity associated with that source. Of primary interest in seismic analysis and design is the aggregate seismicity for all sources that may impact the structure of interest. This requires that the rate of seismicity for all sources is estimated. The recurrence interval of the maximum credible earthquake along a specific fault is often based on its slip rate and the rupture area required for an event of that magnitude (McGuire 2004). The likelihood of ground motions of a certain level is then a function of the rate of seismicity and the length of the time over which the observation is made. The time interval is referred to alternatively as the exposure time, mean return time, or recurrence interval, and it is specified for each project based on the importance of the structure.

Following ODOT specifications, new bridges are classified and designed in terms of AASHTO criteria as either “essential” or “other” bridges (Section 1.1.10.1 of the ODOT Bridge Design and Drafting Manual). The exposure times associated with these designations are 500 and 1,000 years, respectively. The intensity and duration of the ground motions at a given site will be different for these two return periods, and the liquefaction hazard will clearly reflect these differences.

Establishing Ground Motions for Analysis and Design

Estimation of site-specific ground motion parameters for a given exposure time combines the spatial and temporal source information previously addressed, and empirical attenuation relationships. Attenuation relationships provide estimates of ground motion parameters (e.g., PGA, PGV, spectral response ordinates) as functions of the style of faulting, earthquake magnitude, and source-to-site distance. Many of the attenuation relationships commonly used in practice have been presented in a volume of the Seismological Research Letters (1997). Utilization of the attenuation models facilitates direct estimates of the ground motion parameter of interest. For the “simplified liquefaction procedure” routinely applied in practice (Youd et al 2001) the peak horizontal ground acceleration (PGA) is the primary measure of the strength of shaking. Once the fault locations, seismicity rates, and ground motion attenuation have been established the PGA can be estimated. The process of estimating the PGA for a specified exposure interval involves one or both of the following procedures: (1) a *deterministic* analysis wherein a single earthquake magnitude is prescribed to a given source and the PGA determined based on the source-to-site distance, or (2) a *probabilistic* analysis that includes the aggregate contribution of all of the seismic sources, along with uncertainties in the recurrence rates and ground motion levels, in the resulting PGA value. Introductions to both procedures along with applications have been well presented (Cornell 1968, Kramer 1996, McGuire 2004) therefore these concepts are only briefly covered in this document.

Deterministic Analysis

A common method of estimating strong ground motions involves assigning a *Maximum Credible Earthquake* to a specific fault, then using an attenuation relationship to determine the PGA at the project site. This method, referred to as the *deterministic*

approach, focuses only on the largest reasonably possible earthquake associated with a source. The recurrence interval of this Maximum Credible Earthquake is not specified therefore the temporal aspect of the seismic hazard is not addressed. This method of seismic hazard analysis was common up through the 1970's and many practitioners continue to regard deterministic PGA analyses as independent of exposure interval. In contemporary practice, deterministic analyses are rarely performed without at least an indirect accounting for the exposure time of interest.

The deterministic analysis can accommodate seismicity rates associated with individual sources by incorporating the exposure interval of interest (500 or 1,000 years for most ODOT projects) and estimating the magnitude of the event having this return period. Once the magnitude is known an attenuation relationship is used to directly obtain a PGA value. This procedure can be carried out for all of the seismic sources that contribute significant ground motions at the site. Uncertainty in the resulting ground motion estimates is assessed by incorporating the standard deviations in both the seismicity rates and the attenuation relationships. The advantage of this approach for liquefaction hazard evaluation is that both the intensity of ground shaking (PGA) and the duration of the motions, as related to the earthquake magnitude, are known. The primary disadvantages of this approach include; (1) the PGA values do not necessarily reflect the cumulative, or aggregate, hazard in the region, and (2) assessing the influence of uncertainties in factors such as earthquake magnitude or source-to-site distance on the resulting PGA are accounted for by performing additional parametric studies of each variable. This task can be simplified by the use of spreadsheets incorporating the various attenuation relationships.

Probabilistic Analysis

As an alternative to the deterministic method of estimating PGA, probabilistic procedures can be used that combine the contributions of all sources in a cumulative estimate of the ground motion parameter of interest. This procedure is illustrated in Figure 1. Probability distributions of key variables such as rupture location along a fault, location of random sources, seismicity rates, and ground motion estimates from attenuation relationships can be incorporated into one seismic hazard analysis. Uncertainties associated with other factors such as the likelihood of activity along mapped faults, the direction of fault rupture propagation, and predominant style of faulting can be incorporated into the evaluation (e.g., Ang and Tang 1975, Kramer 1997, Vick 2002, McGuire 2004).

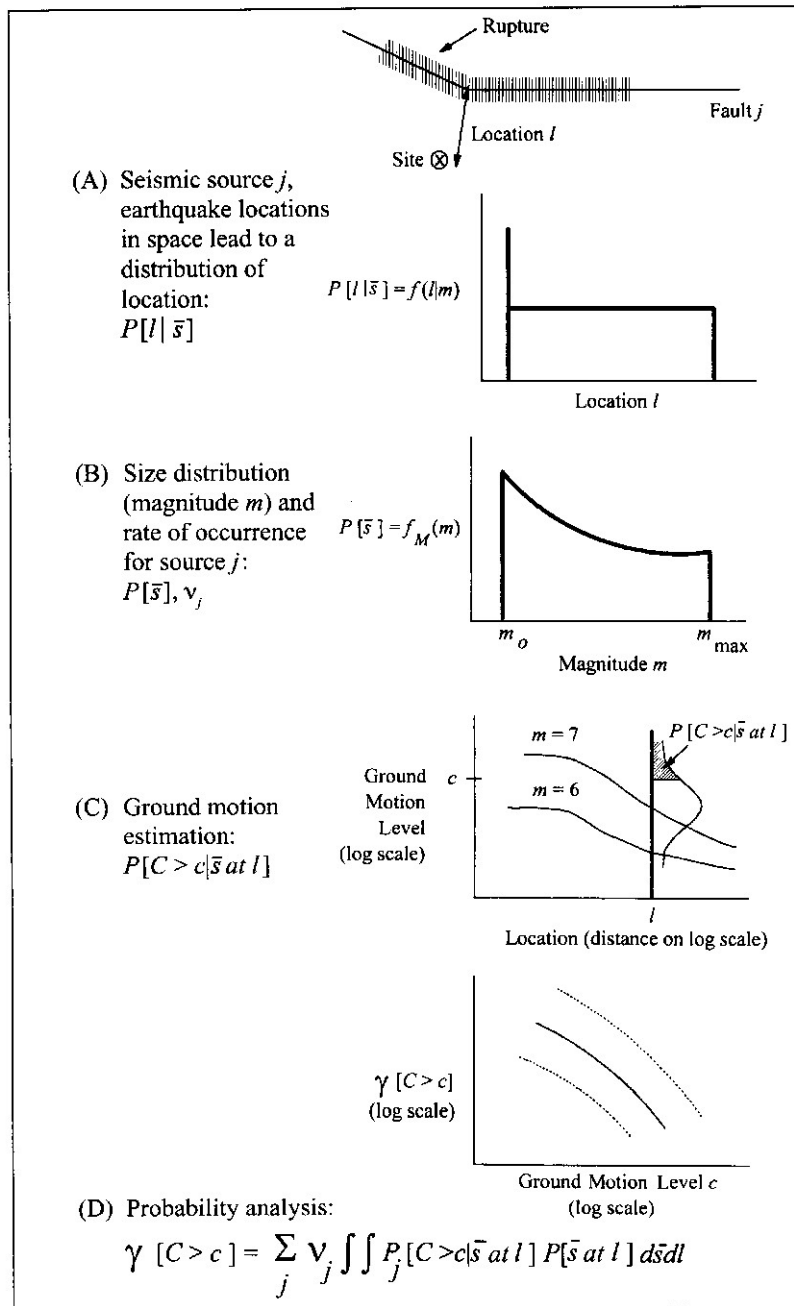


Figure 1: The steps in performing a Probabilistic Seismic Hazard Analysis (from McGuire, 2004).

A primary advantage of probabilistic seismic hazard analysis is that by assigning locations and seismicity rates to all sources the ground motion parameter of interest expected at a specific site can be determined along with its probability distribution, which is useful for illustrating uncertainty in the ground motion variable. Repeating the analysis for multiple locations, specified as grid points, throughout a region allows for the creation of contour maps of the ground motion parameters for specified exposure intervals. These

maps have been referred to as “uniform” or “aggregate” hazard maps as the contributions of all sources have been incorporated into a single ground motion value. An example for peak horizontal accelerations at rock sites in Oregon having a 5 percent probability of exceedence in 50 years (i.e. 975 year average return period) is presented in Figure 2. The map provides the spatial variation in PGA due to all of the seismic sources in the region. This map is similar in form to the ground motion maps used in seismic design provisions and codes for buildings. Once the Probabilistic Seismic Hazard Analysis (PSHA) has been completed, similar ground motion maps can be obtained for any specified exposure interval. The disadvantage of these maps with respect to liquefaction hazard evaluations is that the magnitude of the earthquake(s) associated with the PGA value is not indicated on the map therefore the duration of the ground motion and the Magnitude Scaling Factor cannot be determined.

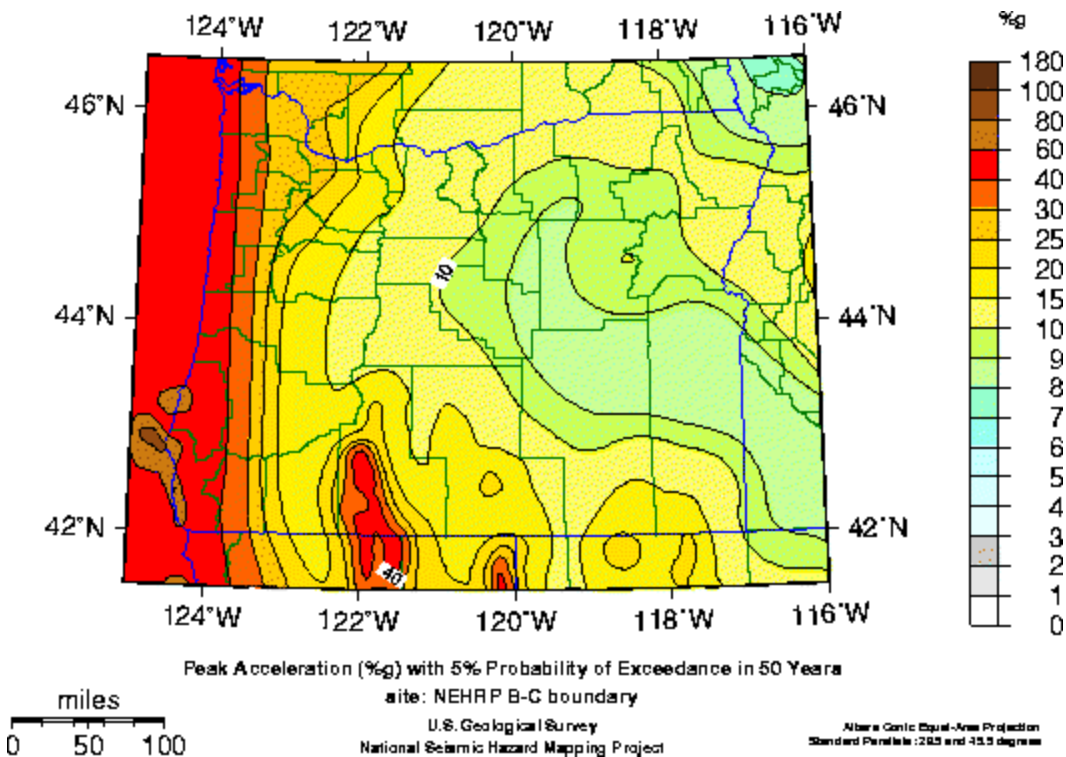


Figure 2: Peak ground acceleration on Site Class B rock for a 975 year mean return time (USGS Seismic Hazard Mapping Program web site, 1996 data).

U.S. Geological Survey Seismic Hazard Maps

The seismic hazard mapping program of the U.S. Geological Survey (USGS) has synthesized spatial and temporal seismicity data from many sources in its comprehensive probabilistic hazard maps for the United States (USGS 2004). The maps provide the latest estimates of ground motion parameters (peak ground acceleration, and spectral accelerations for 0.2 sec, 0.3 sec, and 1.0 sec periods) for specific exposure intervals of

approximately 500, 1,000, 2,500, and 5,000 years. The ground motion values are estimated for sites at the boundary of NEHRP Site Class B and C (transition from competent rock to more highly fractured and weathered rock). The USGS seismic hazard mapping web site is interactive and it allows users to input site location (zip code or latitude-longitude), and choose from the four mean return times. The variation of peak acceleration with exposure time for six locations in the State of Oregon is provided in Figure 3. Although the time-dependent trends in PGA are similar, the hazard levels around the state quite different.

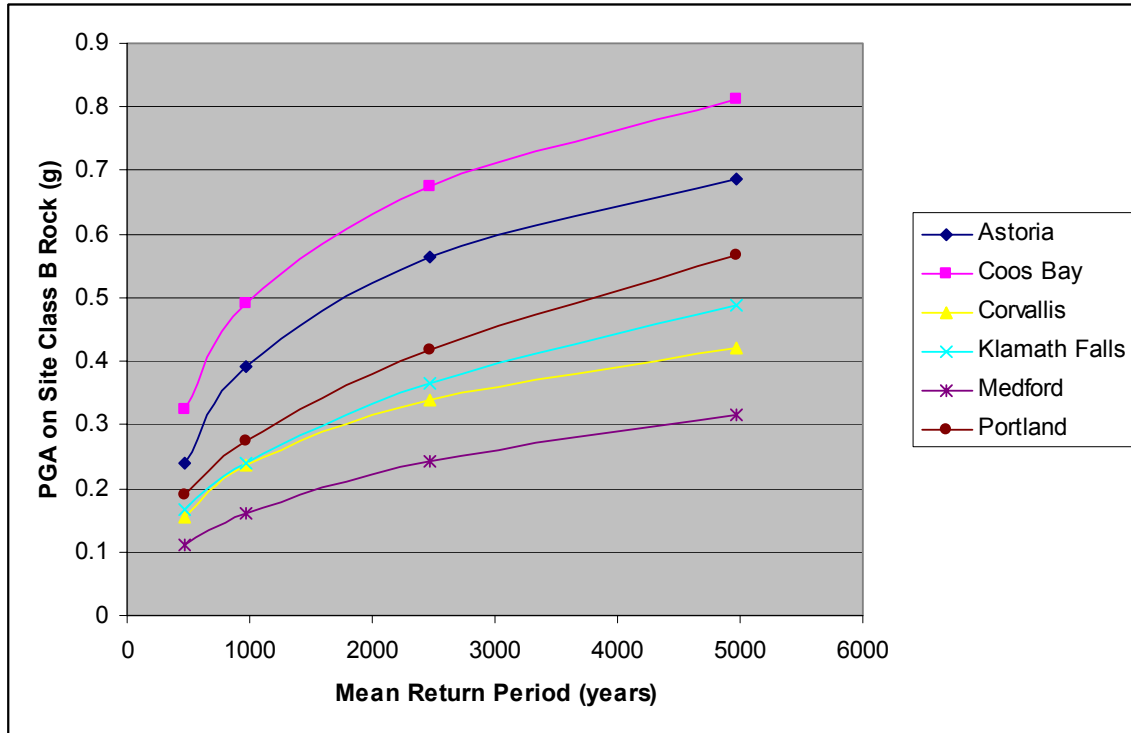


Figure 3: Variation of peak ground acceleration on Site Class B bedrock with exposure interval for six cities in Oregon (USGS Seismic Hazard Mapping Project, 2002 data).

The USGS seismic hazard mapping website is a tremendous resource to the engineering community and the ground motion information that is provided is widely used in practice. For example, this ground motion data has become the basis for the NEHRP provisions for seismic design of new buildings (FEMA 2004) and the International Building Code (IBC 2003). The ground motion parameters used in these procedures have a mean return time of 2,500 years. These are referred to as the “Maximum Considered” earthquake motions, not to be confused with “Maximum Credible” earthquake motions, which would be larger in all cases. This is evident in Figure 3 as the PGA values continue to increase for return periods greater than 2,500 years.

The basis for much of the USGS probabilistic analysis of Oregon and adjacent regions was originally obtained from the Geomatrix (1995) ground motion investigation prepared

for ODOT. This data has been continually updated as more is learned about the characteristics of seismic sources in the Pacific Northwest and the ground motions produced by these sources. An example of the evolving consensus pertaining to seismic source characterization includes the specification of the easternmost portion of the CSZ plate boundary that is thought to be capable of generating significant ground motions. This boundary was moved to the west along much of the Oregon coast in the 2002 analysis thereby reducing the peak accelerations computed onshore (USGS 2004b). The variations in PGA values provided in western Oregon on the 1996 and 2002 maps are due largely to this change. Another important difference between the probabilistic seismic hazard maps produced by Geomatrix and the current USGS maps is the use of different ground motion attenuation models. The current USGS maps employ as many as five different models in the estimation of ground motion parameters associated with shallow crustal earthquakes, and two models for motions generated by subduction zone events. The ground motion values obtained by the models for specific faulting styles are used with equal weighting (i.e. mean value) in the probabilistic model. It is important to know which attenuation models have been adopted by the USGS if attempts are made to match the ground motions provided on the hazard maps. It is therefore highly recommended that ODOT personnel charged with seismic analysis and design use the following references pertaining to the modeling of seismic sources and ground motions in the Pacific Northwest (USGS 2004b, c, f).

The ODOT Bridge Engineering Section has mandated the use of the USGS Seismic Hazard Mapping Program data as the basis for bedrock ground motions used in geologic and geotechnical hazard evaluations. The PGA and spectral values provided by the USGS can be used directly in force-based seismic design procedures, however for analyses incorporating ground motion time histories or duration-dependent scaling factors the magnitudes of the earthquakes that contribute to the uniform hazard must be known. This information cannot be obtained from the maps directly, it must be determined from the seismic source data and ground motion estimates for each of the sources independently. The relative contribution of the various sources to the PGA value provided on the map is determined in the probabilistic framework by assessing the PGA induced by each source. Source locations are defined by gridding the region around the site by azimuth and distance, and the magnitude distributions of all sources are lumped in groups of nearly equivalent magnitude referred to as *bins*. By evaluating the relative contribution of each source to the cumulative ground motion value the hazard can be *de-aggregated* to highlight the magnitudes of the events and the source-to-site distances that dominate the seismic hazard.

DEAGGREGATION OF SEISMIC HAZARD

The evaluation of liquefaction triggering and ground deformation is more involved than most seismic analysis in that both the intensity and the duration of the ground motions are needed. As previously outlined, the intensity of the motions can be estimated using empirical attenuation relationships once the magnitude (*M*) and source-to-site distance (*R*) are known. The duration of the motions can be evaluated using a variety of procedures (e.g. bracketed duration, equivalent uniform cycles). The *Simplified Procedure* utilizes a magnitude-dependent scaling factor that was originally based on an

equivalent uniform cycle concept (Youd et al 2001, Idriss and Boulanger, 2004). The Magnitude Scaling Factor (MSF) used in the procedure relates the relative duration of earthquake motions as a function of magnitude. The MSF is therefore a surrogate for the actual ground motion duration. The advantage of this simple MSF is that it is based only on the magnitude of the earthquake of interest. The PGA and MSF required for the *Simplified Procedure* are therefore only functions of M and R. The difficulty in obtaining this information from a PSHA is that the PGA maps reflect all of the seismic sources in the region and a single M-R pair cannot be determined from the ground motion maps alone.

The process of deaggregating the cumulative seismic hazard into the contributing M-R pairs has become a common part of PSHA. By identifying the most probable sources contributing to the overall hazard the engineer can assess the relative impact of the various seismic sources. This is especially useful in most regions of Oregon where the seismic hazard is *multi-modal*, meaning that there are multiple scenario earthquakes. Very useful, practice-oriented explanations of the probabilistic deaggregation process have been presented by Bazzurro and Cornell (1999), Harmsen and Frankel (2001), and McGuire (2004). These papers provide very useful background information on the probabilistic operations, assumptions and limitations, and applications to case studies. Only the chief aspects of these papers as they apply to the USGS deaggregations and liquefaction hazard evaluations will be presented in this document.

A basic deaggregation analysis highlights the relative contributions of M-R pairs to the overall seismic hazard. A probability distribution (e.g. probability density function or probability mass function) is established for all sources and either the mean or modal values of M and R are determined. The mean deaggregation provides the weighted mean values of M and R for all sources that contribute to the hazard. The modal value(s) yields the M and R pair having the largest contribution in the hazard deaggregation of each grid location. For regions exhibiting more than one significant seismic source the modal values are much more representative, and mean values of M and R are not recommended for use in liquefaction hazard analyses as explained in the following example.

The shortcoming of mean M-R values can be illustrated by simplifying the seismic hazard for Portland. In the Portland region the seismic hazard includes; (1) large Cascadia Subduction Zone earthquakes, (2) deep intraslab earthquakes like historic earthquakes in the Puget Sound region (1949, 1965, 2001), (3) local, shallow crustal earthquakes along mapped faults, and (4) local, shallow crustal earthquakes on unknown faults (random areal sources, or *gridded seismicity* using the terminology applied in the USGS studies). For the 975 mean return time this scenario can be simplified for the sake of illustration to include a M 8.6 CSZ event located 100 km from Portland, and a M 6.2 crustal event occurring along a mapped fault such as the West Hills Fault or a comparable spatially random event at a source to site distance of 14 km. The mean M-R for this simplified scenario is M 7.4 and source-to-site distance of 57 km. The mean M-R is unrealistic in that it does not represent a feasible earthquake scenario. Utilization of the mean M-R values to specify the PGA and MSF would yield ground motion parameters that are inappropriate for both of the scenarios in this simplified example. The significant

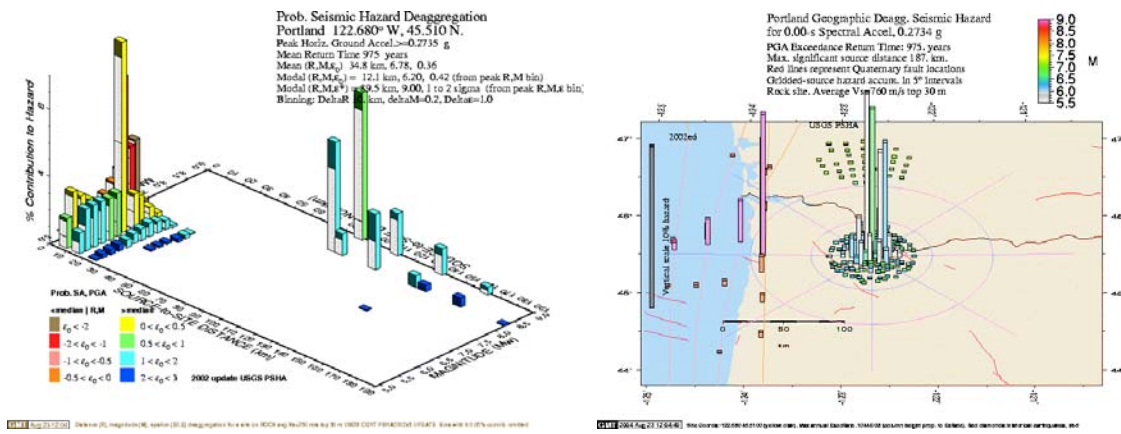
contribution of both seismic sources would be indicated in modal M-R values, and the deaggregation would highlight the need for two liquefaction hazard evaluations, one for the CSZ event and one for the local crustal event. A final note provided by this example, it is clearly not appropriate to use the median PGA from the hazard map in a liquefaction evaluation for the M 8.6 and M 6.2 events as the PGA value reflects numerous M-R pairs that contribute to the cumulative hazard in the region.

It is often helpful to then assess how the individual PGA values from modal M-R pairs compare to the single, median value shown on the ground motion map. The difference between the values determined using attenuation relationships for each modal M-R and the mapped value is denoted by the parameter epsilon, ϵ . Epsilon is generally defined as the number of standard deviations from the median ground motion as predicted by an attenuation relationship (Bazzurro and Cornell 1999, Harmsen and Frankel 2001, USGS 2004e). Incorporation of the deviation of the ground motion from the mapped median value as predicted by an attenuation relationship given M and R provides a very useful additional measure of the relative contribution of each M-R in the overall hazard assessment. Positive values of ϵ indicate that the PGA for the specific M-R pair is less than the mapped value and a negative value demonstrates that the PGA for this source exceeds the median mapped value. This information is conveniently presented in 3-D M-R- ϵ plots, and in geographic deaggregation plots as shown in Figure 4.

Deaggregation of M-R- ϵ provides necessary information regarding the relative contributions of various seismic sources and it allows the practitioner to apply attenuation relationships for each of the primary sources identified. This is necessary for liquefaction evaluations given the need for PGA and MSF. In regions of multiple sources the modal values of M-R can be used in conjunction with attenuation relationships to estimate the representative value of PGA from each of the primary sources. Note that it is very unlikely that the PGA values obtained from attenuation relationships for the modal M-R pairs will yield the median PGA value therefore no single event will ever be able to fully describe the seismic threat at the site (Bazzurro and Cornell 1999). In specific regions of the western United States the PGA values provided for the predominant M-R pairs are often within about 20% of the median value (Bazzurro and Cornell 1999, Harmsen and Frankel 2001) however this should be assessed on a case by case basis. This generalization does not apply in much of western Oregon. For example, in the Portland region the ground motions induced by the CSZ events are not within 20% of the median mapped PGA value. In regions where the hazard is dominated by multiple events liquefaction hazard evaluations should be conducted for all predominant M-R combinations

The M-R- ϵ deaggregation plots in Figure 4 clearly illustrate the multi-modal nature of the seismic hazard in the Portland region. The primary sources are associated with the local shallow crustal earthquakes and the distant CSZ events. The 3-D plot (Figure 4a) illustrates the relative contribution of the numerous M-R pairs in bar chart format. The range of ϵ is indicated by color coding individual M-R bars. The warm, earth tones (orange, red, brown) indicate negative values of ϵ , and the cooler colors (yellow, green, blue) identify positive values of ϵ . In this example it is clear that the PGA values in

Portland due to CSZ earthquakes are less than the median PGA that is shown on the map for the 975 year mean return interval. The earthquakes that contribute ground motions in excess of the median PGA value are the M 6.5 to 7.0 events that occur within 15 km of the site. This same information is shown in a geographical context in Figure 4b. In this figure the sources have been assigned to distance and azimuth zones, and the relative contributions shown in relation to the height of the bars. The coloring scheme in this plot is used to identify the magnitude of the earthquakes. Together these plots demonstrate the modal M-R pairs that contribute the most to the hazard, and the relative contributions of the PGA values to the median. Similar plots are provided in the appendixes for Coos Bay, Klamath Falls, Medford, and Portland for mean return times of 475 and 975 years.



a. Three dimensional M-R-ε plot.

b. Geographic deaggregation

Figure 4: M-R-ε plots for ground motions in Portland having a 975 mean return time (USGS 2004).

Comparison of Mean PGA from Deaggregation and PGA from Modal M-R Pairs

The earthquake source that yields the greatest percent contribution to the ground motion hazard is listed in the deaggregation figures provided at the USGS web site (e.g., Figure 4a and 4b). The modal values of M-R-ε for mean return times of 475 and 975 years are listed in Table 1 for the four highlighted cities in Oregon. In most cases the seismic hazard is dominated by one M-R pair; however, the contributions of additional sources should be assessed. This can be easily checked using the tabular data in the appendixes. As an example, the deaggregation data for the 975 year return interval in Portland is examined. The table in Appendix B provides the relative contributions of all M-R pairs that have been considered in the probabilistic hazard model. The relative contribution can be assessed by locating the M-R pairs with the largest “ALL_EPS” values. The largest value (11.30) corresponds to the M 6.2 event occurring 12.1 km from the site. This M-R pair is illustrated in Figure 4a and highlighted in Table 1 as a primary contributor to the overall seismic hazard. Inspection of the “ALL_EPS” data indicates that there are several primary contributors to the ground motion hazard. If a 5% minimum relative contribution

is used as a criterion to identify the most critical M-R pairs then four scenarios are evident; (1) M 6.2, R 12.1 km, 11.30 %, (2) M 9.0, R 89.5 km, 8.74%, (3) M 6.64, R 2.9 km, 8.33%, and (4) M 8.3, R 89.5, 6.56%. The M 9.0 earthquake is also highlighted in Table 1. While it is clear that many other seismic sources contribute to the hazard at this site it is necessary to identify the primary sources for subsequent liquefaction hazard evaluations. The criteria for establishing the minimum relative contribution to be considered for liquefaction analysis is subjective. It will reflect the importance of the structure and this value will involve engineering judgment. As a guide, the largest PGA values associated with the applicable M-R pairs should be evaluated in terms of the number of standard deviations that the specific PGA values are from the mean PGA for the site. For most bridges the use of the mean plus two standard deviation motions may be overly conservative. The specification of an appropriate hazard level (i.e. standard deviations above the mean, or minimum ϵ_0 bin) will reflect the importance of the structure.

Table 1: PSHA Ground Motion and Source Parameters for Four Sites in Oregon

SITE	LAT.	LONG.	Listed Mean PGA (g)		MODAL M & R (M, R, ϵ_0) ^a		MODAL M & R (M*, R*, ϵ^* interval) ^b	
			475 yrs	975 yrs	475 yrs	975 yrs	475 yrs	975 yrs
Portland	45.510	-122.680	0.191	0.274	6.2, 12.2, -0.17	6.2, 12.2, 0.42	6.2, 12.2, 0 to 1 σ	9.0, 89.5, 1 to 2 σ
Medford	42.330	-122.860	0.110	0.160	9.0, 79.8, -0.60	9.0, 79.8, -0.03	8.3, 79.8, 0 to 1 σ	9.0, 79.8, 0 to 1 σ
Coos Bay	43.365	-124.230	0.325	0.490	8.3, 16.3, -0.71	8.3, 16.3, 0.17	8.3, 16.3, 0 to 1 σ	8.3, 16.3, 0 to 1 σ
Klamath Falls	42.220	-121.770	0.168	0.239	6.82, 23.7, 0.40	7.2, 4.3, -1.59	6.82, 23.4, 0 to 1 σ	6.83, 23.5, 1 to 2 σ

^a Modal M-R and ϵ_0 is the mean value of ϵ from the sources in the most likely distance, magnitude bin (i.e. only M and R are considered).

^b Modal M-R and ϵ^* is the interval of epsilons corresponding to the most probable distance, magnitude, and epsilon in the deaggregation (i.e. M, R, and ϵ considered) [after USGS 2004e].

The peak ground accelerations in Portland due to each of the four primary earthquake scenarios have been determined using the attenuation relationships that were employed in the creation of the USGS ground motion hazard maps (Abrahamson and Silva 1997, Boore et al. 1997, Campbell and Bozorgonia 2003, Sadigh et al. 1997, and Youngs 1997). The average PGA values for these four cases are approximately 0.22g (M 6.2, R 12.1 km), 0.55g (M 6.64, R 2.9 km), 0.12g (M 8.3, R 89.5 km), and 0.16g (M 9.0, R 89.5 km). The mean PGA listed for the Portland site is 0.27g. It is interesting to note that the average of the four individual PGA values is 0.27g. Although the average of the four PGA values should be fairly close to the mean PGA value listed for Portland, the exact agreement is considered to be a rather circumstantial and fortuitous outcome. The selection of a different minimum relative contribution may have yielded a different average value of PGA. Note that as the specified value of the minimum relative contribution is decreased the agreement between the average PGA and the mean value listed should increase.

The liquefaction hazard evaluation for this site could be performed in a straightforward manner for all four of these scenarios using spreadsheets. A potentially laborious aspect of the investigation involves the site specific dynamic soil response analyses required to obtain the ground surface PGA and the cyclic stress ratios at the depths of interest. Guidelines for this aspect of the analysis are provided by Dickenson and others (2002). For this example the site response would be evaluated for four scenarios. If three bedrock earthquake records are used to account for the influence of ground motion uncertainty on the computed soil response for each of the four scenarios, as is commonly performed in practice, this would entail 12 analyses. Once the ground surface PGA values, or the CSR values at depth, are known the liquefaction hazard can be readily determined. A straightforward comparison of the relative impact of the four scenarios can be illustrated using the following; simplified ground motion amplification factors (Dickenson et al. 2002), Magnitude Scaling Factors (Youd et al, 2001), and the well known formulation for estimating the cyclic stress ratio (CSR) at depth:

$$(CSR)_{M 7.5} = 0.65(a_{max}/g)(\sigma_{vo}/\sigma'_{vo})(r_d/MSF) \quad \text{Equation 1}$$

Where a_{max} is the peak horizontal acceleration at the ground surface, g is the acceleration of gravity, σ_{vo} is the total vertical stress at the depth of interest, σ'_{vo} is the effective vertical stress at the same depth, r_d is the stress reduction factor, and MSF is the magnitude scaling factor.

The relative intensity of the cyclic loading associated with the four earthquakes can be compared for equivalent field conditions by normalizing to the CSR for a M 7.5 earthquake. The collection of terms $(0.65(\sigma_{vo}/\sigma'_{vo})(r_d))$ can be held constant yielding the following expression for a simple index parameter related to the cyclic loading (CSR*):

$$(CSR^*)_{M 7.5} = (PGA_{BR})(SAF)(1/MSF) \quad \text{Equation 2}$$

Where PGA_{BR} is the peak horizontal acceleration in bedrock and SAF is the soil amplification factor. Multiplying the averaged PGA values obtained using the attenuation relationships for rock sites, the soil amplification factors provided in Dickenson et al (2002), and the MSF values from Youd et al (2001) as indicated in Equation 2 yields CSR* values of 0.17, 0.33, 0.23, 0.35, for the magnitude 6.2, 6.64, 8.3, and 9.0 earthquakes respectively. This simple comparison, along with the relative contribution to the ground shaking hazard provided in the table of Appendix B (M 6.64, 8.33%; M 9.0 8.74%) demonstrates that the CSZ and local crustal sources are almost equally important in assessing the liquefaction potential. In practice it is recommended that generalized soil amplification factors be replaced by the results of the site specific dynamic response analyses. The results of a simple evaluation such as this may be used to highlight the two most important earthquake scenarios, thereby reducing the number of dynamic soil response analyses from the 12 previously indicated to a more efficient number (6 in this case).

Alternative Methods of Utilizing De-Aggregation Data

The most appropriate method of liquefaction analysis using the results of PSHA would be to continue the probabilistic framework to include uncertainty in liquefaction susceptibility and ground failure (i.e. a coupled probabilistic evaluation). This procedure has been adopted on large bridge projects; however, it is not routinely performed for most projects. The simplification of specifying a minimum relative contribution and identifying the most significant M-R pairs is one possible method for reducing the number of liquefaction evaluations that are performed. Other methods have been suggested. Dobry and others (1999) has recommended that the design magnitude can be selected as that for which 80 percent of the deaggregated ground acceleration hazard is from lesser magnitude earthquakes. In Portland for example, the magnitude corresponding to the 80% level is 8.3 for both the 475 year and 975 year return intervals. This approach should be used with caution in the Pacific Northwest where ground motions due to great earthquakes ($M > 8$) make up a considerable portion of the overall seismic hazard. Arbitrarily truncating the maximum magnitude at 80% (or any other value) of the deaggregated hazard could lead to unconservative estimates of M for many sites in western and central Oregon. This approach also overlooks seismic sources that are smaller magnitude yet closer to the site, thereby leading to large values of PGA.

The integration of probabilistic and deterministic ground motion values (i.e., spectral accelerations) for use in structural design based on current codes has been addressed by Leyendecker and others (2000). The recommendations found in that paper have been suggested by others for use in liquefaction hazard analyses, despite the fact that they were established for structural engineering applications only. Leyendecker and his colleagues provide a thorough justification for the use of a 1.5 multiplication factor on spectral ground motion values obtained in deterministic hazard analysis. The 1.5 factor represents a “seismic margin” that was estimated on the basis of expert judgment for collapse prevention of structures. The multiplier was also found to be approximately one standard deviation above the median ground motion. The recommendations provided by Leyendecker for the scaling of deterministic ground motions are applicable for structural design only; however, and should not be applied for liquefaction hazard analyses. It is recommended that the actual, unscaled ground motion value(s) from the appropriate M-R pairs should be for the liquefaction hazard evaluation.

General Notes Regarding the Relative Contributions to Mean PGA

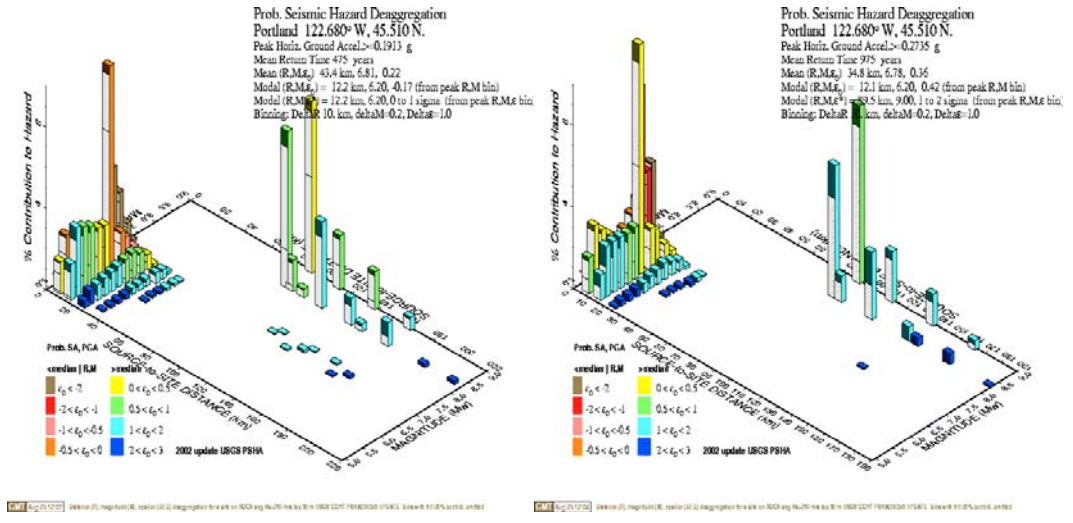
The M-R- ϵ plots demonstrate the *relative* contribution of each source to the ground motion hazard. The relative contribution changes with time for each source as the rate of seismicity is different for each and the likelihood of an earthquake close to the site increases with time. This is particularly evident in regions with a significant component of the hazard derived from random areal sources. Although the magnitude of the earthquake associated with a given fault will increase with exposure interval, the relative contribution could decrease due to greater seismicity rates on other faults, or to the occurrence of earthquakes closer to the site. This should not preclude the former from consideration in liquefaction analyses. For many sites in the Pacific Northwest, as the return period is increased, the relative hazard contribution from closer earthquakes becomes larger. One reason for this is that the larger ground motion associated with the

longer return period is more likely to be generated by earthquakes closer to the site (Harmsen and Frankel 2001). This is relevant for liquefaction hazard analysis because a casual review of the relative contributions may lead some to believe that the hazard due to larger, more distant sources is unimportant. This may be unconservative as the large subduction zone events are de-emphasized despite their long duration ground motions.

For most regions located between the Coast Range and the Cascades the relative contribution of the CSZ earthquakes to the median PGA decreases (this is not necessarily the case for mid- to long-period spectral accelerations). In Portland, for example, the relative contributions to the hazard for the 475 year mean return time are; CSZ roughly 31%, shallow gridded seismicity (random areal sources) 52%, and local crustal events on mapped faults 16%. This changes when considering the 2,500 year motions where the relative contribution is; CSZ roughly 10%, shallow gridded 45%, and 38% local faults. The variations in relative contribution with mean return time are illustrated in Figure 5 and provided in tabular form in the appendixes for the four cities previously listed. It must be acknowledged that the damaging impact of a large CSZ earthquake does not decrease with exposure time. In fact the opposite is true. In a probabilistic framework the PGA generated by a specific source will continue to increase even after the exposure time exceeds the mean return period for that source. This occurs because there is a higher likelihood that ground motions will exceed the mean PGA estimated from the attenuation relationships (i.e. the mean plus 1σ or 2σ PGA). The CSZ event should not be dismissed because the *relative contribution* falls below a certain value. This situation merely indicates that there are numerous local sources that result in PGA values that exceed the PGA produced by the larger, more distant subduction zone event. When the duration and MSF associated with the subduction zone earthquakes are accounted for the liquefaction hazards may be more significant with the CSZ event than the smaller, more local earthquakes as indicated in the example for Portland. The CSZ event should therefore still be evaluated for liquefaction hazards due to the different MSF's applied to the various M-R scenarios.

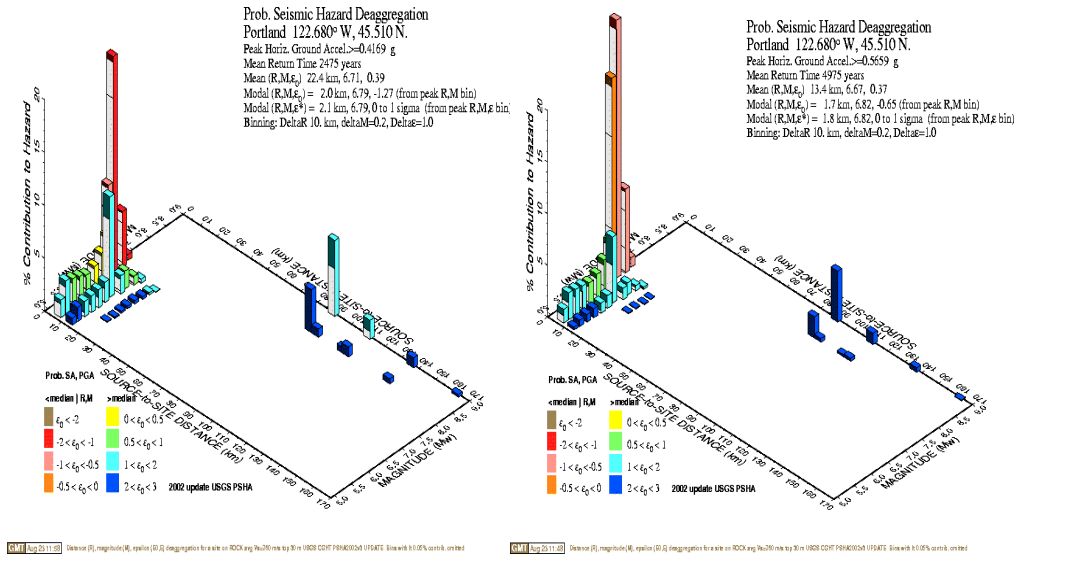
Deaggregation provides a useful framework for identifying the predominant seismic sources, or more appropriately, the most likely range of M-R combinations, in a region. The results of the deaggregation can be used to identify the M-R scenarios that contribute the most significantly to the PGA, as well as short period and long period components of ground motions. Although ground motion characteristics due to near fault effects and rupture directivity have not been incorporated into the USGS PSHA studies inspection of the M-R plots and tables will help to identify situations where these effects should be included in seismic analysis. This would merely require the application of suitable attenuation relationships for the M-R pair of interest. This should be considered for sources located within 10 to 15 km of the site. Note that this was not done in the USGS PSHA for the M 6.64, R 2.9 km pair in Portland. The ground motions used as the basis for liquefaction analyses should reflect the modal M-R combinations and not just the median PGA indicated on seismic hazard maps. The recommended procedures for utilizing the M-R relationships from the USGS PSHA in liquefaction evaluations are presented in the following section. The proposed methodology is followed by two applications for generic embankment geometries, one for a loose sandy soil that is highly

susceptible to liquefaction and the second for a medium dense sand in which partial pore pressure generation is anticipated.



a. 475 year mean return time.

b. 975 year mean return time.



c. 2,475 year mean return time.

d. 4,975 year mean return time.

Figure 5: Change in relative contribution of CSZ and local crustal sources to PGA with exposure interval in Portland (from USGS seismic hazard mapping website).

RECOMMENDED PROCEDURES FOR EVALUATING LIQUEFACTION HAZARDS AT BRIDGE SITES

The procedures that follow are intended to serve as guidelines for the performance of liquefaction hazard evaluations. This is not an internal standard or code. This outline is presented in a step-by-step format for the ease of reference. It should not be construed as a rigid framework as site specific aspects of each project may warrant modifications from this general procedure. This outline supplements the methods and considerations presented in other pertinent references (Youd et al 2001, Dickenson et al 2002, Seed et al 2003, Idriss and Boulanger, 2004). A flow chart is provided in Appendix J that outlines the steps for the liquefaction hazard and ground deformation analysis.

Step 1: Identify the seismic sources that contribute to the regional seismic hazard.

As the fundamental first step in any seismic hazard evaluation this task may require input from geoscientists, knowledgeable personnel from other state or federal agencies (DOGAMI, USACE), or external experts. Although the comprehensive PSHA evaluation prepared for ODOT by Geomatrix (1995) has served as the most authoritative reference on this subject since it was produced, the document presents the state-of-knowledge as it existed in 1994. This document is still considered a valuable reference on seismic sources, fault characterization, and ground motion attenuation in the Pacific Northwest; however, the recommendations should be updated with more recent literature from the geoscience, seismological, and engineering fields. USGS references associated with the National Seismic Hazard Mapping Program provide useful updates (Frankel et al 2002, USGS 2004a, c, f).

The goal of this step is to determine the cumulative annual frequency versus magnitude relationships for the region. For each of the potential sources a magnitude can be specified for the given mean return time, or exposure interval. In the case of mapped sources this step will satisfy both the spatial and temporal aspects of the earthquakes, but not the uncertainty in recurrence intervals. For “gridded” sources only the magnitude can be ascertained, the source-to-site distance is not well constrained.

Step 1b: Determine the Peak Horizontal Bedrock Acceleration Associated with the Return Period of Interest

The general magnitude and distance information determined in Step 1 is supplemented with the results of the USGS PSHA. The PGA on Site Class B rock can be readily determined at the USGS Seismic Hazard Mapping Program website (USGS 2004). The return periods of interest are 475 and 975 years, following ODOT specifications. The interactive website provides the hazard determination for any location using the local zip code, latitude and longitude, or interpolation from contour maps. This step will result in a single, median PGA value for the location and return period selected. This value represents the cumulative, or aggregate, hazard due to all of the seismic sources in the region and it should not be used as the basis for the liquefaction hazard evaluation.

Step 1c: Perform Seismic Hazard Deaggregation

In order to identify the seismic sources that contribute the most to the hazard at the site a deaggregation can be performed using the USGS interactive web site <http://eqint.cr.usgs.gov/eq-men/html/deaggint2002.html>. The user is prompted for straightforward information and an in-depth knowledge of PSHA principles is not required. Specific information that is required for the on-line deaggregation includes: (a) *Site Name*, (b) *Location of Interest* (latitude and longitude), (c) *Return Time* (percent probability of exceedance in a specified time interval), (d) *SA Frequency* (this refers to the period of interest for spectral accelerations – in this case the user should select “PGA”), (e) *Geographic Deaggregation* (select Fine angle-Fine distance for this plotting option), and (f) *Seismograms* (none are usually required).

The results of the deaggregation are provided in terms of mean and modal values. The M-R- ϵ values will be necessary for subsequent applications of attenuation relationships.

Mean values of M and R should not be used in liquefaction hazard evaluations.

The modal values should be used. The modal values are given in terms of as M-R- ϵ_0 or as M*-R*- ϵ^* values. The subtle differences in these magnitude, distance, and ground motion variability parameters are defined in useful references by Harmsen and Frankel (2001) and the USGS (2004e). The percent contribution to the mean PGA provided by each M-R pair is listed in the USGS deaggregation data (refer to the Appendixes for the four cities highlighted herein) under the heading “ALL_EPS.” This data highlights the relative contributions to the seismic hazard made by each M-R pair considered. Selecting the pertinent M-R pairs for liquefaction hazard analyses is now left to the discretion of the engineer. The number of pairs incorporated into the liquefaction analysis will depend on the importance of the structure, the number of sources making a significant contribution, and the resources available to the project.

Judgment will be required to determine what constitutes a “significant” contribution to the seismic hazard. It is clear that a balance must be struck between an adequate consideration of individual sources and the practical issue of time necessary to perform the liquefaction analyses for each source. The example provided in this report focused on sources providing at least 5% relative contribution to the overall hazard. This value was arbitrarily selected to provide reasonable balance for the sake of demonstration. The results were useful for demonstrating the PGA values associated with each source, and the variation between the mean PGA for all sources affecting Portland and the average of the PGA determined for the four primary sources. By selecting 5% as the minimum relative contribution it is apparent that several seismic sources have been omitted that would yield PGA values greater than the four values obtained. This situation will be unconservative for a limited number of M-R pairs; however, it is not recommended that liquefaction hazard analyses be performed for ground motions that are approaching mean plus 2σ for the site. Employing these large motions will likely lead to compounding conservatism in assessing liquefaction and ground failure hazards, as well as in resulting mitigation strategies. As M-R pairs yielding smaller minimum percentage of relative contributions are considered the number of source scenarios increases thereby increasing

the ground motion levels used in evaluation. For the four cities highlighted in this report the number of M-R pairs associated with a 5% relative contribution cutoff (975 year return period) are; Coos Bay (4), Klamath Falls (6), Medford (5), and Portland (4). These are considered to be a reasonable number of cases for most applications.

For much of western Oregon the relative significance of CSZ earthquakes *decreases* with increasing return period in regions where there are moderate, yet infrequent earthquakes on local faults. This reduction in the relative contribution of CSZ ground motions should not be confused with a reduction in the liquefaction potential posed by CSZ earthquakes. The PGA values due to the CSZ events increases with return period. The decrease in relative contribution is due largely to the fact that the cumulative median PGA value is increasing in response to closer shallow crustal sources (mapped faults and gridded sources). Recall that the PGA is a short-period ground motion parameter. At most sites along the I-5 corridor, and similar longitude, the longer period contributions of the CSZ earthquakes will continue to dominate the seismic hazard as evident in the PSHA values for the moderate period ($T = 1$ second) spectral acceleration. A worthwhile and quick check of the influence of a large CSZ earthquake at the site would involve returning to the frequency-magnitude relationships in Step 1. This plot will clearly indicate the magnitude of interest for CSZ events given the return time. The USGS PSHA is based on a two-magnitude scenario where M 8.3 and M 9.0 events are given equal weighting at all return intervals. The mean return time for the M 9 earthquake is 500 years, longer than the recurrence interval for the M 8.3 event. For the exposure times of interest for ODOT projects (475 and 975 years) the CSZ earthquakes will be significant for all sites in western Oregon.

Step 2: Determine the PGA on Rock for Modal M-R Pairs using Attenuation Relationships

Once the M-R- ϵ parameters are known attenuation relationships can be used to establish the PGA on rock due to each of the primary sources. The M and R values provided in the deaggregation are used in the empirical attenuation relationships to obtain PGA values. The source-to-site distances used in the USGS deaggregations are explained at their web site (USGS 2004f). In this step it is necessary to know the style of faulting associated with the modal M-R pairs. This is necessary because numerous attenuations relationships have been used in the preparation of the USGS seismic hazard maps, and it is recommended that the same relationships be used for comparison. This information can be ascertained from the tabulations and M-R- ϵ plots that accompany the deaggregation output (refer to appendixes). The CSZ interplate (*mega-thrust*) earthquakes are specified as M 8.3 or M 9.0, the CSZ intra-plate (*deep intra-slab*) events can be identified as sources in the M 6.5 to 7.5 range located at source to site distances that are generally greater than 50 km, and the shallow crustal sources (local faults and gridded seismicity) are generally in the ranges of M 5.0 – 7.0 and R 5 – 40 km. The specific attenuation relationships provided by source or style of faulting are; (a) CSZ interface earthquakes (Youngs et al 1997, Sadigh et al 1997), (b) shallow crustal earthquakes in regions of extensional tectonics such as the Basin and Range province (Abrahamson and Silva, 1997, Boore et al 1997, Campbell and Bozorgnia 2003, Sadigh et al 1997, Spudich et al

1999), and (c) non-extensional areas (Abrahamson and Silva, 1997, Boore et al 1997, Campbell and Bozorgnia 2003, Sadigh et al 1997). All of the relationships are used with equal weighting for the specific applications therefore for a direct comparison to be made to the median PGA value provided on the USGS maps all of the appropriate attenuation relationships must be used. This exercise serves as a worthwhile comparison; however, it is not considered to be necessary for routine liquefaction hazard assessments.

For the purpose of estimating PGA based on the M-R data, attenuation relationships other than the ones used by the USGS can be employed. For example, recent investigations of subduction zone earthquake motions have lead to the development of ground motion relationships for CSZ earthquakes (Gregor et al 2002, Atkinson and Boore 2003). These relationships for estimating peak ground accelerations supplement earlier efforts by Cohee and others (1991) and Crouse (1991). In light of the absence of strong motion records in Oregon for CSZ earthquakes, and the uncertainty inherent in empirical and numerically-based ground motion estimates, it is recommended that two or three methods be used on each project. The attenuations relationships can be formatted for use with spreadsheets thereby making it very efficient to obtain PGA values for any source.

The PGA values obtained on the basis of modal M-R pairs will most likely not match the median PGA value provided on USGS maps or listed in summary tables for the mean return time of interest. The resulting ground motion estimates may be larger or smaller than the median mapped value. This can be assessed in advance by noting the ϵ value for the modal M-R pair. Given the median PGA from the map and the ϵ value from the deaggregation an estimate of the PGA due to the specific M-R pair can be made. This data is provided in tabular form (refer to the appendixes) thereby supplementing the use of attenuation relationships to obtain PGA.

The remaining steps in the liquefaction hazard evaluation follow the recommendations provided at length in other recent publications (Youd et al 2001, Dickenson et al 2002, Seed et al 2003, Idriss and Boulanger 2004). For the sake of brevity the specific tasks will be outlined in a very cursory fashion. Practitioners are encouraged to refer to the supplementary references for the details of these portions of the evaluation.

Steps 3 and 4: Select Representative Acceleration Time Histories and Perform Dynamic Soil Response Analysis

Dynamic soil response analysis is required to determine the cyclic loading at selected depths in the soil profile. One-dimensional site response analyses using simple models such as SHAKE are commonly used in practice for computing time histories of acceleration, shear stress, and shear strain in the layers of interest. The computed cyclic stress ratio ($CSR = \tau_{avg}/\sigma_v'$, where τ_{avg} is the equivalent, average cyclic shear stress induced by the earthquake and σ_v' is the vertical effective stress prior to shaking) is used directly in the *Simplified Procedures* for evaluating the potential for the triggering of liquefaction. It is recommended that 2 or 3 input, rock motions be used for each M-R scenario in order the capture the range of variability in the rock motions, as well as the

variability in the dynamic response of the soil column. The selection criteria for the bedrock motions have been well addressed by Dickenson et al (2002).

As previously addressed the incorporation of multiple M-R pairs for evaluation can dramatically increase the number of dynamic response analyses required. In situations such as this (i.e. Portland region) the following procedure can be considered for screening the most important earthquake scenarios for dynamic modeling:

1. Apply the appropriate attenuation relationships for all M-R pairs that are identified as contributing a significant relative contribution to the hazard.
2. Estimate the soil amplification factor from charts or from prior dynamic soil response analyses in similar geologic settings, and at similar seismic load levels.
3. Estimate the ground surface PGA by multiplying the bedrock PGA values by the soil amplification factor(s).
4. Assess the relative cyclic load level using an approach similar that to outlined in the text (CSR*, Equation 2). Both the PGA and the duration of the motions must be accounted for in such a procedure.
5. Select the 2 or 3 most significant earthquake scenarios for subsequent modeling. In many regions of Oregon (e.g., Medford, Klamath Falls) the primary M-R scenarios represent similar sources. In these situations the number of scenarios warranting investigation may be reduced to 1 or 2.

Steps 5 and 6: Determine the Liquefaction Resistance of the Soil and Estimate the Post-Cyclic Loading Strength of the Soil

The cyclic resistance of the soil can be estimated using the straightforward, widely-adopted procedures outlined in the consensus document by Youd and others (2001) and in subsequent publications (Seed et al. 2003, Idriss and Boulanger, 2004). An extensive example problem has been prepared by Dickenson and others (2002) for a site located along the Columbia River adjacent to Portland International Airport, and this reference provides in-depth discussion of the steps involved. The resulting Cyclic Resistance Ratio ($CRR = \tau_{avg}/\sigma_v'$, where τ_{avg} is the equivalent, average cyclic shear strength of the soil and σ_v' is the vertical effective stress prior to shaking) is compared to the intensity of the cyclic loading (CSR) generated by the design level earthquakes. The factor of safety against liquefaction is the ratio of CRR/CSR.

Once the factor of safety against liquefaction has been determined the excess pore pressure can be estimated and the shear strength evaluated. The methods used for determining the shear strength of sandy soils is presented in Dickenson et al (2002), with updated relationships for the post-liquefaction strength of sandy soil proposed by Olson and Stark (2003). If several scenarios (i.e. M-R pairs) are being considered it may be necessary in subsequent stability analyses for all, or at least a subset, of the cases to be evaluated. As an example, for sites located along the I-5 corridor the local, shallow crustal events may yield the lowest factors of safety against liquefaction, although the hazard to the bridge may be greater due to CSZ earthquakes given their longer duration. The duration would have been accounted for by use of the MSF; however, subsequent

deformation analyses (e.g., Newmark sliding block, Makdisi and Seed) may indicate that ground deformations due to the larger CSZ events are greater.

Step 7: Estimate the Seismic Stability of the Embankment

The dynamic and post-cyclic loading shear strengths of the soils, determined as a part of Step 6, are used in standard slope stability analyses to estimate the margin of safety against failure of slopes and embankments. The seismic stability of the slope can be estimated using pre-earthquake strengths with a pseudostatic lateral force coefficient representing the earthquake loading, or by incorporating the post-cyclic loading shear strengths and performing a “static” analysis. The former method is not recommended for analysis of sites with potentially liquefiable soils, sensitive fine-grained soils, or brittle materials such as lightly cemented soils. The second method can be used to obtain a post-cyclic loading factor of safety (FS_{eq}). If FS_{eq} is less than unity then the slope will fail during and after the strong ground shaking. Estimates of the ground deformation associated with this mode of failure can only be determined using 2D and 3D numerical models with slip surface and large-strain capability. In regions where the seismic hazard is dominated by both large CSZ earthquakes and smaller local crustal events it may be necessary to perform multiple stability analyses. Situations that would require only one stability analysis are; (1) the case where none of the soil liquefies during shaking by either scenario, and (2) the case where the same soil layers liquefy in both events. For cases where the factors of safety against liquefaction are different (yet between 1.0 and 1.4), or the extent of liquefaction is different during the scenario events, multiple stability analyses are recommended.

Step 8: Estimate the Lateral Deformation of the Embankment

In many cases FS_{eq} is greater than unity. This indicates that the slope is stable for post-earthquake static conditions. It is possible however that FS_{eq} can drop below unity during the earthquake due to the cyclic loads imposed on the soils during shaking. In this case a critical, or yield, acceleration (a_{crit}) can be determined to assess the margin of stability that the slope may have during cyclic loading. The critical acceleration is the acceleration that is needed to bring the slope to a state of marginal stability ($FS = 1$). The slide mass will begin to move when the acceleration of the slope exceeds the critical acceleration. During an earthquake this acceleration only exists for a short duration therefore the slope is temporarily stable, then unstable, and stable once again. The acceleration time history computed using the dynamic soil response model in Step 5 is used to determine if the value of a_{crit} will be exceeded during the ground shaking. By double integrating the acceleration pulses that exceed a_{crit} the cumulative displacement of the slope can be estimated. This procedure has been applied for a portion of the Columbia River levee in Portland (Dickenson et al 2002). A useful tool for performing this sliding block type of analysis is available through the USGS (Jibson and Jibson 2003). Deformations should be computed for all scenarios judged to significantly contribute to the liquefaction hazard. In most cases evaluated by the author for sites along the I-5 corridor this has required only 2 scenarios.

Step 9: Develop Recommendations for Soil Improvement if Necessary

If the results of the seismic stability analysis indicate FS_{eq} below unity, or computed ground deformations that are greater than tolerable limits, then mitigation strategies are required. In many cases this includes soil improvement to treat weak, liquefiable, or sensitive soils. The vertical and lateral extent of the ground treatment will depend on factors such as geologic conditions, site and construction constraints, size of the structures, and cost. Evaluating the effectiveness of soil improvement for minimizing ground deformations requires an iterative process of slope stability analyses that incorporates the strength of the treated soil. The vertical and lateral extent of the treated soil is enlarged until the ground deformations computed using procedures such as the sliding block, or more sophisticated numerical models, are acceptable. This modeling may involve different modes of improvement (soil densification, cementation, dewatering, etc), site reconfiguration and grading, or structural mitigation measures (piers, piles, retaining walls). In most cases complex soil-foundation-structure interaction is involved and this must be addressed with knowledgeable engineering judgment, input from specialty contractors, and local experience. It must be noted that the stability analysis must not focus solely on the original critical failure surface determined for the un-improved soil. It is common in cases involving ground treatment for the location of the critical surface to change as the extent of the ground treatment changes. This should be anticipated and accounted for in the deformation analyses.

An example of this procedure is provided in the following section. The application for analysis involves a bridge approach embankment of simple geometry underlain by liquefiable soils. Two scenarios will be analyzed for liquefaction potential, slope stability and lateral displacements. The evaluation will incorporate a spreadsheet analysis of liquefaction and post-cyclic shear strength, and a subsequent slope stability analysis using the well-known program XSTABL. Unique aspects of both scenarios and recommendations for practice will be addressed in the following section.

**EXAMPLE PROBLEMS:
ASSESSMENT OF LIQUEFACTION HAZARDS
INCLUDING TRIGGERING AND DEFORMATION POTENTIAL**

In order to demonstrate the application of procedures for establishing design level ground motions and evaluating liquefaction hazards two example problems involving generalized embankment configurations are presented. The methods of analysis follow the procedures outlined in the preceding text, the report by Dickenson and others (2002), and several state-of-the-practice references cited in this report. Standard-of-practice methods of analysis for the complex behavior of embankments underlain by liquefiable soils are applied. In the first example, the foundation soil is a very loose to loose sand containing variable weight percentages of non-plastic silt (Figure 6). The second example features a foundation of medium dense sand that exhibits a greater resistance to liquefaction. The ground motions used in the evaluation are representative for the Portland metropolitan area for a return period of 975 years. Pertinent aspects of the analysis are outlined as follows.

Ground Motions

The ground motions used in the analysis were selected based on de-aggregation data obtained from the USGS Seismic Hazard Mapping Project website. All earthquake M-R scenarios that contributed at least 5% to the cumulative seismic ground motion hazard were considered in the evaluation. Inspection of the tabular PSHA de-aggregation data in Appendix B reveals four M-R pairs that exceed 5% contribution (i.e., "ALL_EPS" > 5.00% for PGA). These scenarios include local, shallow crustal earthquakes, as well as distant large CSZ events, as shown in Table 2. Bedrock PGA values were obtained using all of the attenuation relationships that were utilized in the development of the USGS ground motion maps. This was done for the sake of comparison with the mean PGA value listed at the USGS website. This level of effort is not necessary for routine applications in practice; however, this step is simplified by the use of spreadsheets for each of the attenuation relationships.

The site consists of sandy soils with a depth to bedrock of 55 feet. The soil amplification factors developed by Dickenson and Seed (in Dickenson et al. 2002) were used in the evaluation. Note that simplified ground motion amplification factors are commonly used during the early stages of analysis to facilitate preliminary assessment and screening. They are not recommended for final analysis and design (Dickenson et al, 2002; Youd et al, 2000). It is recommended that a numerical dynamic soil response program such as SHAKE be used for project specific analyses. Soil-dependent ground motion amplification factors are used herein for the sake of simplicity and demonstration purposes only.

Table 2: Earthquake Scenarios used in the Example Problems

PORTLAND SITE: 975 YEAR MEAN RETURN PERIOD		
Earthquake Scenario (M-R Pair)	PGA on Bedrock (g)	PGA at the Ground Surface (g)
M 6.2, R 12.1 km	0.195	0.26
M 6.64, R 2.9 km	0.520	0.49
M 8.3, R 89.5 km	0.12	0.18
M 9.0, R 89.5 km	0.16	0.22
Mean of the 4 scenarios	0.249	0.29
Mean from USGS PSHA	0.274	0.33*

*Soil response amplification factor of Seed & Dickenson (1994) applied to the USGS PSHA bedrock PGA.

CASE NO. 1: FOUNDATION OF VERY LOOSE TO LOOSE SANDY SOIL

Modeling and Assumptions

The embankment configuration and geotechnical conditions for this problem are illustrated in Figure 6. The *Simplified Procedure* for liquefaction evaluation has been prepared in a spreadsheet (Appendix I), which makes the application for multiple earthquake scenarios very efficient. The fine sand has been modeled with a fines content that varies with depth as follows; 4% by weight non-plastic silt in the upper 15 ft, 12% at depths of 15 to 25 ft, and 35% at depths between 25 and 40 ft. The Cyclic Stress Ratios (CSR) induced by the ground motions at the depths of interest (i.e. the elevation of each of the SPT data points) were computed using the ground surface PGA value, which was converted to approximate CSR-values at the depths of interest using the standard formulation by Seed and Idriss (in Youd et al, 2000). This is a simplification that is useful for preliminary screening; however, the results of dynamic soil response analyses using programs such as SHAKE are preferable for computing the CSR at specific depths.

The existence of sloping ground conditions results in stresses that vary with distance from the centerline of the embankment toward the free-field. At any specified elevation the vertical stress and shear stress will depend on the location of the point relative to the embankment slope. This complicates the liquefaction hazard evaluation for the following reasons; (1) the vertical effective stress at a given elevation is not constant across the entire site, (2) the computation of CSR is dependent on the vertical total and effective stresses, and (3) the residual undrained shear strength of liquefied soil is a function of the vertical effective stress. The latter two items require that the CSR, the corresponding factor of safety against liquefaction (FS_{liq}), and the residual shear strength vary vertically and laterally. This results in an additional degree of complexity when performing limit equilibrium slope stability analyses, in which soil layers are usually modeled with material properties (ϕ' , c' , c_u) and FS_{liq} that remain constant in the lateral direction. In order to clearly demonstrate the procedures for evaluating liquefaction hazards and slope stability, simplifying assumptions have been made throughout the two cases presented. The primary simplifications are related to the modeling of soil properties in the lateral

dimension. For example, the CSR values have been computed for the stress conditions that exist under the centerline of the embankment and for the free-field conditions beyond the toe of the slope. Instead of computing the FS_{liq} with depth for both vertical profiles, establishing the corresponding shear strengths, and incorporating the laterally dependent soil strengths into the slope stability analyses, the CSR values have been averaged. This approximation has been adopted herein for the sake of brevity. The impact of the simplification will obviously depend on the configuration of the embankment and the cyclic resistance of the soil. A second approximation involves the estimation of the undrained residual shear strength of the liquefied soils. This strength is a function of the pre-earthquake vertical effective stress therefore the shear resistance of the soil will vary depending on lateral location relative to the centerline of the embankment, slope face, toe, or free-field. The undrained shear strengths were estimated using the vertical effective stresses that exist under the centerline of the embankment. This will yield larger shear strengths than would be computed for the soils underneath the sloping portion of the embankment and in the free-field. It is recommended that the impact of these approximations be evaluated for project specific analyses.

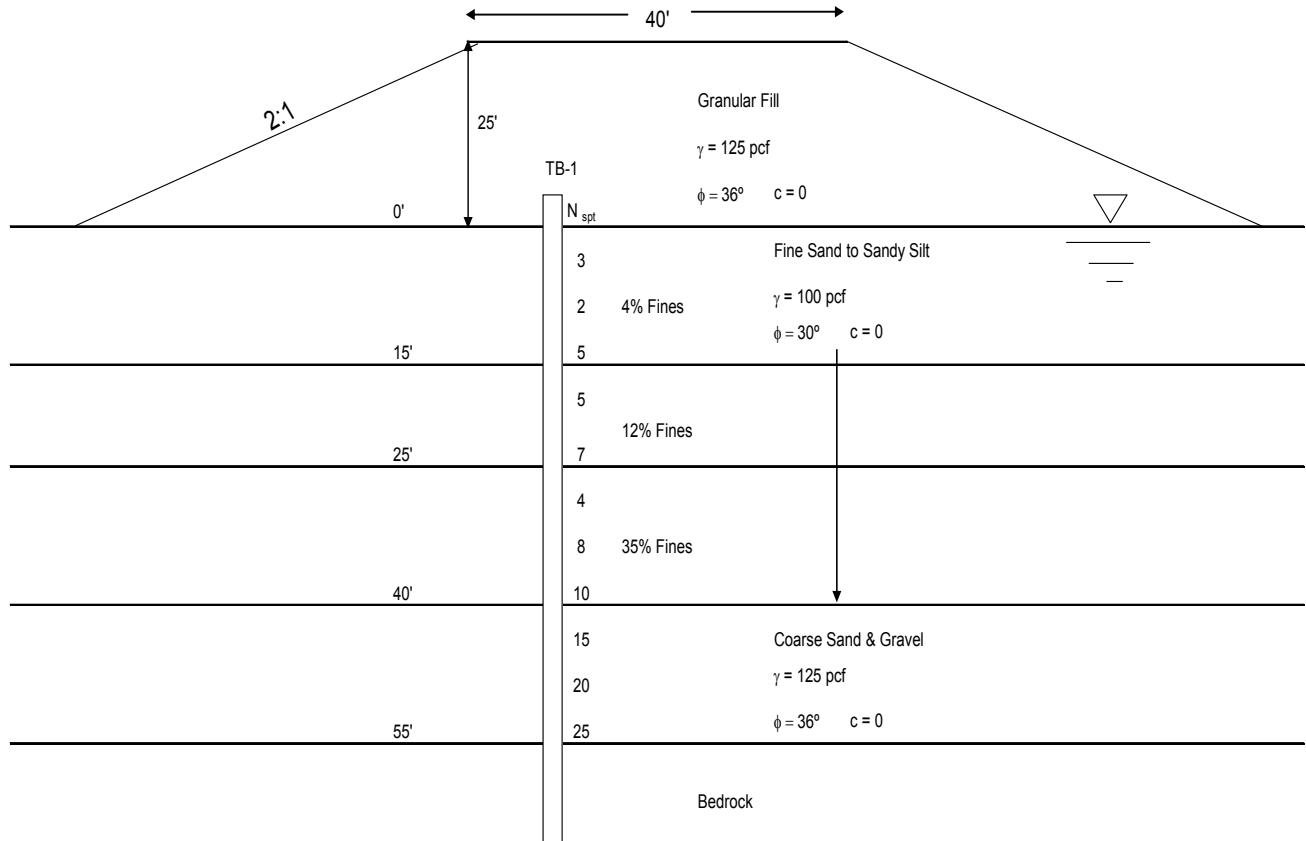


Figure 6: Embankment configuration and foundation conditions for the liquefaction hazard example problems (Case 1).

Results for Case No. 1

The analyses demonstrated that the fine sand is liquefiable throughout its entire thickness for all four of the earthquake scenarios evaluated. This is not surprising given the low penetration resistances of the fine sand. Note that the underlying coarse sand is also indicated to be liquefiable in three of the four earthquake scenarios.

The prevalence of liquefiable soils in the foundation of embankment highlights the need for subsequent analyses of embankment stability. Standard limit equilibrium methods of analysis can be used for this purpose. These methods are useful for estimating the margin of stability for slopes and embankments along circular or wedge-shaped failure planes. The overall factor of safety against sliding is evaluated along discrete failure planes. This

procedure is routinely performed in practice to locate “critical surfaces” having the lowest margin of stability, and it is useful for highlighting the portion of the embankment that exhibits the greatest potential for failure. There are; however, several significant limitations in the use of limit equilibrium analyses are cases involving liquefaction, soil-structure interaction (e.g., pile foundations in slopes, bridge abutments and appurtenant structures near slopes), and ground treatment. The procedure is limited in that the pattern of deformations cannot be assessed. This is an important need for performance-based seismic design involving structures. Another limitation involves the modeling of liquefied soil. In routine practice, the undrained residual strength of the liquefied sand is estimated using empirical relationships developed in back-analysis of failed slopes. The residual strength is used in the slope stability analysis as a constant value of shear resistance despite the fact that the strength varies with strain level, and drainage during and after ground shaking. Finally, the limit equilibrium methods are poorly equipped to account for complex modes of failure and deformation that may arise adjacent to structures, embedded foundations or earth retention systems, or treated ground. Numerical models have been developed that can account for many of these shortcomings; however, they are resource intensive and may not be justified for evaluations of more routine bridge embankment configurations. Used properly, the limit equilibrium methods can be applied with a reasonable degree of confidence for applications involving embankments founded on liquefiable soils.

Slope stability analyses involving liquefied soil require that the shear resistance of the softened soil be estimated. In light of the complex nature of excess pore pressure generation, large-strain development, and post-liquefaction strength gain accompanying drainage and large strain, most methods used in practice for estimating the residual strength of liquefied soil rely on back-analysis of field case studies involving slope failures. The most widely used methods have been developed by Seed and Harder (1990), Stark and his co-workers (Olsen and Stark, 2002), and Dobry and colleagues (Baziar and Dobry, 1995). The former method correlates the residual undrained strength with SPT N -value, while the method proposed by Stark relates the strength to SPT and CPT data as functions of pre-earthquake vertical effective stress. Dobry’s approach is presented in the form of an undrained strength ratio for small or large deformations. It has been observed that potentially large variations in the estimated residual shear strengths can result when using these procedures. No formal consensus has been proposed regarding the use of one method over another, and it is recommended that all three be used to bracket the range of likely values. Seed has recommended (Seed et al, 2003) that the methods proposed by Seed and Harder, and Olson and Stark be used. He recommends that a weighted average can then be obtained using weighting factors of 75% for the former relationship and 25% for the latter. No rationale was given for these relative weighting factors. In the analyses performed for this example problem these two methods were used with equal weighting (i.e. the average of the two values). The shear strength values varied with depth, but were held constant in the lateral direction. This was adopted for the sake of simplification. The residual shear strengths should vary with vertical effective stress, and therefore with position relative to the embankment (e.g. under the centerline, under the slope face, or past the toe of the slope). This refinement should be accounted for in actual analysis and design.

The slope stability computations were performed using the commercially available program XSTABL. The factor of safety against failure was evaluated using Spencer's method and Bishop's method. The residual undrained shear strengths were employed for liquefiable soils, and drained shear strengths were used for the embankment soils. The post-earthquake static factor of safety was computed for several cases; including deep seated failure and slope-face failures. The factor of safety against shallow surface failure (sloughing) is roughly 1.27, which may at first appear to be acceptable; however, this does not account for the stability during seismic loading or the overall stability of the embankment. The factor of safety against deep seated rotational failure through the liquefied soil is substantially less than unity (0.46). The critical surfaces are shown in Figure 7. This indicates that the embankment would not be stable under static conditions if liquefied strengths apply. This is representative of "end of shaking" conditions. The embankment and foundation soils will undergo considerable deformation during all four of the earthquake scenarios. The range of likely deformations will be a function of the duration of shaking and the number of significant loading cycles. Limit equilibrium methods cannot be used to estimate the displacement due to the very low factor of safety. Utilization of simple charts based on 2D numerical non-linear, effective stress modeling for estimating displacement of embankments on liquefied soils (Dickenson et al, 2002, Figures 7.7 and 7.8) indicates that the maximum deformations may range from 4 to 10 feet, well beyond tolerable limits for most bridge approach embankments. For this scenario it would be necessary to implement a ground treatment program to mitigate the liquefaction hazards at the site.

Several pertinent points can be made regarding the stability analyses for the four earthquake scenarios used in this evaluation. First, it may appear based on the results of the limit equilibrium analyses that it makes no difference to the stability which earthquake or ground motion parameter has been used, the post-earthquake static factor of safety is 0.46 regardless of earthquake scenario. This is not the case. The characteristics of the individual earthquake motions were incorporated into the analysis by way of the liquefaction susceptibility analysis. It was determined that the soils would liquefy under all four cases. Given that the soil liquefied, the same undrained residual shear strength is applicable for all four earthquake scenarios, therefore the same factor of safety is computed for all cases. The seismically induced embankment deformations will reflect the intensity, duration, and frequency content of the ground motions. This can be accounted for in advanced numerical models employing time history analyses, non-linear soil behavior, and large-strain capability. The geomechanical model FLAC was used to generate the charts for estimating maximum embankment deformation for cases involving liquefaction of foundations soils underneath bridge approach embankments. The PGA and magnitude of each event is required to estimate the resulting slope deformations. This simplified procedure allows deformation estimates to be made for each earthquake scenario. The approximate deformations associated with each of the four earthquakes in Table 2 are listed in order as; M 6.2 event yields approximately 4 to 6 ft. of displacement, M 6.64 – 8 to 10 ft., M 8.3 – 4 to 6 ft., and M 9.0 - 4 to 6 ft. The influence of earthquake size and source-to-site distance is evident in these estimates. It is

interesting to note that the large CSZ events and the local M 6.2 earthquake yield similar displacements estimates.

A final note should be added regarding the large deformations indicated in Figures 7.7 and 7.8 of Dickenson and others (2002). The estimates are considered to be conservative for three reasons; (1) the use of earthquake time histories that exhibited greater energy (Arias Intensity) than would be considered average for that magnitude, (2) several of the crustal earthquake time histories represent near-fault motions and contain velocity components that yield larger displacements than would be computed using far-field motions, and (3) the numerical model used to simulate the soil deformations did not have a plasticity-based strain-hardening function to model dilation at large strain and strength gain due to drainage during straining. The resulting displacements are conservative, but not unreasonable in light of an extensive review of failures of embankments underlain by liquefiable soils. From a practical perspective, displacements greater than 1.5 to 2.0 ft are considered academic only as these ground deformations would be damaging to most bridge foundations and ancillary components.

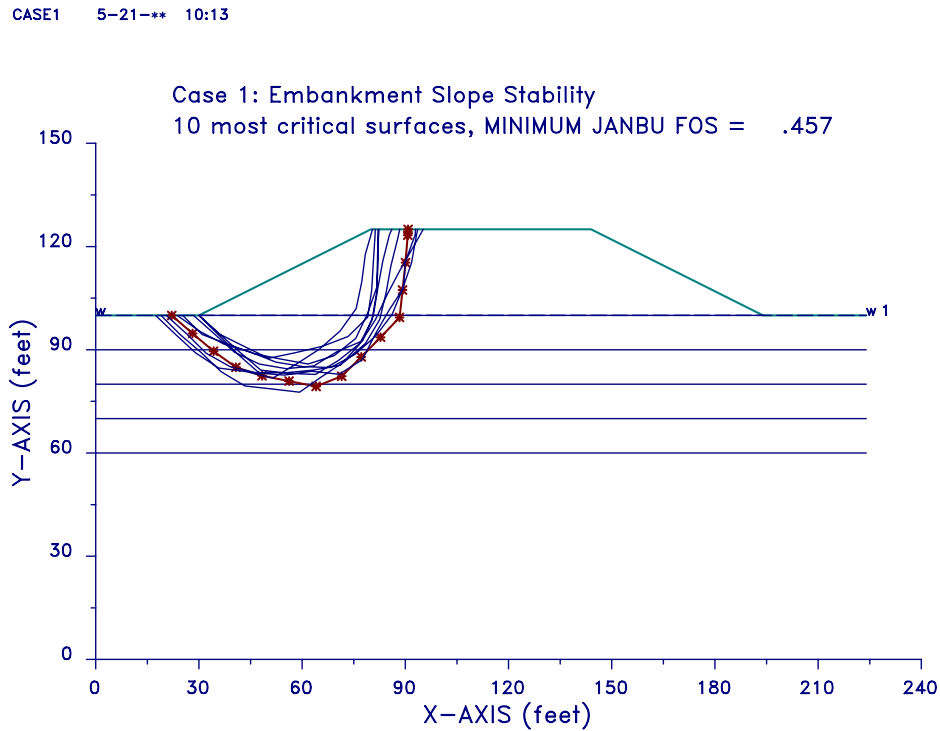


Figure 7: Results of Slope Stability Analyses for Case No. 1 (Full Liquefaction of the Foundation Layer)

CASE NO. 2: FOUNDATION OF MEDIUM DENSE TO DENSE SANDY SOIL

The analysis of liquefaction susceptibility and slope stability has been performed for a case involving medium dense to dense sandy soil. The SPT N-values in the fine sand have been changed for this analysis. The angle of internal friction and saturated unit weight of the fine sand have also been changed to correspond with the increase in penetration resistance ($\phi' = 36^\circ$, $\gamma_{\text{sat}} = 125$ pcf). The modified penetration resistances are shown in Figure 8. In this case the sandy soils have a greater cyclic resistance and they are not found to be fully liquefiable in all cases. In these design examples the factor of safety against liquefaction varies from less than 0.5 to more than 2.0. The post-cyclic loading shear strengths were estimated following the recommendations outlined by Dickenson and others (2002) as follows:

1. $FS_{\text{liq}} > 1.4$ – Use the drained friction values.
2. $1.4 > FS_{\text{liq}} > 1.0$ – Compute an equivalent friction angle that accounts for the excess pore pressure generation during shaking.
3. $FS_{\text{liq}} < 1.0$ – Use the empirical relationships developed by Seed and Harder (1990), Baziar and Dobry (1995), or Olson and Stark (2000) for estimating the residual undrained shear strength of the liquefied sand.

It has been determined that the M 6.2 and M 8.3 scenarios resulted in the generation of very low excess pore pressure in the upper portion of the fine sand, which controls overall embankment stability. Conversely, significant excess pore pressures were computed for the M 6.64 and M 9.0 events. In both of the latter cases the generation of excess pore pressure resulted in a significant reduction in soil strength at depths below 20 ft. from the original ground surface. The spreadsheets used for the liquefaction susceptibility and strength evaluation are provided in Appendix I. The strength parameters computed in this evaluation were used directly in the XSTABL analyses of seismic slope stability.

Post-earthquake stability analyses were performed to determine the factor of safety against sliding for each scenario, and these analyses were supplemented with rigid body slope deformation analyses using the Newmark procedure. The strength parameters used in each of the four slope stability analyses and the resulting factors of safety against sliding are provided in Tables 3 through 6. Note that the critical surfaces for the static conditions are all rather shallow circular slide planes that extend from the edge of the slope crest to points that are not that far from the toe of the slope (Figure 9). The vertical stress conditions under this region of the embankment are clearly less than the stresses at equivalent elevations under the centerline of the embankment. This is an important observation for two reasons: (1) the vertical effective stresses are different than those assumed in the liquefaction susceptibility evaluation, and (2) the vertical effective stresses are different than those assumed in estimating residual undrained shear strengths for the soils that liquefied. In practice, the influence of these simplifications on overall stability should be addressed. The incorporation of more refined vertical stress patterns in the analyses would yield lower factors of safety against sliding.

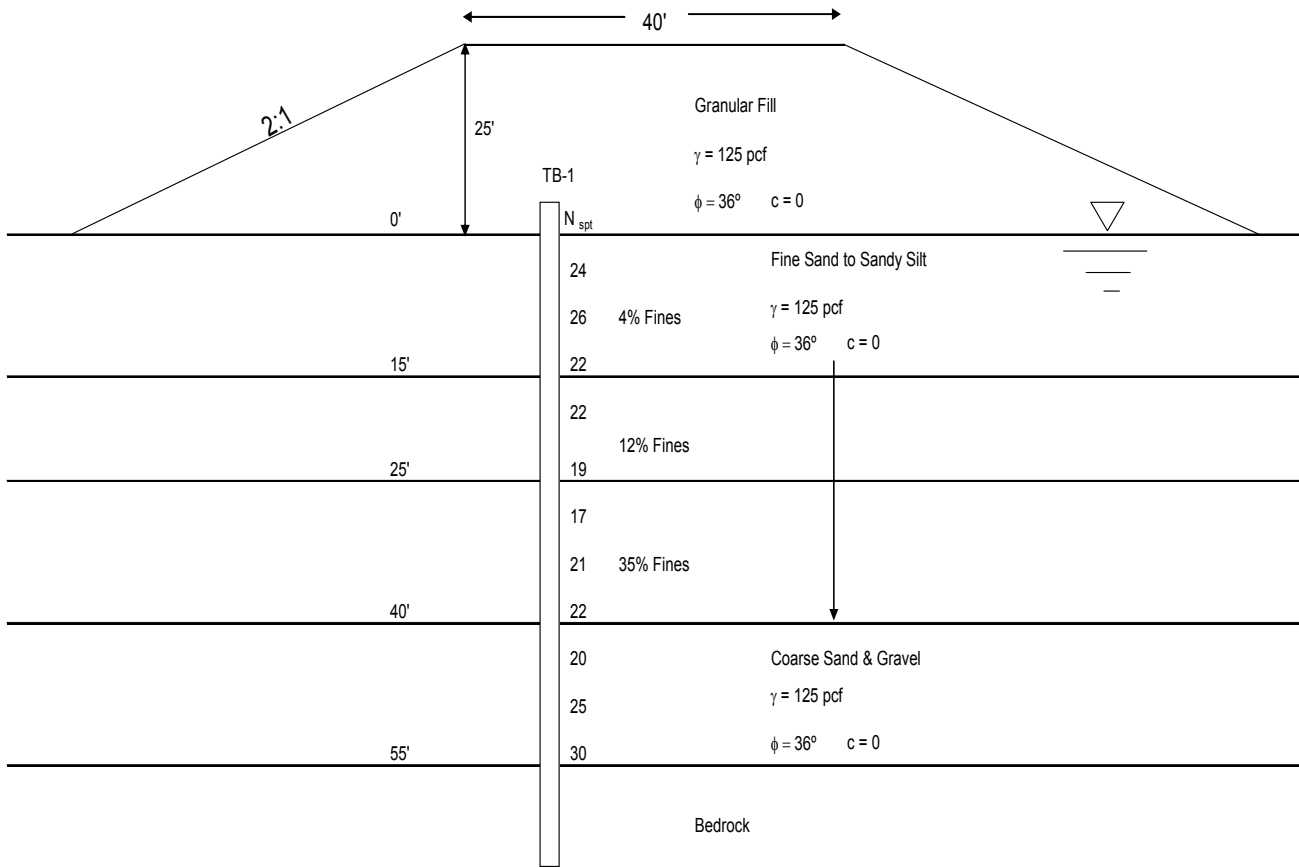


Figure 8: Embankment configuration and foundation conditions for the liquefaction hazard example problems (CASE 2).

**Table 3: Analysis Results for the M 6.2 Earthquake Scenario
(PGA = 0.26g)**

Depth (ft)	N _{field} (blow/ft)	FS _{liq}	Strength Parameter		FS (a _y)	Slope Stability		
			S _{ur} (psf)	Φ _{equiv} (degrees)		Maximum Deformation (ft)		
						Newmark	Makdisi & Seed	Dickenson et al
5	24	2.97	n/a	36	1.61 (0.22)	< 0.01	< 0.01	0.5
10	26	2.52	n/a	36				
15	22	2.80	n/a	36				
20	22	2.71	n/a	36				
25	19	1.45	n/a	36				
30	17	1.77	n/a	36				
35	21	2.78	n/a	36				
40	22	2.61	n/a	36				
45	20	1.03	n/a	14				
50	25	1.31	n/a	30				
55	30	1.66	n/a	36				

**Table 4: Analysis Results for the M 6.64 Earthquake Scenario
(PGA = 0.49g)**

Depth (ft)	N _{field} (blow/ft)	FS _{liq}	Strength Parameter		FS (a _y)	Slope Stability		
			S _{ur} (psf)	Φ _{equiv} (degrees)		Maximum Deformation (ft)		
						Newmark	Makdisi & Seed	Dickenson et al
5	24	1.32	n/a	30	1.33 (0.09)	1.33 (mean) 0.83 (median) 3.10 (mean + 1σ)	0.9	4.0
10	26	1.12	n/a	24				
15	22	1.25	n/a	29				
20	22	1.21	n/a	28				
25	19	0.65	717	n/a				
30	17	0.79	727	n/a				
35	21	1.24	n/a	29				
40	22	1.16	n/a	26				
45	20	0.46	894	n/a				
50	25	0.59	997	n/a				
55	30	0.74	1100	n/a				

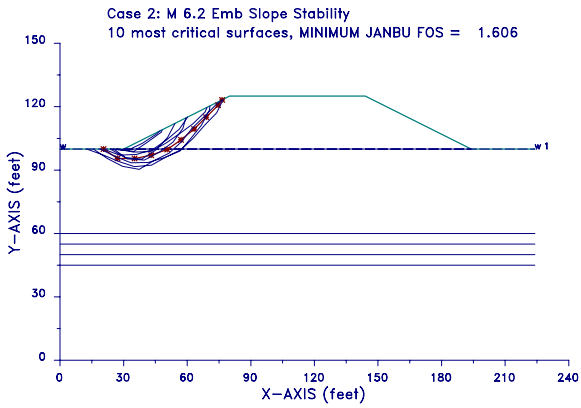
**Table 5 Analysis Results for the M 8.3 Earthquake Scenario
(PGA = 0.18g)**

Depth (ft)	N _{field} (blow/ft)	FS _{liq}	Strength Parameter		Slope Stability			
			S _{ur} (psf)	Φ _{equiv} (degrees)	FS (a _y)	Maximum Deformation (ft)		
						Newmark	Makdisi & Seed	Dickenson et al
5	24	2.23	n/a	36	1.65 (0.20)	0	0	1.0
10	26	1.90	n/a	36				
15	22	2.11	n/a	36				
20	22	2.04	n/a	36				
25	19	1.09	n/a	22				
30	17	1.33	n/a	30				
35	21	2.09	n/a	36				
40	22	1.96	n/a	36				
45	20	0.78	894	n/a				
50	25	0.99	997	n/a				
55	30	1.25	n/a	29				

**Table 6 Analysis Results for the M 9.0 Earthquake Scenario
(PGA = 0.22g)**

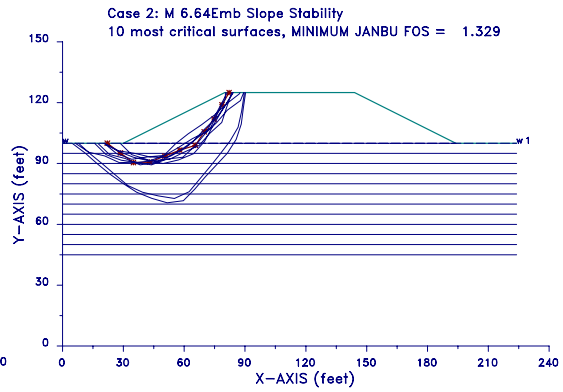
Depth (ft)	N _{field} (blow/ft)	FS _{liq}	Strength Parameter		Slope Stability			
			S _{ur} (psf)	Φ _{equiv} (degrees)	FS (a _y)	Maximum Deformation (ft)		
						Newmark	Makdisi & Seed	Dickenson et al
5	24	1.35	n/a	31	1.41 (0.11)	0.25	>> 3.0	3.0
10	26	1.15	n/a	26				
15	22	1.27	n/a	30				
20	22	1.23	n/a	29				
25	19	0.66	717	n/a				
30	17	0.80	727	n/a				
35	21	1.27	n/a	30				
40	22	1.19	n/a	27				
45	20	0.47	894	n/a				
50	25	0.60	997	n/a				
55	30	0.75	1100	n/a				

CASE2M62 5-21-*** 10:28



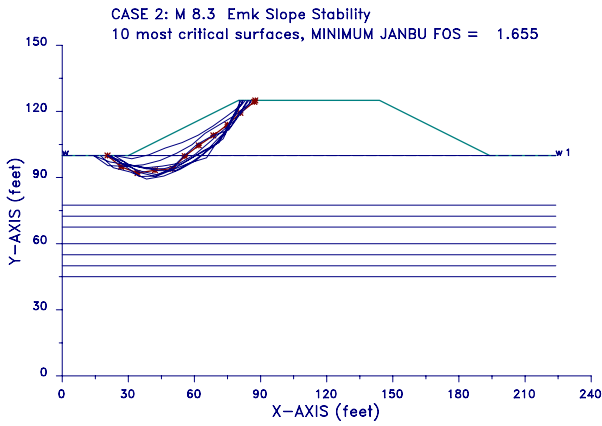
a. M 6.2 Scenario

CASE2M66 5-21-*** 10:53



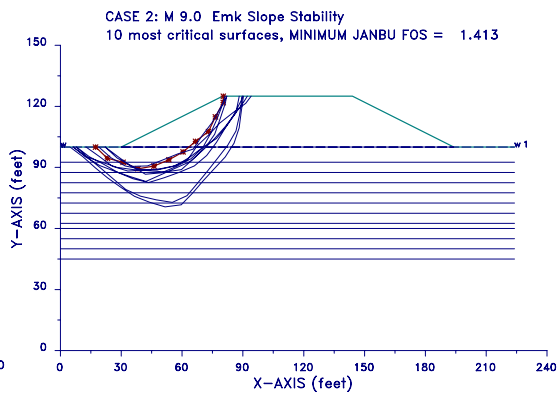
b. M 6.64 Scenario

CASE2M83 5-21-*** 11:11



c. M 8.0 Scenario

CASE2M90 5-21-*** 11:01



d. M 9.0 Scenario

Figure 9: Critical Slip Surfaces for Static Analyses Employing Post-Cyclic Loading Shear Strengths. (CASE 2)

The yield, or critical, acceleration (alternatively listed in the literature as a_{crit} , a_y , k_y) that is required to bring the slope to a state of marginal stability was determined by iterative solution using the XSTABL program. The yield acceleration values associated with each earthquake scenario are 0.22g, 0.09g, 0.20g, and 0.11g for the earthquake scenarios in order of smallest magnitude to largest. For three of the four cases (M 6.2, M 6.64, and M 9.0) evaluated, the peak ground acceleration exceeds the yield acceleration and therefore some degree of deformation is anticipated. The peak acceleration at the ground surface is considered appropriate for these examples given the height of the embankment, and the geometry of the slide mass. The yield acceleration is not exceeded for the case of the M 8.3 earthquake and permanent deformations would be expected to be negligible using the sliding block procedure.

The permanent earthquake induced slope deformations were estimated using three simple methods; (1) the Newmark sliding block procedure (Jibson and Jibson, 2003), (2) the chart solution developed by Makdisi and Seed (1978) for compacted earth dams, and (3) the design chart developed by Dickenson and others (2002) for cases involving liquefaction in the foundation soils. The Newmark model as prepared by Jibson and Jibson (2003) was used to perform the sliding block evaluations. The first two methods are similar in that no permanent deformation would be computed for cases where the yield acceleration is greater than the peak ground acceleration. The chart developed by Dickenson et al (2002) often indicates nominal permanent deformations for cases in which limit equilibrium analyses indicate that the yield acceleration is not exceeded by the peak ground acceleration. This is due to the method of 2D FDM numerical modeling approach used to develop the chart. Several aspects of the numerical simulation give rise to computed deformations despite global factors of safety greater than unity. These include:

1. The deformation provided by the design chart represents the vector summation of the computed vertical and horizontal components of displacement.
2. The constitutive models employed in the FDM modeling account for settlement due to the volumetric change that follows cyclic loading. Soils that experience FS_{liq} less than 1.1 to 1.2 will undergo volumetric strains in excess of 0.5 to 1.0%. Therefore, cases that involve liquefaction at depth will exhibit vertical deformation even though the overall factor of safety against sliding is greater than 1.0.
3. The computed deformations used in the development of the chart represent the maximum value obtained at any point in the model. This includes deep-seated failures, slope failures involving the toe or slope face, as well as surficial sloughing.

The results of the deformation analyses demonstrate the influence that the magnitude and source-to-site distance have on the computed slope movement. This is due primarily to the intensity and duration of the ground motions, although the frequency content of the motions can be important for near-fault effects and for the CSZ motions that exhibit significant long period components. The ground motions used in the Newmark analysis

were selected from the catalog of records obtained in the package of Jibson and Jibson (2003). Candidate time histories were selected to be representative of the motions for each scenario. The following criteria were used to select ground motions for the Newmark analyses; M 6.2 scenario ($6.0 < M < 6.4$, $6 \text{ km} < R < 18 \text{ km}$, strike slip and oblique normal fault style, stiff soil and soil rock soil condition, all records scaled to $0.26g$), M 6.64 ($6.3 < M < 6.9$, $1 \text{ km} < R < 10 \text{ km}$, strike slip and oblique normal faults, stiff soil and soft rock condition, all records scaled to $0.49g$), and for the M 9.0 earthquake a collection of motions was used that should likely bracket the problem. Four motions were used, all scaled to $0.22g$. The time histories included records from the 1985 Michoacan, Mexico earthquake, 1985 Valparaiso, Chile earthquake, and the 1978 Miyagi-ken Oki, Japan earthquake. Note that the magnitudes of the available records are all less than the M 8.3 to 9.0 scenario earthquakes recommended by the USGS. The computed deformations are considered to be slightly less than what would be anticipated had records from M 8.3 and 9.0 earthquakes been applied.

Practical Interpretation of the Results

The simple methods of estimating ground deformation are standard of practice screening tools that provide likely ranges of soil displacement. They do not provide estimates to be used in project specific analysis of pile foundations and abutments. None of the analyses account for the existence of deep foundations, embedded walls, anchors, or abutments fixed by bridge decks and superstructure adjacent to the slope. Additionally, the pattern of deformations is not provided therefore the impact on structural components such as deep foundations cannot be directly assessed. The ranges of estimated displacement should be viewed as indicators of relative seismic performance. It is recommended that the deformations be interpreted in light of tolerable limits and performance requirements for common bridge components.

In many sectors involving transportation infrastructure earthquake risk is defined in terms of return periods. Two-level earthquake hazard design has been adopted by several state transportation departments. The two level earthquake hazard levels are the Functional Evaluation Earthquake (FEE), sometimes referred to as the Operating Level Earthquake (OLE), and the Safety Evaluation Earthquake (SEE), or Contingency Level Earthquake (CLE). The FEE is defined as the earthquake (or more appropriately *the ground motions*) having a mean return period of 500 years. The SEE corresponds to a 2,500 year return period. These ground motion criteria can be modified to incorporate the 1,000 year exposure interval. The limit states and tolerable deformations are defined for each design level hazard. In addition to the earthquake hazards the bridge and appurtenant structures can be defined in terms of importance as lifelines. Portions of the bridge and approaches may be deemed “Critical Access Paths” or “Critical Infrastructure” and designed to a higher level of performance than those outside of the Critical Access Path (Parsons Brinckerhoff 1999). As an example, the design criteria for CAP structures subjected to FEE motions is usually elastic response, no below grade damage to deep foundations, minimal structural damage that can be quickly repaired, and the structure remains fully operational immediately after the earthquake. Non-CAP structures may be designed to a relaxed standard of performance that allows limited, repairable damage. For the SEE the

structure should remain functional without shoring or major repairs. Collapse is prevented for both CAP and non-CAP structures.

The approximate deformation limits for various bridge components can be established in consultation with bridge structural engineers. Possible classifications could include:

- Abutment walls supported on spread footings.
- Abutment walls supported on piles.
- Spread footings for interior piers.
- Deep foundations for interior piers.
- Embankment adjacent to critical structures, foundations, etc.
- Embankments in open area (no adjacent structures).

For example, in the case of the Cooper River Bridge in South Carolina the seismic settlement criteria for FEE allowed 1 in of settlement for CAP structures, and 2 in for non-CAP structures. SEE requirements specified no more than 4 in of settlement for CAP structures and less than 8 in to 20 in for Non-CAP components. Associated embankment deformation criteria are provided in Table 7. These criteria should be amended based on structure type.

Table 7: Allowable Embankment Deformations as Functions of Earthquake Hazard Level and Importance along Access Path (from Parson Brinckerhoff, 1999)

	Allowable Embankment Deformation (in) (FEE/SEE)	
	Embankment in Critical Access Path	Embankment in Non-Critical Access Path
Embankment adjacent to critical structures, foundations, etc.	≤ 2.0/6.0	≤ 2.0/6.0
Embankment in open area	≤ 12.0/39.0	≤ 24.0/79.0

The hazard analyses performed in this report were based on 1,000 yr motions. If this is considered a SEE hazard evaluation for a CAP structure, then it is evident that the risk of excessive embankment deformations is unacceptably high. The deformations induced by the M 6.64 and M 9.0 earthquakes may lead to more than 3 ft of deformation. A strategy for remedial ground treatment would be necessary for these critical cases. The zone of treated soil can be modeled with the limit equilibrium slope stability analyses by increasing the shear resistance of the soil, and an iterative suite of analyses performed to identify the optimal location and extent of soil to be improved. It must be noted that the slope stability analyses must be performed to search for new critical surfaces, as it is unlikely that the new critical circle, or wedge, will lie at the same location as the pre-treatment surface. The extent and type of treatment (e.g., densification, cementation and soil mixing, grouting) is varied until the computed displacements are less than the tolerable deformations for the hazard event and importance of the structure.

References

- Abrahamson, N.A. and Silva, W.J. (1997). "Empirical response spectral attenuation relations for shallow crustal earthquakes," *Seismological Research Letters*, vol. 68, no. 1, pp. 94-127.
- Andrus, R. D., Stokoe II, K.H., and Juang, C.H. (2004). "Guide for Shear-Wave-Based Liquefaction Potential Evaluation," *Earthquake Spectra*, Journal of the Earthquake Engineering Research Institute, vol. 20, no. 2, pp. 285-308.
- Ang, A. H-S and Tang, W.H. (1975), "Probability Concepts in Engineering Planning and Design", Vol. 1 – Basic Principles, J. Wiley and Sons.
- Atkinson G.M., and Boore, D.M. (2003). "Empirical Ground-Motion Relations for Subduction Zone Earthquakes and Their Application to Cascadia and Other Regions," *Bulletin of the Seismological Society of America*, vol. 93, no. 4, pp. 1703-1729.
- Baziar, M.H, and Dobry, R.. (1995). "Residual Strength and Large Deformation Potential of Loose Silty Sand," *Journal of Geotechnical Engineering*, ASCE, vol. 121, no. 4, pp. 896-906.
- Bazzurro, P., and Cornell, C.A. (1999). "Disaggregation of Seismic Hazard," *Bulletin of the Seismological Society of America*, vol. 89, no. 2, pp. 501-520.
- Boore, D.M., Joyner, W.B., and Fumal, T.E. (1997). "Equations for estimating horizontal response spectra and peak acceleration from western North American earthquakes: a summary of recent work," *Seismological Research Letters*, vol. 68, no. 1, pp. 128-153.
- Campbell, K.W., and Bozorgnia, Y. (2003). "Updated near-source ground motion (attenuation) relations for the horizontal and vertical components of peak ground acceleration and acceleration response spectra," *Bulletin of the Seismological Society of America*, vol. 93, no. 1, pp. 314-331.
- Cohee, B.P., Somerville, P.G., and Abrahamson, N.A. (1991). "Simulated Ground Motions for Hypothesized $M_w = 8$ Subduction Zone Earthquakes in Washington and Oregon," *Bulletin of the Seismological Society of America*, vol. 81, no. 1, pp. 28-56.
- Cornell, C.A. (1968). "Engineering seismic risk analysis," *Bulletin of the Seismological Society of America*, vol. 58, pp. 1583-1606.
- Crouse, C.B. (1991). "Ground-Motion Attenuation Equations for Earthquakes on the Cascadia Subduction Zone," *Earthquake Spectra*, EERI, vol. 7, no. 2, pp. 201-236.
- Dickenson, S.E., McCullough, N.J., Barkau, M.G., and Wavra, B.J. (2002). Assessment and Mitigation of Liquefaction Hazards to Bridge Approach Embankments in Oregon, Final report to the Oregon Department of Transportation, SPR 361, Report no. FHWA-OR-RD-03-04, 210 p.
- Dobry, R. Ramos, R, and Power, M.S. (1999) Site Factors and Site Categories in Seismic Codes, Technical Report MCEER-99-0010.
- EduPro Civil Systems (2002), ProShake and EduShake: User's manual, available at the web site www.proshake.com.
- Federal Emergency Management Agency (2004). "2003 Edition: NEHRP Recommended Provisions for Seismic Regulations for New Buildings and Other Structures," Part 1: Provisions (FEMA 425), and Part 2: (FEMA 425), Building Seismic Safety Council, Washington, D.C., available at <http://www.fema.gov/hazards/earthquakes/nehrrp/fema-368.shtm>.

Frankel, A.D., Petersen, M.D., Mueller, C.S., Haller, K.M., Wheeler, R.L., Leyendecker, E.V., Wesson, R.L., Harmsen, S.C., Cramer, C.H., Perkins, D.M., and Rukstales, K.S. (2002). "Documentation for the 2002 Update of the National Seismic Hazard Maps," United States Geological Survey, Open File Report 02-420, 33 p., (pdf file available at <http://pubs.usgs.gov/of/2002/ofr-02-420/>).

Geomatrix Consultants, Inc. (1995). Seismic Design Mapping State of Oregon, Final report to the Oregon Department of Transportation, Personal services contract 11688, Jan. 1995, Project No. 2442.

Gregor, N.J., Silva, W.J., Wong, I.G., and Younds, R.R. (2002). "Ground-Motion Attenuation Relationships for Cascadia Subduction Zone Megathrust Earthquakes Based on a Stochastic Finite-Fault Model," *Bulletin of the Seismological Society of America*, vol. 92, no. 5, pp. 1923-1932.

Harmsen, S., and Frankel, A. (2001). "Geographic Deaggregation of Seismic Hazard in the United States," *Bulletin of the Seismological Society of America*, vol. 91, no. 1, pp. 13-26.

Idriss, I.M., and Boulanger, R.W. (2004). "Semi-Empirical Procedures for Evaluating Liquefaction Potential during Earthquakes," *Proc. of the joint 11th International Conference on Soil Dynamics and Earthquake Engineering and 13th International Conference on Earthquake Geotechnical Engineering*, pp. 32-56.

Jibson, R.W. and Jibson, M.W. (2003). "Java programs for using Newmark's method and simplified decoupled analysis to model slope performance during earthquakes," U.S. Geological Survey Open File Report 03-005, available on CD from the first author.

Kramer, S.L. (1996). Geotechnical Earthquake Engineering, Prentice Hall Publishers, 653 p.

Lee, M.K.W., and Finn, W.D.L. (1991). "DESRA-2C – Dynamic Effective Stress Response Analysis of Soil Deposits with Energy Transmitting Boundary Including Assessment of Liquefaction Potential," University of British Columbia, Faculty of Applied Science.

Leyendecker, E.V., Hunt, J., Frankel, A.D., and Rukstales, K.S. (2000). "Development of Maximum Considered Earthquake Ground Motion Maps," *Earthquake Spectra*, EERI, vol. 16, no. 1, pp. 21-40.

Li, X.S., Wang, Z.L., and Shen, C.K. (1992). "SUMDES – A Nonlinear Procedure for Response Analysis of Horizontally-Layered Sites Subjected to Multi-Directional Earthquake Loading", Department of Civil Engineering, University of California, Davis, 81 p.

McGuire, R.K. (2004), Seismic Hazard and Risk Analysis, EERI Monograph Series MNO-10, Earthquake Engineering Research Institute, 221 p.

Olson, S.M., and Stark, T.D. (2002). "Liquefied strength ratio from liquefaction flow failure case histories," *Canadian Geotechnical Journal*, vol. 39, pp. 629-647.

Parsons Brinckerhoff (1999). "Final Report: Supplemental Design Criteria for Seismic Design for U.S. 17 Cooper River Bridges, Charleston, South Carolina," submitted to the South Carolina Department of Transportation.

Poulos, H.G., and Davis, E.H. (1991). Elastic Solutions for Soil and Rock Mechanics, Centre for Geotechnical Research, University of Sydney, Australia, (originally published by John Wiley & Sons, Inc., 1974), 410 p.

Robertson, P.K., and Wride, C.E. (1997). "Evaluation of cyclic liquefaction potential based on the CPT," *Proc. of Seismic Behavior of Ground and Geotechnical Structures*, Seco e Pinto (ed.), Balkema, pp. 269-276.

Sadigh, K., Chang, C.Y., Egan, J., Makdisi, F., and Youngs, R. (1997). "Attenuation relationships for shallow crustal earthquakes based on California strong motion data," *Seismological Research Letters*, vol. 68, no. 1, pp. 180-189.

Schnabel, P.B., Lysmer, J., and Seed, H.B. (1972), SHAKE: A computer program for earthquake response analysis of horizontally layered sites, Earthquake Engineering Research Center, U.C. Berkeley, EERC Report No. EERC 72-12, 88 p. (This user's manual can be obtained through PEER or NISEE at U.C. Berkeley).

Seed, R.B., Cetin, K.O., Moss, R.E.S., Kammerer, A.M., Wu, J., Pestana, J.M., Riemer, M.F., Sancio, R.B., Bray, J.D., Kayen, R.E., and Faris, A. (2003), Recent Advances in Soil Liquefaction Engineering: A Unified and Consistent Framework, 26th Annual Spring Seminar of the ASCE Los Angeles Geotechnical Section, Long Beach, CA, 71 p.

Seed, R.B., and Harder, L.F., Jr. (1990). "SPT-Based Analysis of Cyclic Pore Pressure Generation and Undrained Residual Strength," Proc. of the Memorial Symposium for H. Bolton Seed, Vol. 2, Bi-Tech Publishers, pp. 351-376.

Seismological Research Letters (1997). **Special Issue on Estimation of Ground Motions**, Seismological Society of America, vol. 68, No. 1, 255 p.

Spudich, P., Joyner, W.B., Lindh, A.G., Boore, D.M., Margaris, B.M., and Fletcher, J.B. (1999). "SEA99 – A revised ground motion prediction relation for use in extensional tectonic regimes," *Bulletin of the Seismological Society of America*, vol. 89, pp. 1156-1170.

Strong Motion Databases (2004). California Geological Survey (<http://www.consrv.ca.gov/cgs/smip/>), Consortium of Organizations for Strong Motion Observation Systems: COSMOS (<http://www.cosmos-eq.org>), Multidisciplinary Center for Earthquake Engineering Research: MCEER (<http://mceer.buffalo.edu/links/agrams.asp>), Pacific Earthquake Engineering Research Center: PEER (<http://peer.berkeley.edu/smcat/>), U.S. Geological Survey (<http://eqhazmaps.usgs.gov/>).

Sunitsakul, J. (2004). "The Cyclic Behavior of Silt Soils," Dissertation submitted in partial fulfillment of the Doctor of Philosophy in Civil Engineering, Department of Civil, Construction and Environmental Engineering, Oregon State University, 236 p.

U.S. Geological Survey (2004). U.S.G.S. Seismic Hazard Mapping Program website: (<http://eqhazmaps.usgs.gov/>). Specific references are found at the following URLs:

- a. Publications Associated with the Seismic Hazard Mapping Program, (<http://eqhazmaps.usgs.gov/html/docmain.html>)
- b. Documentation for the 2002 Update of the National Seismic Hazard Maps, (<http://pubs.usgs.gov/of/2002/ofr-02-420/>)
- c. "Quaternary Faults and Fold Database of the United States," (<http://qfaults.cr.usgs.gov/>)
- d. "The 2002 Interactive Deaggregation Web Page," (http://eqint.cr.usgs.gov/eq/html/2002_Deagg_Readme.html)
- e. "What are epsilon (ϵ) and epsilon0 (ϵ_0)?" (http://eqint.cr.usgs.gov/eq/html/What_is_epsilon.html)
- f. "What Distances Are Reported in the Seismic Hazard Deaggregations?" (http://eqint.cr.usgs.gov/eq/html/distances_in_deaggs.html)

Vick, S.G. (2002). Degrees of Belief: Subjective Probability and Engineering Judgment, ASCE press, 472p.

Youngs, R.R., Chiou, S.J., Silva, W.J., and Humphrey, J.R. (1997). "Strong ground motion attenuation relationships for subduction zone earthquakes," *Seismological Research Letters*, vol. 68, no. 1, pp. 58-73.

Youd, T.L., Idriss, I.M. (chairmen) and others (2001). "Liquefaction Resistance of Soils: Summary Report from the 1996 NCEER and 1998 NCEER/NSF Workshops on Evaluation of Liquefaction Resistance of Soils", *Journal of Geotechnical and Geoenvironmental Engineering*, ASCE, vol. 127, no. 10, pp. 817-833.

Appendix A

Deaggregation of Seismic Hazard for Portland
Return Period 475 Years (10% Probability of Exceedance in 50 Years)

Summary Tables, Plot of Relative Contributions, and Map of Geographic Hazard

*** Deaggregation of Seismic Hazard for PGA & 2 Periods of Spectral Accel. ***
 *** Data from U.S.G.S. National Seismic Hazards Mapping Project, 2002 version ***
 PSHA Deaggregation. %contributions. site: Portland long: 122.680 W., lat: 45.510 N.
 USGS 2002-03 update files and programs. dM=0.2. Site descr:ROCK
 Return period: 475 yrs. Exceedance PGA =0.1913 g.

#Pr[at least one eq with median motion>=PGA in 50 yrs]=0.03381

DIST(KM)	MAG(MW)	ALL_EPS	EPSILON>2	1<EPS<2	0<EPS<1	-1<EPS<0	-2<EPS<-1	EPS<-2
5.9	5.05	1.589	0.090	0.536	0.846	0.117	0.000	0.000
13.5	5.05	1.759	0.407	1.218	0.134	0.000	0.000	0.000
23.6	5.05	0.312	0.289	0.022	0.000	0.000	0.000	0.000
6.0	5.20	2.756	0.136	0.835	1.480	0.305	0.000	0.000
13.6	5.20	3.406	0.635	2.286	0.485	0.000	0.000	0.000
23.7	5.20	0.689	0.577	0.113	0.000	0.000	0.000	0.000
33.3	5.21	0.067	0.067	0.000	0.000	0.000	0.000	0.000
6.0	5.40	2.244	0.094	0.596	1.198	0.355	0.000	0.000
13.7	5.40	3.232	0.443	1.970	0.819	0.000	0.000	0.000
23.8	5.40	0.779	0.528	0.251	0.000	0.000	0.000	0.000
33.8	5.41	0.117	0.117	0.000	0.000	0.000	0.000	0.000
6.1	5.60	1.792	0.065	0.414	0.890	0.421	0.001	0.000
13.8	5.60	3.023	0.307	1.613	1.100	0.004	0.000	0.000
23.9	5.60	0.870	0.433	0.437	0.000	0.000	0.000	0.000
34.1	5.60	0.171	0.170	0.001	0.000	0.000	0.000	0.000
6.1	5.80	1.400	0.045	0.287	0.648	0.404	0.017	0.000
13.9	5.80	2.762	0.212	1.226	1.269	0.055	0.000	0.000
24.0	5.80	0.949	0.324	0.614	0.011	0.000	0.000	0.000
34.2	5.80	0.226	0.202	0.024	0.000	0.000	0.000	0.000
6.6	6.01	1.525	0.046	0.289	0.688	0.464	0.037	0.000
13.7	6.00	2.649	0.155	0.945	1.351	0.198	0.000	0.000
23.5	6.00	1.015	0.218	0.705	0.091	0.000	0.000	0.000
33.7	6.01	0.312	0.223	0.090	0.000	0.000	0.000	0.000
44.0	6.01	0.065	0.065	0.000	0.000	0.000	0.000	0.000
7.0	6.21	1.827	0.051	0.327	0.801	0.574	0.074	0.000
12.2	6.20	10.237	0.445	2.817	5.313	1.652	0.011	0.000
23.8	6.20	1.143	0.185	0.743	0.215	0.000	0.000	0.000
33.8	6.21	0.298	0.160	0.138	0.000	0.000	0.000	0.000
43.6	6.21	0.094	0.088	0.006	0.000	0.000	0.000	0.000
6.8	6.40	2.031	0.051	0.327	0.820	0.698	0.134	0.001
14.8	6.42	1.927	0.081	0.514	0.988	0.342	0.002	0.000
23.8	6.40	1.232	0.139	0.717	0.376	0.000	0.000	0.000
34.0	6.40	0.334	0.127	0.207	0.000	0.000	0.000	0.000
44.1	6.40	0.112	0.092	0.020	0.000	0.000	0.000	0.000
3.1	6.63	4.414	0.099	0.630	1.582	1.539	0.510	0.055
13.7	6.59	1.447	0.049	0.310	0.708	0.364	0.016	0.000
23.7	6.61	1.012	0.090	0.522	0.400	0.001	0.000	0.000
35.9	6.61	0.522	0.161	0.360	0.001	0.000	0.000	0.000
44.5	6.59	0.128	0.084	0.044	0.000	0.000	0.000	0.000
2.4	6.85	2.946	0.065	0.410	1.031	1.026	0.373	0.041
15.0	6.80	0.792	0.026	0.166	0.386	0.205	0.010	0.000
24.1	6.80	0.742	0.050	0.317	0.356	0.019	0.000	0.000
35.7	6.80	0.457	0.092	0.349	0.015	0.000	0.000	0.000
44.6	6.80	0.099	0.056	0.043	0.000	0.000	0.000	0.000
128.2	6.81	0.072	0.046	0.026	0.000	0.000	0.000	0.000
162.1	6.81	0.071	0.071	0.000	0.000	0.000	0.000	0.000
3.0	7.03	1.257	0.028	0.175	0.439	0.438	0.161	0.017
16.0	6.95	0.409	0.013	0.081	0.198	0.115	0.003	0.000
25.0	6.95	0.185	0.011	0.073	0.096	0.005	0.000	0.000
35.0	6.97	0.152	0.024	0.112	0.016	0.000	0.000	0.000
44.8	6.95	0.062	0.028	0.034	0.000	0.000	0.000	0.000
113.2	7.02	0.058	0.017	0.040	0.000	0.000	0.000	0.000
136.1	7.00	0.126	0.073	0.053	0.000	0.000	0.000	0.000
170.0	7.00	0.139	0.139	0.000	0.000	0.000	0.000	0.000
1.3	7.26	0.114	0.002	0.016	0.039	0.039	0.016	0.002
117.5	7.15	0.055	0.015	0.039	0.000	0.000	0.000	0.000
140.0	7.15	0.054	0.026	0.029	0.000	0.000	0.000	0.000
156.4	7.15	0.072	0.057	0.015	0.000	0.000	0.000	0.000
89.5	8.30	7.725	0.807	5.058	1.861	0.000	0.000	0.000
93.6	8.30	1.537	0.173	1.084	0.280	0.000	0.000	0.000
101.7	8.30	0.432	0.057	0.361	0.013	0.000	0.000	0.000
115.2	8.30	4.247	0.774	3.473	0.000	0.000	0.000	0.000
136.7	8.30	1.307	0.383	0.924	0.000	0.000	0.000	0.000
144.9	8.30	0.380	0.137	0.243	0.000	0.000	0.000	0.000
164.2	8.30	1.172	0.707	0.465	0.000	0.000	0.000	0.000

191.6	8.30	0.164	0.164	0.000	0.000	0.000	0.000	0.000
213.6	8.30	0.174	0.174	0.000	0.000	0.000	0.000	0.000
89.5	9.00	8.441	0.516	3.207	4.718	0.000	0.000	0.000
110.4	9.00	2.642	0.206	1.283	1.154	0.000	0.000	0.000
136.4	9.00	1.864	0.205	1.283	0.377	0.000	0.000	0.000
162.9	9.00	0.629	0.102	0.527	0.000	0.000	0.000	0.000

Summary statistics for above PSHA PGA deaggregation, R=distance, e=epsilon:
 Mean src-site R= 43.4 km; M= 6.81; eps0= 0.22. Mean calculated for all sources.
 Modal src-site R= 12.2 km; M= 6.20; eps0= -0.17 from peak (R,M) bin
 Gridded source distance metrics: Rseis Rrup and Rjb
 MODE R*= 12.2km; M*= 6.20; EPS.INTERVAL: 0 to 1 sigma % CONTRIB.= 5.313

Principal sources (faults, subduction, random seismicity having >10% contribution)
 Source Category: % contr. R(km) M epsilon0 (mean values)
 WUS shallow gridded 51.78 14.4 5.85 0.28
 Wash-Oreg faults 16.06 8.6 6.48 -1.25
 M 9.0 Subduction 13.58 103.4 9.00 0.50
 M 8.3 Subduction 17.19 109.2 8.30 1.07
 Individual fault hazard details if contrib.>1%:
 Bolton f 0.98 11.8 6.20 -0.59
 Grant Butte f 6.56 11.4 6.20 -0.14
 Portland Hills f 2.07 1.3 6.95 -3.10
 Portland Hills f 4.73 2.1 6.70 -2.69
 ***** Pacific Northwest region *****

Prob. Seismic Hazard Deaggregation

Portland 122.680° W, 45.510 N.

Peak Horiz. Ground Accel. ≥ 0.1913 g

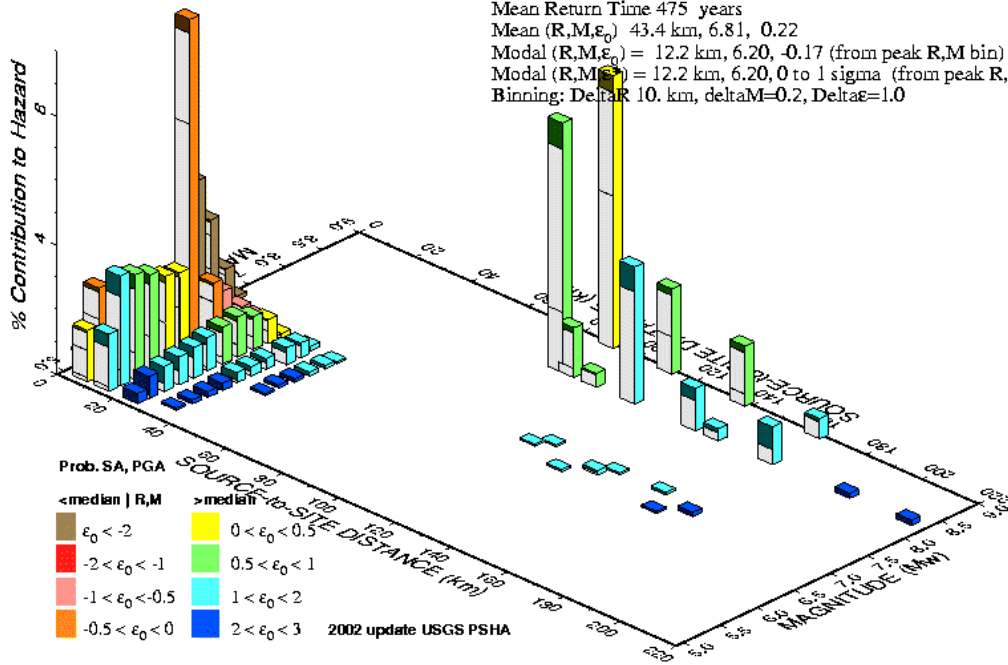
Mean Return Time 475 years

Mean (R,M, ϵ_0) 43.4 km, 6.81, 0.22

Modal (R,M, ϵ_0) = 12.2 km, 6.20, -0.17 (from peak R,M bin)

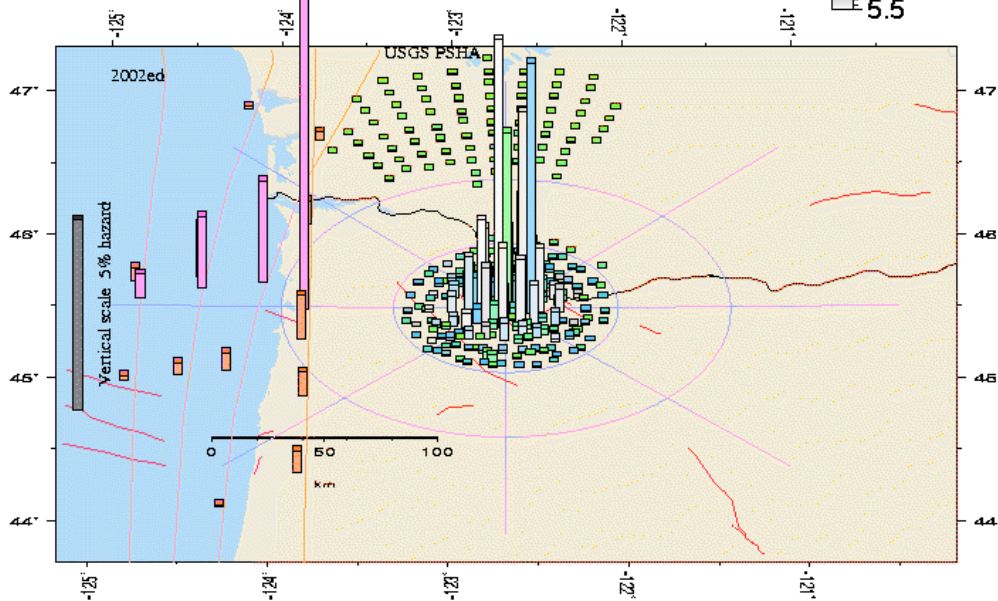
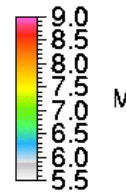
Modal (R,M, ϵ_0) = 12.2 km, 6.20, 0 to 1 sigma (from peak R,M, ϵ bin)

Binning: Delta R 10. km, delta M = 0.2, Delta ϵ = 1.0



GMT Aug 23 12:07 Distance (R), magnitude (M), epsilon (ϵ_0) deagg region for a site on ROCK avg $V_s=760$ m/s top 30 m USGS CGHT PSHA2002v3 UPDATE. Bins with lt 0.05% contrib. omitted

Portland Geographic Deagg. Seismic Hazard
for 0.00-s Spectral Accel, 0.1913 g
PGA Exceedance Return Time: 475. years
Max. significant source distance 199. km.
Red lines represent Quaternary fault locations
Gridded-source hazard accum. in 5° intervals
Rock site. Average $V_s=760$ m/s top 30 m



GMT 2004 Aug 23 12:07:02 Site Coords: 122.680 45.510 (yellow dot). Max annual ExceedRate: .1784E-03 (oo lunn height prop. to ExRate). Red diamonds: historical earthquakes, Mw6

Appendix B

Deaggregation of Seismic Hazard for Portland
Return Period 975 Years (5% Probability of Exceedance in 50 Years)

Summary Tables, Plot of Relative Contributions, and Map of Geographic Hazard

*** Deaggregation of Seismic Hazard for PGA & 2 Periods of Spectral Accel. ***
 *** Data from U.S.G.S. National Seismic Hazards Mapping Project, 2002 version ***
 PSHA Deaggregation. %contributions. site: Portland long: 122.680 W., lat: 45.510 N.
 USGS 2002-03 update files and programs. dM=0.2. Site descr:ROCK
 Return period: 975 yrs. Exceedance PGA =0.2735 g.

#Pr[at least one eq with median motion>=PGA in 50 yrs]=0.01518

DIST(KM)	MAG(MW)	ALL_EPS	EPSILON>2	1<EPS<2	0<EPS<1	-1<EPS<0	-2<EPS<-1	EPS<-2
5.9	5.05	1.758	0.183	0.912	0.663	0.000	0.000	0.000
13.2	5.05	1.234	0.600	0.634	0.000	0.000	0.000	0.000
22.8	5.05	0.092	0.092	0.000	0.000	0.000	0.000	0.000
5.9	5.20	3.174	0.281	1.463	1.430	0.000	0.000	0.000
13.2	5.20	2.493	1.027	1.466	0.000	0.000	0.000	0.000
23.1	5.20	0.233	0.233	0.000	0.000	0.000	0.000	0.000
5.9	5.40	2.739	0.194	1.058	1.443	0.043	0.000	0.000
13.3	5.40	2.517	0.788	1.661	0.068	0.000	0.000	0.000
23.3	5.40	0.309	0.305	0.004	0.000	0.000	0.000	0.000
6.0	5.60	2.326	0.135	0.775	1.235	0.182	0.000	0.000
13.4	5.60	2.524	0.588	1.679	0.258	0.000	0.000	0.000
23.5	5.60	0.396	0.358	0.038	0.000	0.000	0.000	0.000
6.0	5.80	1.935	0.093	0.563	1.008	0.271	0.000	0.000
13.6	5.80	2.485	0.428	1.536	0.522	0.000	0.000	0.000
23.7	5.80	0.485	0.359	0.126	0.000	0.000	0.000	0.000
6.5	6.01	2.182	0.094	0.589	1.123	0.375	0.000	0.000
13.3	6.00	2.567	0.316	1.369	0.882	0.000	0.000	0.000
23.1	6.01	0.583	0.321	0.262	0.000	0.000	0.000	0.000
33.2	6.01	0.091	0.091	0.000	0.000	0.000	0.000	0.000
6.9	6.21	2.718	0.106	0.674	1.340	0.584	0.014	0.000
12.1	6.20	11.289	0.920	5.098	5.083	0.188	0.000	0.000
23.3	6.19	0.688	0.303	0.385	0.000	0.000	0.000	0.000
33.4	6.21	0.103	0.099	0.003	0.000	0.000	0.000	0.000
6.7	6.40	3.266	0.106	0.673	1.539	0.898	0.051	0.000
14.4	6.42	2.127	0.167	0.901	0.995	0.064	0.000	0.000
23.4	6.40	0.816	0.270	0.522	0.023	0.000	0.000	0.000
33.6	6.40	0.130	0.115	0.015	0.000	0.000	0.000	0.000
2.9	6.64	8.331	0.204	1.293	3.207	2.824	0.741	0.062
13.4	6.59	1.804	0.102	0.621	0.923	0.158	0.000	0.000
23.4	6.61	0.690	0.184	0.470	0.036	0.000	0.000	0.000
35.6	6.61	0.191	0.173	0.018	0.000	0.000	0.000	0.000
2.8	6.82	3.985	0.095	0.602	1.509	1.415	0.331	0.032
14.6	6.80	0.952	0.053	0.332	0.487	0.080	0.000	0.000
23.6	6.81	0.539	0.103	0.371	0.064	0.000	0.000	0.000
35.4	6.80	0.203	0.152	0.051	0.000	0.000	0.000	0.000
2.3	6.98	4.200	0.095	0.604	1.517	1.472	0.457	0.055
15.8	6.95	0.495	0.026	0.166	0.275	0.028	0.000	0.000
24.6	6.95	0.137	0.024	0.096	0.018	0.000	0.000	0.000
34.6	6.97	0.068	0.043	0.025	0.000	0.000	0.000	0.000
136.7	7.00	0.071	0.071	0.000	0.000	0.000	0.000	0.000
1.3	7.26	0.232	0.005	0.032	0.081	0.081	0.029	0.004
89.5	8.30	6.557	1.650	4.907	0.000	0.000	0.000	0.000
93.6	8.30	1.274	0.353	0.920	0.000	0.000	0.000	0.000
112.8	8.30	3.300	1.622	1.678	0.000	0.000	0.000	0.000
136.4	8.30	0.703	0.681	0.023	0.000	0.000	0.000	0.000
142.2	8.30	0.396	0.396	0.000	0.000	0.000	0.000	0.000
162.5	8.30	0.542	0.542	0.000	0.000	0.000	0.000	0.000
188.1	8.30	0.086	0.086	0.000	0.000	0.000	0.000	0.000
89.5	9.00	8.738	1.052	6.607	1.079	0.000	0.000	0.000
110.4	9.00	2.490	0.419	2.070	0.000	0.000	0.000	0.000
136.4	9.00	1.556	0.418	1.138	0.000	0.000	0.000	0.000
162.9	9.00	0.463	0.209	0.254	0.000	0.000	0.000	0.000

Summary statistics for above PSHA PGA deaggregation, R=distance, e=epsilon:
 Mean src-site R= 34.8 km; M= 6.78; eps0= 0.36. Mean calculated for all sources.
 Modal src-site R= 12.1 km; M= 6.20; eps0= 0.42 from peak (R,M) bin
 Gridded source distance metrics: Rseis Rrup and Rjb
 MODE R*= 89.5km; M*= 9.00; EPS.INTERVAL: 1 to 2 sigma % CONTRIB.= 6.607

Principal sources (faults, subduction, random seismicity having >10% contribution)

Source Category:	% contr.	R(km)	M	epsilon0 (mean values)
WUS shallow gridded	49.97	11.4	5.91	0.48
Wash-Oreg faults	23.18	6.4	6.55	-1.02
M 9.0 Subduction	13.25	101.5	9.00	1.04
M 8.3 Subduction	12.89	104.1	8.30	1.55

Individual fault hazard details if contrib.>1%:				
Bolton f	1.29	11.6	6.20	-0.01
Grant Butte f	7.13	11.4	6.20	0.47
Helvetia f	0.95	14.1	6.37	0.27
Portland Hills f	4.14	1.3	6.95	-2.33
Portland Hills f	9.21	2.1	6.71	-2.00

Prob. Seismic Hazard Deaggregation

Portland 122.680° W, 45.510 N.

Peak Horiz. Ground Accel. ≥ 0.2735 g

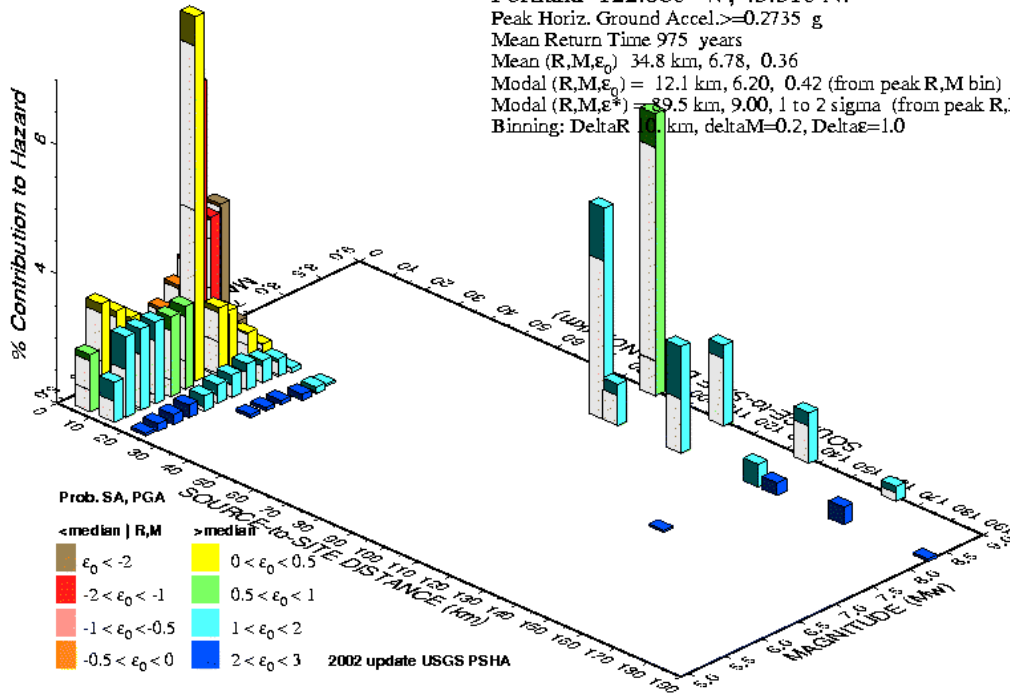
Mean Return Time 975 years

Mean (R,M, ϵ_0) 34.8 km, 6.78, 0.36

Modal (R,M, ϵ_0) = 12.1 km, 6.20, 0.42 (from peak R,M bin)

Modal (R,M, ϵ^*) = 89.5 km, 9.00, 1 to 2 sigma (from peak R,M, ϵ bin)

Binning: DeltaR = 1 km, deltaM=0.2, Delta ϵ =1.0



GMT Aug 23 12:04 Distance (R), magnitude (M), epsilon (E0,E) deaggregation for a site on ROCK avg V_s=760 m/s top 30 m USGS CGHT PSHA2002v3 UPDATE. Bins with lt 0.05% contrib. omitted

Portland Geographic Deagg. Seismic Hazard

for 0.00-s Spectral Accel, 0.2734 g

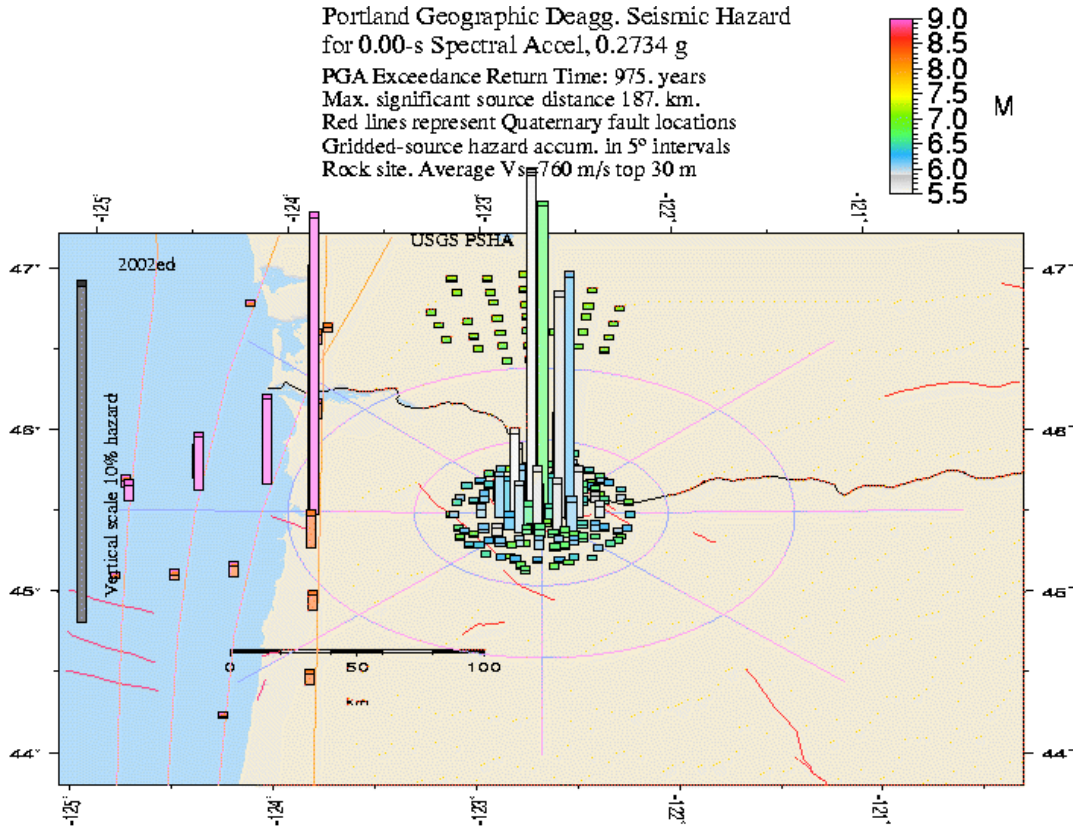
PGA Exceedance Return Time: 975. years

Max. significant source distance 187. km.

Red lines represent Quaternary fault locations

Gridded-source hazard accum. in 5° intervals

Rock site. Average V_s=760 m/s top 30 m



GMT 2004 Aug 23 12:04:40 Site Coords: -122.680 45.510 (yellow d.M). Max annual ExcdRate: .1044E-03 (column height prop. to ExRate). Red diamonds: historical earthquakes, M=6

Appendix C

Deaggregation of Seismic Hazard for Medford
Return Period 475 Years (10% Probability of Exceedance in 50 Years)

Summary Tables, Plot of Relative Contributions, and Map of Geographic Hazard

*** Deaggregation of Seismic Hazard for PGA & 2 Periods of Spectral Accel. ***
 *** Data from U.S.G.S. National Seismic Hazards Mapping Project, 2002 version ***
 PSHA Deaggregation. %contributions. site: Medford long: 122.860 W., lat: 42.330 N.
 USGS 2002-03 update files and programs. dM=0.2. Site descr:ROCK
 Return period: 475 yrs. Exceedance PGA =0.11014 g.

#Pr[at least one eq with median motion>=PGA in 50 yrs]=0.05382

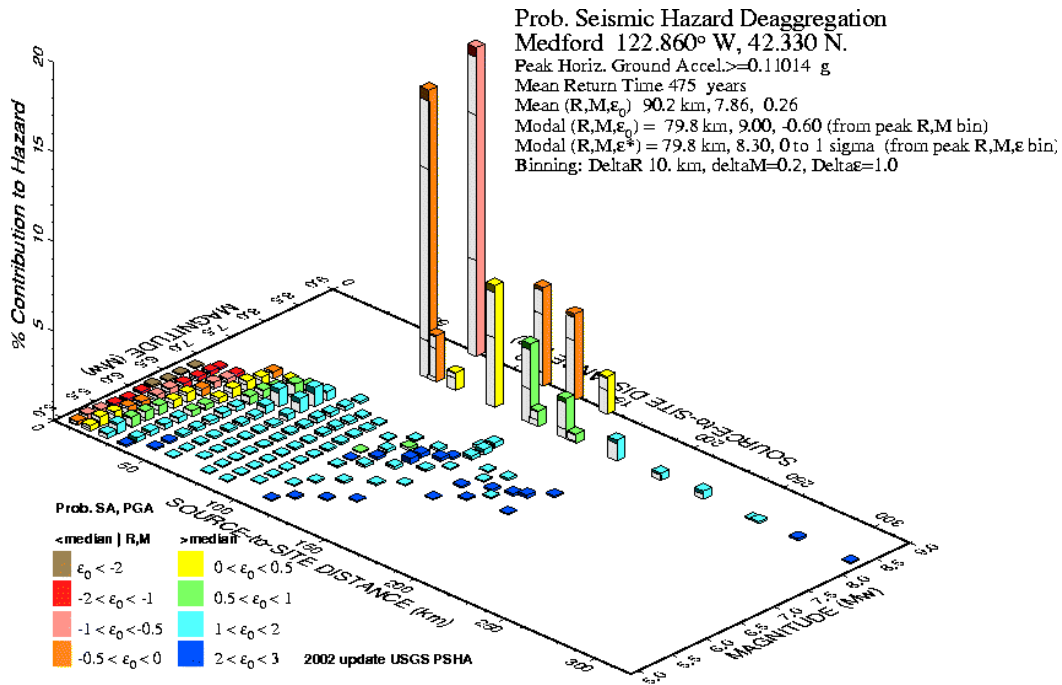
DIST(KM)	MAG(MW)	ALL_EPS	EPSILON>2	1<EPS<2	0<EPS<1	-1<EPS<0	-2<EPS<-1	EPS<-2
7.5	5.05	0.214	0.007	0.045	0.109	0.052	0.000	0.000
14.5	5.05	0.285	0.021	0.131	0.129	0.003	0.000	0.000
24.0	5.05	0.286	0.081	0.203	0.002	0.000	0.000	0.000
34.6	5.05	0.106	0.094	0.012	0.000	0.000	0.000	0.000
7.5	5.20	0.354	0.011	0.069	0.171	0.103	0.000	0.000
14.6	5.20	0.516	0.033	0.206	0.262	0.015	0.000	0.000
24.1	5.20	0.571	0.123	0.423	0.025	0.000	0.000	0.000
34.7	5.20	0.232	0.174	0.057	0.000	0.000	0.000	0.000
44.9	5.20	0.095	0.095	0.000	0.000	0.000	0.000	0.000
54.9	5.20	0.054	0.033	0.020	0.001	0.000	0.000	0.000
74.7	5.20	0.050	0.019	0.031	0.000	0.000	0.000	0.000
85.0	5.20	0.055	0.034	0.022	0.000	0.000	0.000	0.000
109.3	5.21	0.060	0.060	0.000	0.000	0.000	0.000	0.000
7.5	5.40	0.270	0.008	0.048	0.120	0.090	0.004	0.000
14.7	5.40	0.443	0.023	0.144	0.249	0.027	0.000	0.000
24.2	5.40	0.563	0.085	0.397	0.082	0.000	0.000	0.000
34.8	5.40	0.258	0.136	0.122	0.000	0.000	0.000	0.000
45.1	5.40	0.121	0.117	0.004	0.000	0.000	0.000	0.000
54.9	5.40	0.070	0.050	0.015	0.005	0.000	0.000	0.000
64.7	5.40	0.058	0.028	0.029	0.000	0.000	0.000	0.000
74.7	5.40	0.056	0.020	0.036	0.000	0.000	0.000	0.000
85.0	5.40	0.058	0.024	0.034	0.000	0.000	0.000	0.000
95.4	5.40	0.051	0.034	0.016	0.000	0.000	0.000	0.000
115.2	5.40	0.080	0.080	0.000	0.000	0.000	0.000	0.000
7.6	5.60	0.202	0.005	0.033	0.083	0.071	0.009	0.000
14.8	5.60	0.372	0.016	0.100	0.209	0.049	0.000	0.000
24.4	5.60	0.546	0.059	0.333	0.154	0.000	0.000	0.000
34.9	5.60	0.282	0.095	0.187	0.000	0.000	0.000	0.000
45.2	5.60	0.148	0.118	0.030	0.000	0.000	0.000	0.000
54.8	5.60	0.087	0.069	0.010	0.007	0.000	0.000	0.000
64.5	5.60	0.072	0.044	0.025	0.004	0.000	0.000	0.000
74.6	5.60	0.064	0.027	0.037	0.000	0.000	0.000	0.000
85.0	5.60	0.064	0.024	0.041	0.000	0.000	0.000	0.000
95.3	5.60	0.055	0.026	0.029	0.000	0.000	0.000	0.000
106.6	5.61	0.056	0.041	0.015	0.000	0.000	0.000	0.000
125.1	5.60	0.074	0.074	0.000	0.000	0.000	0.000	0.000
7.6	5.80	0.148	0.004	0.023	0.058	0.053	0.011	0.000
14.9	5.80	0.304	0.011	0.069	0.159	0.064	0.001	0.000
24.5	5.80	0.516	0.041	0.254	0.219	0.002	0.000	0.000
35.0	5.80	0.301	0.066	0.226	0.010	0.000	0.000	0.000
45.3	5.80	0.175	0.095	0.079	0.000	0.000	0.000	0.000
54.8	5.80	0.105	0.079	0.018	0.008	0.000	0.000	0.000
64.4	5.80	0.088	0.062	0.017	0.008	0.000	0.000	0.000
74.6	5.80	0.076	0.040	0.034	0.002	0.000	0.000	0.000
85.0	5.80	0.072	0.028	0.044	0.000	0.000	0.000	0.000
95.3	5.80	0.062	0.025	0.037	0.000	0.000	0.000	0.000
111.2	5.80	0.098	0.059	0.039	0.000	0.000	0.000	0.000
134.4	5.80	0.060	0.060	0.000	0.000	0.000	0.000	0.000
6.9	6.01	0.138	0.003	0.020	0.051	0.049	0.014	0.000
15.4	6.01	0.314	0.010	0.063	0.154	0.083	0.004	0.000
24.8	6.00	0.475	0.029	0.186	0.247	0.012	0.000	0.000
35.0	6.00	0.335	0.050	0.246	0.039	0.000	0.000	0.000
45.2	6.00	0.198	0.073	0.125	0.000	0.000	0.000	0.000
55.0	6.01	0.137	0.079	0.050	0.009	0.000	0.000	0.000
64.8	6.00	0.105	0.073	0.019	0.013	0.000	0.000	0.000
74.8	6.00	0.089	0.052	0.027	0.009	0.000	0.000	0.000
85.0	6.00	0.077	0.035	0.042	0.001	0.000	0.000	0.000
95.0	6.01	0.079	0.031	0.048	0.000	0.000	0.000	0.000
119.4	6.00	0.116	0.065	0.051	0.000	0.000	0.000	0.000
5.9	6.19	0.117	0.003	0.016	0.041	0.041	0.015	0.001
15.4	6.20	0.360	0.010	0.064	0.162	0.115	0.009	0.000
25.0	6.20	0.525	0.025	0.161	0.304	0.034	0.000	0.000
35.0	6.20	0.299	0.031	0.187	0.082	0.000	0.000	0.000
44.6	6.20	0.268	0.062	0.198	0.008	0.000	0.000	0.000
55.1	6.20	0.160	0.069	0.082	0.009	0.000	0.000	0.000

64.8	6.20	0.127	0.070	0.043	0.014	0.000	0.000	0.000
74.9	6.21	0.105	0.062	0.026	0.017	0.000	0.000	0.000
85.0	6.20	0.103	0.052	0.042	0.010	0.000	0.000	0.000
95.1	6.20	0.079	0.037	0.041	0.001	0.000	0.000	0.000
107.8	6.21	0.097	0.029	0.068	0.000	0.000	0.000	0.000
130.0	6.20	0.103	0.056	0.047	0.000	0.000	0.000	0.000
7.1	6.40	0.081	0.002	0.011	0.028	0.028	0.011	0.001
15.7	6.39	0.309	0.008	0.052	0.130	0.105	0.014	0.000
25.7	6.40	0.438	0.018	0.115	0.244	0.061	0.000	0.000
35.0	6.41	0.329	0.025	0.157	0.147	0.001	0.000	0.000
44.6	6.40	0.256	0.040	0.185	0.031	0.000	0.000	0.000
54.9	6.40	0.197	0.059	0.127	0.010	0.000	0.000	0.000
65.2	6.40	0.151	0.062	0.074	0.015	0.000	0.000	0.000
74.6	6.40	0.125	0.063	0.042	0.020	0.000	0.000	0.000
84.9	6.40	0.106	0.055	0.032	0.019	0.000	0.000	0.000
95.2	6.40	0.102	0.049	0.044	0.009	0.000	0.000	0.000
107.4	6.42	0.050	0.041	0.009	0.000	0.000	0.000	0.000
115.5	6.41	0.152	0.053	0.099	0.000	0.000	0.000	0.000
138.1	6.40	0.058	0.026	0.031	0.000	0.000	0.000	0.000
154.9	6.37	0.050	0.044	0.006	0.000	0.000	0.000	0.000
6.7	6.59	0.074	0.002	0.010	0.025	0.026	0.010	0.001
15.3	6.61	0.243	0.006	0.038	0.095	0.086	0.019	0.000
24.3	6.60	0.363	0.012	0.075	0.183	0.091	0.002	0.000
35.3	6.60	0.521	0.040	0.246	0.234	0.002	0.000	0.000
44.4	6.61	0.465	0.068	0.322	0.075	0.000	0.000	0.000
54.2	6.58	0.447	0.152	0.280	0.012	0.002	0.000	0.000
64.9	6.61	0.347	0.150	0.176	0.020	0.000	0.000	0.000
74.9	6.60	0.192	0.108	0.063	0.022	0.000	0.000	0.000
84.8	6.61	0.170	0.096	0.048	0.026	0.000	0.000	0.000
95.0	6.60	0.124	0.076	0.032	0.016	0.000	0.000	0.000
105.7	6.61	0.065	0.012	0.045	0.009	0.000	0.000	0.000
114.4	6.62	0.136	0.136	0.000	0.000	0.000	0.000	0.000
125.3	6.59	0.168	0.075	0.093	0.000	0.000	0.000	0.000
165.0	6.59	0.095	0.077	0.018	0.000	0.000	0.000	0.000
185.4	6.66	0.063	0.063	0.000	0.000	0.000	0.000	0.000
6.7	6.80	0.071	0.002	0.010	0.024	0.024	0.010	0.001
15.4	6.80	0.233	0.005	0.035	0.087	0.084	0.022	0.001
24.9	6.79	0.262	0.008	0.049	0.123	0.078	0.004	0.000
35.2	6.81	0.557	0.032	0.205	0.303	0.017	0.000	0.000
44.5	6.80	0.478	0.054	0.293	0.132	0.000	0.000	0.000
53.9	6.79	0.972	0.249	0.700	0.020	0.004	0.000	0.000
63.8	6.83	0.814	0.294	0.497	0.021	0.003	0.000	0.000
74.9	6.79	0.280	0.126	0.127	0.026	0.000	0.000	0.000
84.6	6.80	0.193	0.093	0.071	0.030	0.000	0.000	0.000
94.7	6.81	0.129	0.065	0.044	0.020	0.000	0.000	0.000
112.8	6.80	0.171	0.060	0.083	0.028	0.000	0.000	0.000
126.4	6.79	0.306	0.306	0.000	0.000	0.000	0.000	0.000
135.5	6.77	0.131	0.055	0.075	0.000	0.000	0.000	0.000
155.9	6.76	0.107	0.099	0.008	0.000	0.000	0.000	0.000
170.8	6.80	0.079	0.051	0.028	0.000	0.000	0.000	0.000
14.4	6.95	0.098	0.002	0.014	0.035	0.035	0.011	0.001
23.9	6.95	0.166	0.004	0.028	0.070	0.058	0.007	0.000
36.2	6.99	0.496	0.026	0.166	0.283	0.021	0.000	0.000
44.9	6.99	0.341	0.030	0.181	0.130	0.000	0.000	0.000
53.7	7.03	0.837	0.124	0.596	0.111	0.006	0.000	0.000
63.9	7.03	1.059	0.364	0.661	0.026	0.009	0.000	0.000
74.8	6.98	0.220	0.085	0.110	0.023	0.002	0.000	0.000
84.9	6.98	0.158	0.054	0.068	0.037	0.000	0.000	0.000
94.7	6.99	0.125	0.037	0.051	0.037	0.000	0.000	0.000
106.0	7.01	0.065	0.029	0.023	0.013	0.000	0.000	0.000
117.8	6.99	0.170	0.033	0.099	0.038	0.000	0.000	0.000
125.8	6.96	0.216	0.212	0.004	0.000	0.000	0.000	0.000
133.6	7.04	0.189	0.168	0.021	0.000	0.000	0.000	0.000
141.5	6.97	0.059	0.025	0.034	0.000	0.000	0.000	0.000
158.4	7.01	0.058	0.020	0.038	0.000	0.000	0.000	0.000
167.0	6.92	0.120	0.120	0.000	0.000	0.000	0.000	0.000
175.4	7.00	0.121	0.121	0.000	0.000	0.000	0.000	0.000
181.0	7.06	0.188	0.169	0.019	0.000	0.000	0.000	0.000
35.1	7.20	0.366	0.015	0.097	0.209	0.044	0.000	0.000
44.5	7.20	0.331	0.023	0.144	0.163	0.001	0.000	0.000
54.2	7.22	0.400	0.047	0.254	0.095	0.003	0.000	0.000
64.1	7.22	0.516	0.101	0.370	0.041	0.005	0.000	0.000

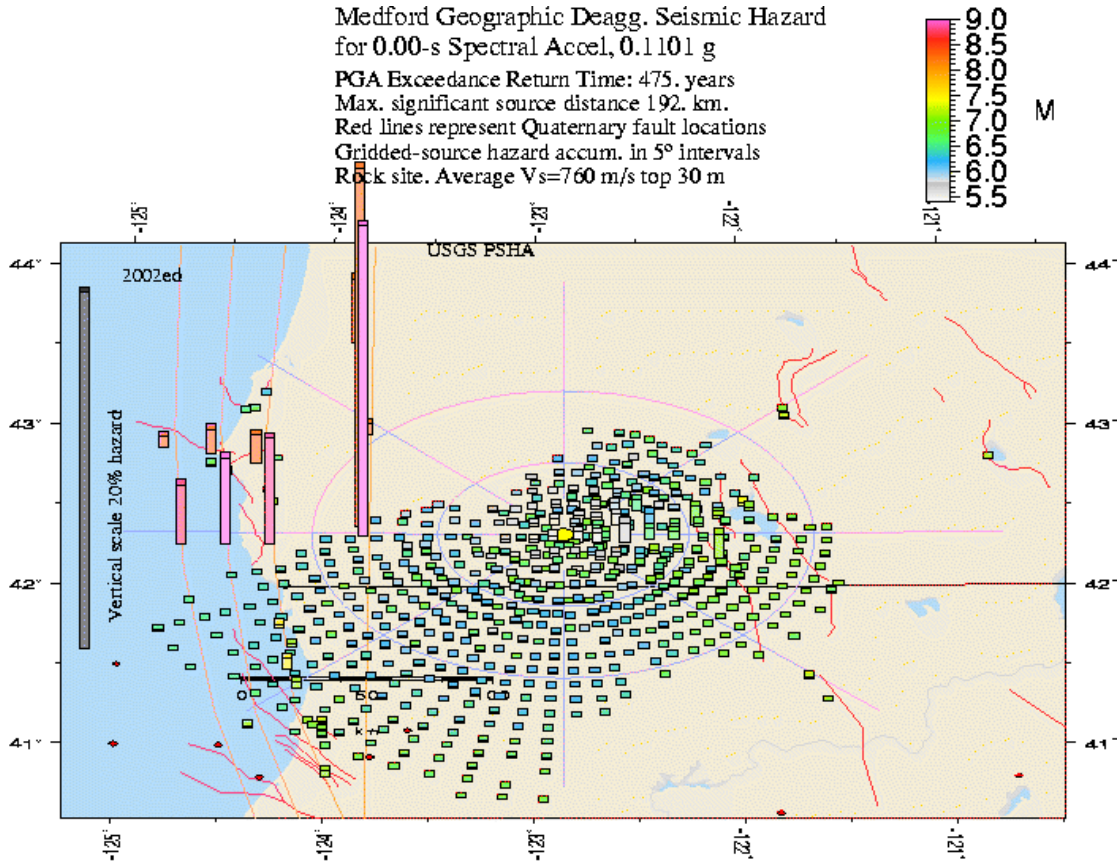
75.2	7.19	0.217	0.076	0.123	0.015	0.004	0.000	0.000
85.1	7.18	0.081	0.026	0.037	0.017	0.001	0.000	0.000
94.2	7.18	0.066	0.021	0.027	0.017	0.000	0.000	0.000
114.3	7.19	0.074	0.044	0.027	0.003	0.000	0.000	0.000
127.0	7.19	0.137	0.049	0.070	0.017	0.000	0.000	0.000
136.0	7.16	0.119	0.100	0.019	0.000	0.000	0.000	0.000
141.6	7.28	0.225	0.132	0.093	0.000	0.000	0.000	0.000
153.9	7.20	0.065	0.049	0.016	0.000	0.000	0.000	0.000
164.6	7.21	0.113	0.077	0.037	0.000	0.000	0.000	0.000
188.3	7.27	0.081	0.081	0.000	0.000	0.000	0.000	0.000
75.3	7.41	0.112	0.030	0.078	0.004	0.000	0.000	0.000
142.1	7.46	0.301	0.187	0.114	0.000	0.000	0.000	0.000
138.6	7.52	0.163	0.044	0.119	0.000	0.000	0.000	0.000
140.6	7.65	0.251	0.092	0.159	0.000	0.000	0.000	0.000
79.8	8.30	16.117	0.623	3.823	9.600	2.072	0.000	0.000
83.8	8.30	2.579	0.104	0.637	1.600	0.238	0.000	0.000
94.6	8.30	0.975	0.044	0.273	0.656	0.002	0.000	0.000
116.2	8.30	6.802	0.405	2.512	3.886	0.000	0.000	0.000
136.0	8.30	4.428	0.350	2.184	1.894	0.000	0.000	0.000
140.3	8.30	0.866	0.073	0.455	0.339	0.000	0.000	0.000
155.5	8.30	2.235	0.238	1.492	0.504	0.000	0.000	0.000
161.2	8.30	0.493	0.058	0.364	0.071	0.000	0.000	0.000
183.9	8.30	1.170	0.205	0.965	0.000	0.000	0.000	0.000
208.3	8.30	0.400	0.109	0.290	0.000	0.000	0.000	0.000
231.8	8.30	0.449	0.198	0.251	0.000	0.000	0.000	0.000
259.5	8.30	0.055	0.043	0.012	0.000	0.000	0.000	0.000
260.7	8.30	0.108	0.086	0.021	0.000	0.000	0.000	0.000
284.4	8.30	0.115	0.115	0.000	0.000	0.000	0.000	0.000
313.6	8.30	0.075	0.075	0.000	0.000	0.000	0.000	0.000
79.8	9.00	17.254	0.533	3.231	8.117	5.374	0.000	0.000
116.9	9.00	5.487	0.211	1.293	3.246	0.737	0.000	0.000
134.5	9.00	4.797	0.210	1.293	3.246	0.047	0.000	0.000
152.5	9.00	2.085	0.105	0.646	1.334	0.000	0.000	0.000

Summary statistics for above PSHA PGA deaggregation, R=distance, e=epsilon:
 Mean src-site R= 90.2 km; M= 7.86; eps0= 0.26. Mean calculated for all sources.
 Modal src-site R= 79.8 km; M= 9.00; eps0= -0.60 from peak (R,M) bin
 Gridded source distance metrics: Rseis Rrup and Rjb
 MODE R*= 79.8km; M*= 8.30; EPS.INTERVAL: 0 to 1 sigma % CONTRIB.= 9.600
 Modal source dmetric: distance to rupture surface (Youngs et al.,SRL,1997)

Principal sources (faults, subduction, random seismicity having >10% contribution)
 Source Category: % contr. R(km) M epsilon0 (mean values)
 WUS shallow gridded 13.97 30.0 5.93 0.42
 M 9.0 Subduction 29.62 100.7 9.00 -0.38
 M 8.3 Subduction 36.90 109.7 8.30 0.21
 Individual fault hazard details if contrib.>1%:
 Sky Lakes FZ 1.01 53.5 6.80 1.26
 2 Cedar Mtn-Mahogany Mtn 1.38 63.6 7.04 1.34
 ***** Southern Oregon site *****



GMT Aug 23 12:17 Distance (R), magnitude (M), epsilon (ϵ_0) deaggregation for site on ROCK avg $V_s=760$ m/s top 30 m USGS CGHT PSHA2002v3 UPDATE. Bins with $\leq 0.05\%$ contrib. omitted



GMT 2004 Aug 23 12:17:55 Site Coords: -122.860 42.3300 (yellow d blk). Max annual ExcdRate: A197E-03 (as linn height prop. to ExRate). Red diamonds: historical earthquakes, Mb6

Appendix D

Deaggregation of Seismic Hazard for Medford
Return Period 975 Years (5% Probability of Exceedance in 50 Years)

Summary Tables, Plot of Relative Contributions, and Map of Geographic Hazard

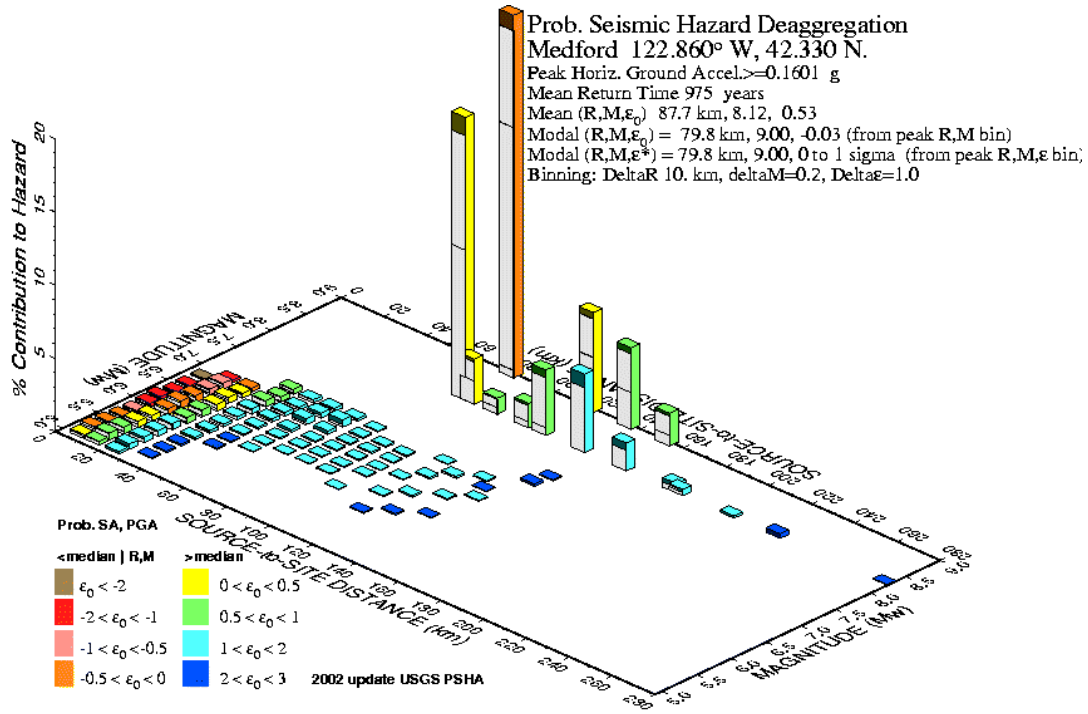
*** Deaggregation of Seismic Hazard for PGA & 2 Periods of Spectral Accel. ***
 *** Data from U.S.G.S. National Seismic Hazards Mapping Project, 2002 version ***
 PSHA Deaggregation. %contributions. site: Medford long: 122.860 W., lat: 42.330 N.
 USGS 2002-03 update files and programs. dM=0.2. Site descr:ROCK
 Return period: 975 yrs. Exceedance PGA =0.1601 g.

#Pr[at least one eq with median motion>=PGA in 50 yrs]=0.01509									
DIST(KM)	MAG(MW)	ALL_EPS	EPSILON>2	1<EPS<2	0<EPS<1	-1<EPS<0	-2<EPS<-1	EPS<-2	
7.4	5.05	0.280	0.015	0.093	0.160	0.013	0.000	0.000	
14.1	5.05	0.259	0.044	0.174	0.041	0.000	0.000	0.000	
23.5	5.05	0.164	0.114	0.050	0.000	0.000	0.000	0.000	
7.5	5.20	0.486	0.022	0.142	0.271	0.052	0.000	0.000	
14.2	5.20	0.494	0.067	0.312	0.115	0.000	0.000	0.000	
23.6	5.20	0.348	0.205	0.143	0.000	0.000	0.000	0.000	
34.0	5.20	0.076	0.076	0.000	0.000	0.000	0.000	0.000	
7.5	5.40	0.395	0.015	0.098	0.213	0.069	0.000	0.000	
14.3	5.40	0.458	0.046	0.249	0.162	0.001	0.000	0.000	
23.8	5.40	0.374	0.163	0.211	0.000	0.000	0.000	0.000	
34.3	5.40	0.102	0.101	0.001	0.000	0.000	0.000	0.000	
7.5	5.60	0.315	0.011	0.068	0.158	0.079	0.000	0.000	
14.4	5.60	0.416	0.032	0.188	0.188	0.009	0.000	0.000	
23.9	5.60	0.397	0.120	0.267	0.010	0.000	0.000	0.000	
34.5	5.60	0.130	0.114	0.016	0.000	0.000	0.000	0.000	
7.5	5.80	0.245	0.007	0.047	0.113	0.074	0.003	0.000	
14.5	5.80	0.369	0.022	0.137	0.191	0.020	0.000	0.000	
24.1	5.80	0.412	0.083	0.282	0.047	0.000	0.000	0.000	
34.6	5.80	0.157	0.107	0.050	0.000	0.000	0.000	0.000	
44.8	5.80	0.060	0.059	0.000	0.000	0.000	0.000	0.000	
113.2	5.80	0.073	0.073	0.000	0.000	0.000	0.000	0.000	
6.9	6.01	0.244	0.006	0.041	0.103	0.081	0.012	0.000	
15.0	6.01	0.408	0.020	0.128	0.217	0.042	0.000	0.000	
24.4	6.00	0.410	0.060	0.268	0.081	0.000	0.000	0.000	
34.8	6.01	0.193	0.096	0.097	0.000	0.000	0.000	0.000	
44.9	6.00	0.079	0.073	0.007	0.000	0.000	0.000	0.000	
55.0	6.01	0.051	0.035	0.011	0.006	0.000	0.000	0.000	
95.1	6.01	0.052	0.026	0.026	0.000	0.000	0.000	0.000	
121.7	6.00	0.074	0.074	0.000	0.000	0.000	0.000	0.000	
5.9	6.20	0.221	0.005	0.033	0.084	0.079	0.019	0.000	
15.1	6.20	0.503	0.021	0.132	0.271	0.080	0.000	0.000	
24.7	6.20	0.493	0.052	0.290	0.151	0.000	0.000	0.000	
34.8	6.20	0.190	0.063	0.126	0.001	0.000	0.000	0.000	
44.3	6.20	0.124	0.091	0.033	0.000	0.000	0.000	0.000	
54.9	6.20	0.066	0.049	0.010	0.008	0.000	0.000	0.000	
64.8	6.20	0.056	0.028	0.022	0.006	0.000	0.000	0.000	
74.8	6.21	0.057	0.017	0.039	0.001	0.000	0.000	0.000	
85.2	6.20	0.059	0.016	0.043	0.000	0.000	0.000	0.000	
109.4	6.20	0.086	0.055	0.031	0.000	0.000	0.000	0.000	
132.0	6.20	0.059	0.059	0.000	0.000	0.000	0.000	0.000	
7.1	6.40	0.154	0.004	0.023	0.058	0.055	0.014	0.000	
15.5	6.39	0.458	0.017	0.106	0.234	0.100	0.002	0.000	
25.2	6.40	0.447	0.037	0.219	0.184	0.007	0.000	0.000	
34.6	6.41	0.234	0.051	0.167	0.016	0.000	0.000	0.000	
44.4	6.40	0.132	0.069	0.062	0.000	0.000	0.000	0.000	
54.8	6.40	0.090	0.064	0.017	0.009	0.000	0.000	0.000	
65.2	6.40	0.068	0.039	0.018	0.010	0.000	0.000	0.000	
74.4	6.40	0.065	0.026	0.033	0.006	0.000	0.000	0.000	
84.8	6.40	0.062	0.017	0.045	0.000	0.000	0.000	0.000	
95.4	6.40	0.060	0.017	0.043	0.000	0.000	0.000	0.000	
116.7	6.40	0.105	0.061	0.044	0.000	0.000	0.000	0.000	
6.7	6.59	0.143	0.003	0.021	0.052	0.051	0.016	0.001	
15.1	6.61	0.393	0.012	0.077	0.184	0.112	0.007	0.000	
23.9	6.60	0.426	0.024	0.153	0.225	0.025	0.000	0.000	
35.2	6.60	0.356	0.081	0.258	0.016	0.000	0.000	0.000	
44.2	6.61	0.235	0.117	0.118	0.000	0.000	0.000	0.000	
54.2	6.59	0.187	0.152	0.024	0.011	0.000	0.000	0.000	
65.1	6.59	0.110	0.073	0.021	0.015	0.000	0.000	0.000	
74.7	6.60	0.081	0.041	0.028	0.012	0.000	0.000	0.000	
85.0	6.61	0.085	0.032	0.048	0.004	0.000	0.000	0.000	
95.3	6.60	0.057	0.018	0.039	0.000	0.000	0.000	0.000	
105.7	6.61	0.062	0.019	0.042	0.000	0.000	0.000	0.000	
126.6	6.60	0.101	0.057	0.044	0.000	0.000	0.000	0.000	
6.7	6.80	0.140	0.003	0.020	0.050	0.049	0.017	0.001	
15.3	6.80	0.396	0.011	0.071	0.176	0.125	0.013	0.000	

24.6	6.79	0.325	0.016	0.100	0.182	0.028	0.000	0.000
34.9	6.81	0.422	0.066	0.294	0.061	0.000	0.000	0.000
44.2	6.80	0.257	0.102	0.155	0.000	0.000	0.000	0.000
53.8	6.81	0.424	0.292	0.116	0.015	0.000	0.000	0.000
64.0	6.81	0.248	0.201	0.026	0.021	0.000	0.000	0.000
74.8	6.79	0.100	0.055	0.028	0.018	0.000	0.000	0.000
84.3	6.81	0.089	0.036	0.040	0.014	0.000	0.000	0.000
94.8	6.80	0.066	0.025	0.038	0.002	0.000	0.000	0.000
111.7	6.80	0.130	0.040	0.091	0.000	0.000	0.000	0.000
134.9	6.79	0.073	0.037	0.036	0.000	0.000	0.000	0.000
14.3	6.95	0.176	0.005	0.029	0.073	0.059	0.011	0.000
23.6	6.95	0.230	0.009	0.057	0.127	0.038	0.000	0.000
36.0	6.99	0.379	0.053	0.265	0.060	0.000	0.000	0.000
44.6	6.99	0.194	0.061	0.131	0.001	0.000	0.000	0.000
53.9	7.02	0.312	0.182	0.110	0.017	0.003	0.000	0.000
63.8	7.03	0.490	0.341	0.114	0.035	0.001	0.000	0.000
74.8	6.98	0.115	0.072	0.022	0.021	0.000	0.000	0.000
84.7	7.00	0.095	0.033	0.039	0.024	0.000	0.000	0.000
94.5	7.00	0.089	0.024	0.051	0.015	0.000	0.000	0.000
117.6	7.00	0.141	0.039	0.102	0.000	0.000	0.000	0.000
131.8	7.00	0.054	0.054	0.000	0.000	0.000	0.000	0.000
35.0	7.20	0.320	0.031	0.185	0.104	0.000	0.000	0.000
44.2	7.21	0.207	0.047	0.156	0.004	0.000	0.000	0.000
53.9	7.21	0.235	0.099	0.125	0.008	0.002	0.000	0.000
64.3	7.22	0.191	0.106	0.066	0.018	0.001	0.000	0.000
74.9	7.19	0.084	0.043	0.023	0.018	0.000	0.000	0.000
108.6	7.16	0.050	0.013	0.033	0.003	0.000	0.000	0.000
126.9	7.16	0.082	0.036	0.046	0.000	0.000	0.000	0.000
140.7	7.42	0.166	0.166	0.000	0.000	0.000	0.000	0.000
142.3	7.63	0.057	0.057	0.000	0.000	0.000	0.000	0.000
79.8	8.30	19.325	1.257	7.816	10.252	0.000	0.000	0.000
83.8	8.30	3.090	0.209	1.303	1.578	0.000	0.000	0.000
94.6	8.30	1.110	0.089	0.558	0.462	0.000	0.000	0.000
109.2	8.30	1.697	0.178	1.117	0.402	0.000	0.000	0.000
117.2	8.30	4.480	0.545	3.424	0.511	0.000	0.000	0.000
135.3	8.30	5.363	0.951	4.412	0.000	0.000	0.000	0.000
154.8	8.30	1.904	0.507	1.398	0.000	0.000	0.000	0.000
178.5	8.30	0.647	0.306	0.342	0.000	0.000	0.000	0.000
181.1	8.30	0.411	0.206	0.205	0.000	0.000	0.000	0.000
205.1	8.30	0.154	0.135	0.019	0.000	0.000	0.000	0.000
226.6	8.30	0.305	0.305	0.000	0.000	0.000	0.000	0.000
276.7	8.30	0.056	0.056	0.000	0.000	0.000	0.000	0.000
79.8	9.00	24.776	1.073	6.608	16.597	0.498	0.000	0.000
116.9	9.00	6.831	0.425	2.643	3.762	0.000	0.000	0.000
134.5	9.00	5.560	0.424	2.643	2.493	0.000	0.000	0.000
152.5	9.00	2.259	0.211	1.322	0.726	0.000	0.000	0.000

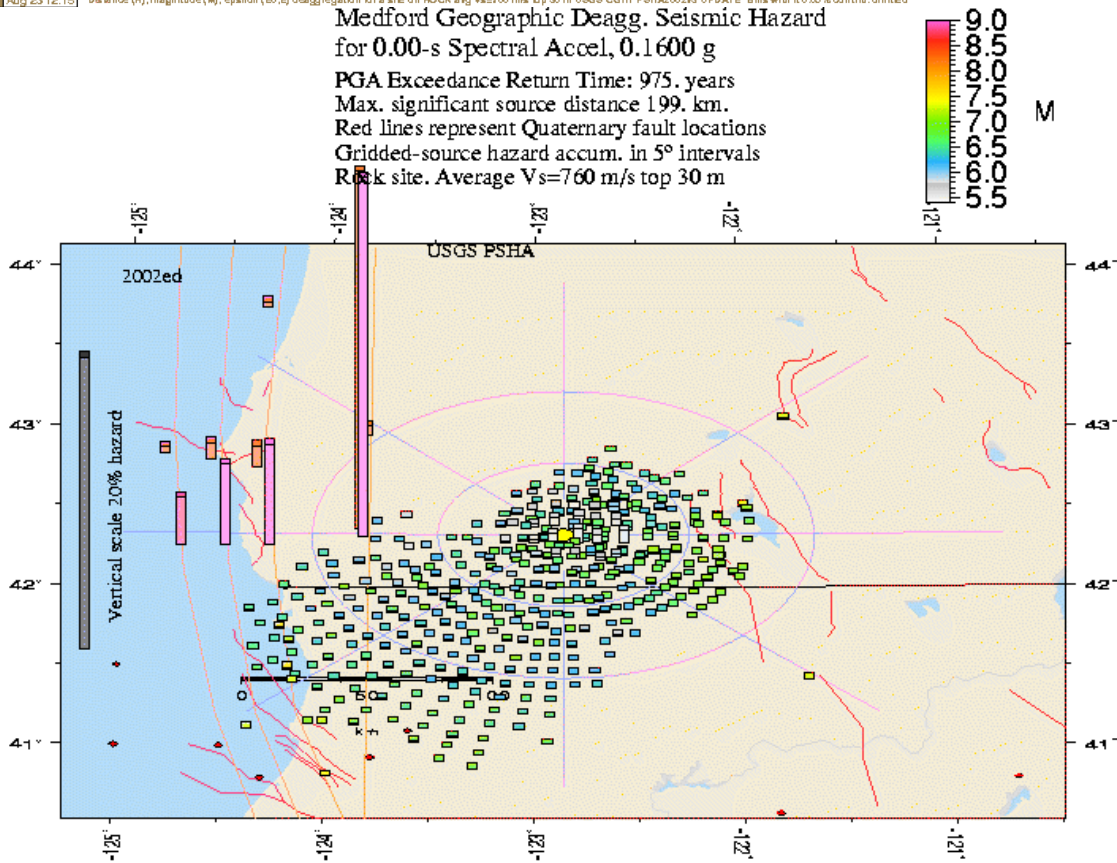
Summary statistics for above PSHA PGA deaggregation, R=distance, e=epsilon:
 Mean src-site R= 87.7 km; M= 8.12; eps0= 0.53. Mean calculated for all sources.
 Modal src-site R= 79.8 km; M= 9.00; eps0= -0.03 from peak (R,M) bin
 Gridded source distance metrics: Rseis Rrup and Rjb
 MODE R*= 79.8km; M*= 9.00; EPS.INTERVAL: 0 to 1 sigma % CONTRIB.= 16.597
 Modal source dmetric: distance to rupture surface (Youngs et al.,SRL,1997)

Principal sources (faults, subduction, random seismicity having >10% contribution)
 Source Category: % contr. R(km) M epsilon0 (mean values)
 WUS shallow gridded 11.83 21.1 5.98 0.44
 M 9.0 Subduction 39.42 98.1 9.00 0.17
 M 8.3 Subduction 38.59 102.5 8.30 0.71
 Individual fault hazard details if contrib.>1%:
 ***** Southern Oregon site *****



GMT Aug 23 12:15 Distance (R), magnitude (M), epsilon (ϵ_0) deaggregation for a site on ROCK avg Vs=760 m/s top 30 m USGS CGHT PSHA2002y3 UPDATE Bins with h 0.05% contrib. omitted

Medford Geographic Deagg. Seismic Hazard
 for 0.00-s Spectral Accel, 0.1600 g
 PGA Exceedance Return Time: 975. years
 Max. significant source distance 199. km.
 Red lines represent Quaternary fault locations
 Gridded-source hazard accum. in 5° intervals
 Rock site. Average Vs=760 m/s top 30 m



GMT 2004 Aug 23 12:15:07 Site Coord: 122.860 42.3300 (yellow dot). Max annual ExceedRate: 2542E-03 (no lumin height prop. to ExRate). Red diamonds: historical earthquakes, Mw < 6

Appendix E

Deaggregation of Seismic Hazard for Coos Bay
Return Period 475 Years (10% Probability of Exceedance in 50 Years)

Summary Tables, Plot of Relative Contributions, and Map of Geographic Hazard

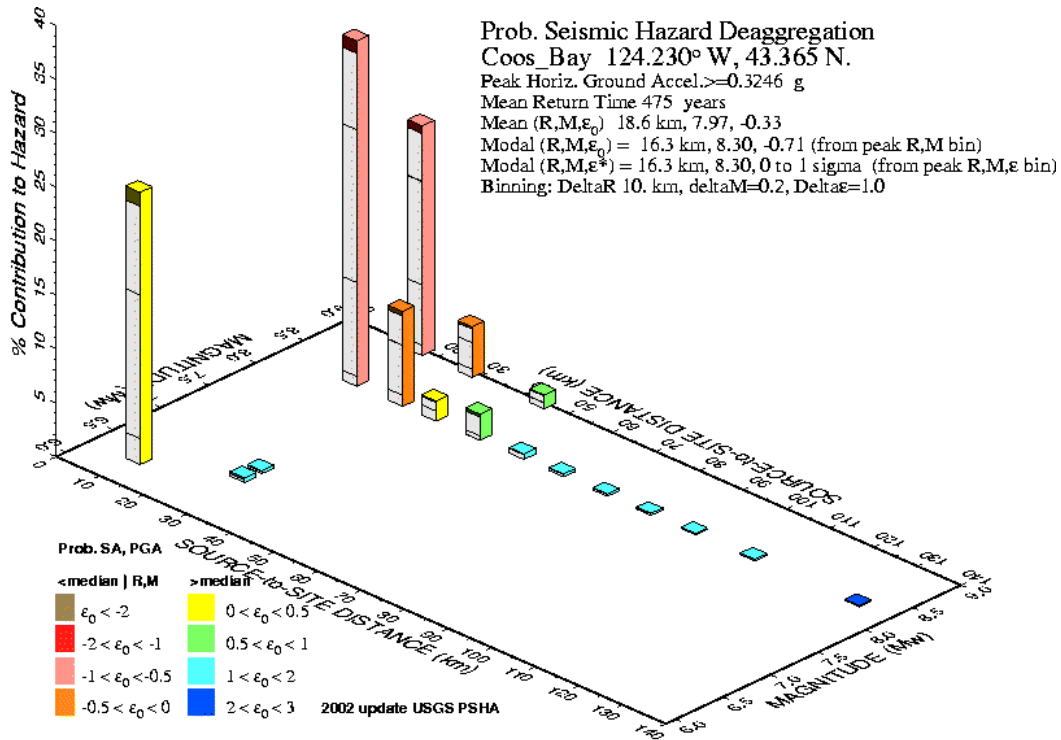
*** Deaggregation of Seismic Hazard for PGA & 2 Periods of Spectral Accel. ***
 *** Data from U.S.G.S. National Seismic Hazards Mapping Project, 2002 version ***
 PSHA Deaggregation. %contributions. site: Coos_Bay long: 124.230 W., lat: 43.365 N.
 USGS 2002-03 update files and programs. dM=0.2. Site descr:ROCK
 Return period: 475 yrs. Exceedance PGA =0.3246 g.

#Pr[at least one eq with median motion>=PGA in 50 yrs]=0.06603

DIST(KM)	MAG(MW)	ALL_EPS	EPSILON>2	1<EPS<2	0<EPS<1	-1<EPS<0	-2<EPS<-1	EPS<-2
10.2	6.30	25.226	1.296	8.229	13.336	2.365	0.000	0.000
27.2	6.62	0.423	0.199	0.224	0.000	0.000	0.000	0.000
27.1	6.81	0.248	0.102	0.146	0.000	0.000	0.000	0.000
16.3	8.30	32.037	1.156	7.071	14.181	8.697	0.933	0.000
26.8	8.30	8.802	0.438	2.703	4.646	1.015	0.000	0.000
34.5	8.30	1.860	0.129	0.806	0.917	0.008	0.000	0.000
44.6	8.30	2.425	0.282	1.744	0.399	0.000	0.000	0.000
54.6	8.30	0.539	0.108	0.431	0.000	0.000	0.000	0.000
63.8	8.30	0.275	0.072	0.203	0.000	0.000	0.000	0.000
73.8	8.30	0.200	0.055	0.145	0.000	0.000	0.000	0.000
83.8	8.30	0.172	0.061	0.112	0.000	0.000	0.000	0.000
94.0	8.30	0.124	0.059	0.065	0.000	0.000	0.000	0.000
107.7	8.30	0.146	0.110	0.036	0.000	0.000	0.000	0.000
131.7	8.30	0.092	0.092	0.000	0.000	0.000	0.000	0.000
16.2	9.00	21.293	0.729	4.449	9.587	5.588	0.940	0.000
27.7	9.00	4.671	0.206	1.271	2.448	0.745	0.000	0.000
44.2	9.00	1.271	0.102	0.636	0.534	0.000	0.000	0.000

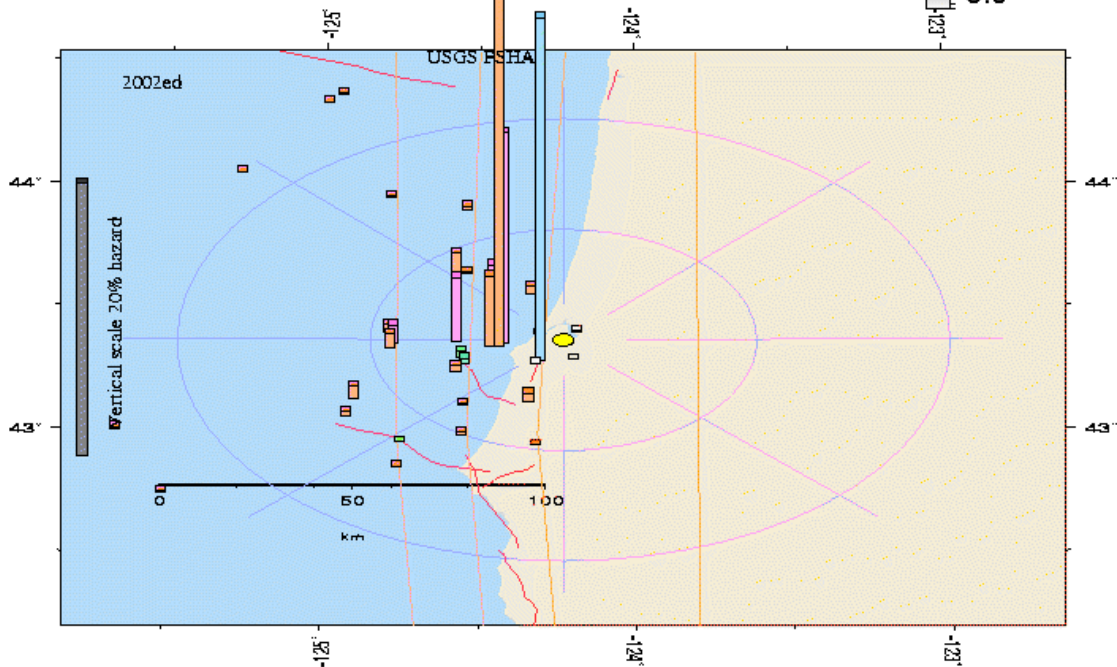
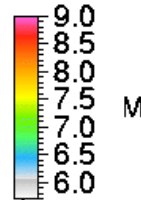
Summary statistics for above PSHA PGA deaggregation, R=distance, e=epsilon:
 Mean src-site R= 18.6 km; M= 7.97; eps0= -0.33. Mean calculated for all sources.
 Modal src-site R= 16.3 km; M= 8.30; eps0= -0.71 from peak (R,M) bin
 Gridded source distance metrics: Rseis Rrup and Rjb
 MODE R*= 16.3km; M*= 8.30; EPS.INTERVAL: 0 to 1 sigma % CONTRIB.= 14.181
 Modal source dmetric: distance to rupture surface (Youngs et al.,SRL,1997)

Principal sources (faults, subduction, random seismicity having >10% contribution)
 Source Category: % contr. R(km) M epsilon0 (mean values)
 Wash-Oreg faults 25.94 10.7 6.31 0.07
 M 9.0 Subduction 27.24 19.5 9.00 -0.63
 M 8.3 Subduction 46.74 22.5 8.30 -0.37
 Individual fault hazard details if contrib.>1%:
 South Slough thrust and reverse 25.22 10.2 6.30 0.02
 ***** Southern Oregon site *****



GMT Aug 23 12:20 Distance (R), magnitude (M), epsilon (ϵ_0) deaggregation for a site on ROCK avg Vs=760 m/s top 30 m USGS CGHT PSHA2002v3 UPDATE. Bins with lt 0.05% contrib. omitted

Coos_Bay Geographic Deagg. Seismic Hazard
 for 0.00-s Spectral Accel, 0.3245 g
 PGA Exceedance Return Time: 475. years
 Max. significant source distance 126. km.
 Red lines represent Quaternary fault locations
 Orange lines show four downdip limits of Cascadia hazard
 Rock site. Average Vs=760 m/s top 30 m



GMT 2004 Aug 23 12:20:58 Site Coords: 124.230 43.3650 (yellow dot). Max annual ExcdRate: 5642E-03 (as lumin height prop. to ExRate). Red diamonds: historical earthquakes, Mb6

Appendix F

Deaggregation of Seismic Hazard for Coos Bay
Return Period 975 Years (5% Probability of Exceedance in 50 Years)

Summary Tables, Plot of Relative Contributions, and Map of Geographic Hazard

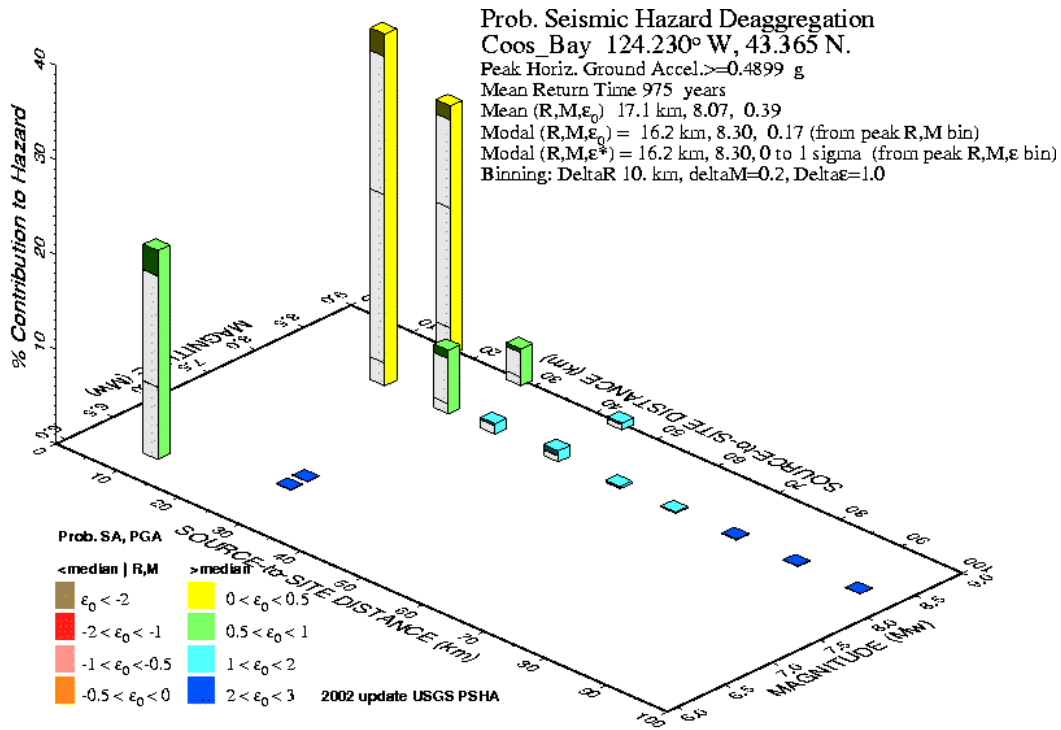
*** Deaggregation of Seismic Hazard for PGA & 2 Periods of Spectral Accel. ***
 *** Data from U.S.G.S. National Seismic Hazards Mapping Project, 2002 version ***
 PSHA Deaggregation. %contributions. site: Coos_Bay long: 124.230 W., lat: 43.365 N.
 USGS 2002-03 update files and programs. dM=0.2. Site descr:ROCK
 Return period: 975 yrs. Exceedance PGA =0.4899 g.

#Pr[at least one eq with median motion>=PGA in 50 yrs]=0.01837

DIST(KM)	MAG(MW)	ALL_EPS	EPSILON>2	1<EPS<2	0<EPS<1	-1<EPS<0	-2<EPS<-1	EPS<-2
10.2	6.30	22.074	2.709	11.768	7.597	0.000	0.000	0.000
27.0	6.61	0.077	0.077	0.000	0.000	0.000	0.000	0.000
26.9	6.80	0.058	0.058	0.000	0.000	0.000	0.000	0.000
16.2	8.30	37.167	2.378	14.625	17.780	2.384	0.000	0.000
26.6	8.30	6.678	0.899	4.733	1.046	0.000	0.000	0.000
34.2	8.30	1.098	0.267	0.831	0.000	0.000	0.000	0.000
44.6	8.30	1.172	0.562	0.610	0.000	0.000	0.000	0.000
54.7	8.30	0.255	0.139	0.117	0.000	0.000	0.000	0.000
63.8	8.30	0.142	0.100	0.042	0.000	0.000	0.000	0.000
73.8	8.30	0.103	0.099	0.004	0.000	0.000	0.000	0.000
83.7	8.30	0.081	0.081	0.000	0.000	0.000	0.000	0.000
93.9	8.30	0.052	0.052	0.000	0.000	0.000	0.000	0.000
16.1	9.00	26.299	1.500	9.303	12.663	2.832	0.000	0.000
27.7	9.00	3.878	0.424	2.556	0.899	0.000	0.000	0.000
44.2	9.00	0.731	0.210	0.521	0.000	0.000	0.000	0.000

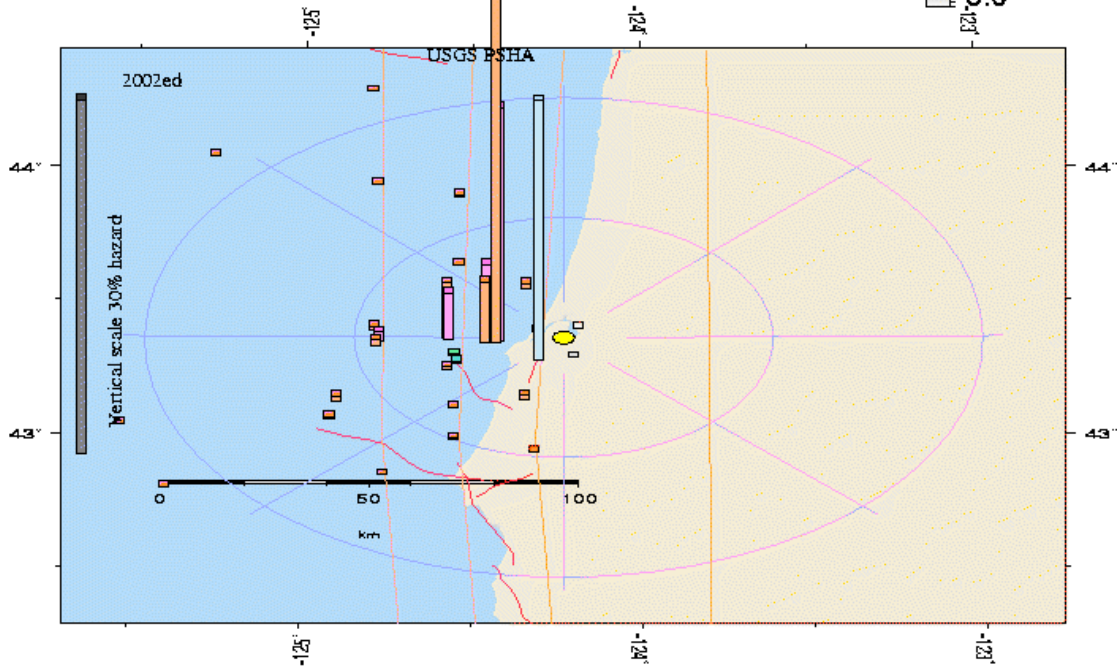
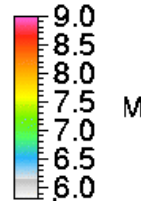
Summary statistics for above PSHA PGA deaggregation, R=distance, e=epsilon:
 Mean src-site R= 17.1 km; M= 8.07; eps0= 0.39. Mean calculated for all sources.
 Modal src-site R= 16.2 km; M= 8.30; eps0= 0.17 from peak (R,M) bin
 Gridded source distance metrics: Rseis Rrup and Rjb
 MODE R*= 16.2km; M*= 8.30; EPS.INTERVAL: 0 to 1 sigma % CONTRIB.= 17.780
 Modal source dmetric: distance to rupture surface (Youngs et al.,SRL,1997)

Principal sources (faults, subduction, random seismicity having >10% contribution)
 Source Category: % contr. R(km) M epsilon0 (mean values)
 Wash-Oreg faults 22.22 10.3 6.30 0.74
 M 9.0 Subduction 30.91 18.2 9.00 0.18
 M 8.3 Subduction 46.82 19.6 8.30 0.37
 Individual fault hazard details if contrib.>1%:
 South Slough thrust and reverse 22.07 10.2 6.30 0.72
 ***** Southern Oregon site *****



GMT Aug 23 13:43 Distance (R), magnitude (M), epsilon (ϵ_0) deaggregation for a site on ROCK avg Vs=760 m/s top 30 m USGS CGHT PSHA2002v3 UPDATE Bins with lt 0.05% contrib. omitted

Coos_Bay Geographic Deagg. Seismic Hazard
 for 0.00-s Spectral Accel, 0.4898 g
 PGA Exceedance Return Time: 975. years
 Max. significant source distance 113. km.
 Red lines represent Quaternary fault locations
 Orange lines show four downdip limits of Cascadia hazard
 Rock site. Average Vs=760 m/s top 30 m



GMT 2004 Aug 23 13:43:53 Site Coord: 124.230 43.36500 (yellow diamond). Max annual ExceedRate 31.14E-03 (column height prop. to ExRate). Red diamonds: historical earthquakes, Mw6

Appendix G

Deaggregation of Seismic Hazard for Klamath Falls
Return Period 475 Years (10% Probability of Exceedance in 50 Years)

Summary Tables, Plot of Relative Contributions, and Map of Geographic Hazard

*** Deaggregation of Seismic Hazard for PGA & 2 Periods of Spectral Accel. ***
 *** Data from U.S.G.S. National Seismic Hazards Mapping Project, 2002 version ***
 PSHA Deaggregation. %contributions. site: Klamath_Falls long: 121.770 W., lat:
 42.220 N.

USGS 2002-03 update files and programs. dM=0.2. Site descr:ROCK

Return period: 475 yrs. Exceedance PGA =0.1683 g.

#Pr[at least one eq with median motion>=PGA in 50 yrs]=0.04525

DIST(KM)	MAG(MW)	ALL_EPS	EPSILON>2	1<EPS<2	0<EPS<1	-1<EPS<0	-2<EPS<-1	EPS<-2
6.7	5.05	0.855	0.045	0.283	0.469	0.058	0.000	0.000
13.3	5.05	1.056	0.183	0.691	0.182	0.000	0.000	0.000
23.0	5.05	0.293	0.218	0.076	0.000	0.000	0.000	0.000
6.7	5.20	1.481	0.069	0.438	0.818	0.156	0.000	0.000
13.4	5.20	2.008	0.280	1.239	0.489	0.000	0.000	0.000
23.1	5.20	0.626	0.398	0.228	0.000	0.000	0.000	0.000
33.5	5.20	0.089	0.089	0.000	0.000	0.000	0.000	0.000
6.8	5.40	1.203	0.048	0.303	0.638	0.213	0.000	0.000
13.5	5.40	1.857	0.195	1.003	0.659	0.000	0.000	0.000
23.2	5.40	0.677	0.325	0.352	0.000	0.000	0.000	0.000
33.8	5.40	0.125	0.125	0.000	0.000	0.000	0.000	0.000
6.8	5.60	0.956	0.033	0.210	0.475	0.238	0.001	0.000
13.6	5.60	1.688	0.135	0.767	0.763	0.023	0.000	0.000
23.4	5.60	0.725	0.244	0.472	0.009	0.000	0.000	0.000
34.0	5.60	0.163	0.150	0.013	0.000	0.000	0.000	0.000
6.8	5.80	0.743	0.023	0.145	0.347	0.219	0.010	0.000
13.7	5.80	1.498	0.093	0.565	0.758	0.082	0.000	0.000
23.5	5.80	0.759	0.173	0.521	0.066	0.000	0.000	0.000
34.1	5.80	0.202	0.151	0.050	0.000	0.000	0.000	0.000
44.0	5.81	0.052	0.052	0.000	0.000	0.000	0.000	0.000
6.9	6.02	0.918	0.025	0.162	0.401	0.297	0.032	0.000
14.1	6.00	1.294	0.068	0.429	0.659	0.138	0.000	0.000
23.5	6.00	0.790	0.125	0.514	0.151	0.000	0.000	0.000
34.1	6.00	0.240	0.135	0.105	0.000	0.000	0.000	0.000
44.4	6.00	0.070	0.067	0.003	0.000	0.000	0.000	0.000
6.5	6.19	0.869	0.023	0.145	0.364	0.283	0.054	0.000
14.8	6.21	1.463	0.066	0.420	0.755	0.221	0.001	0.000
24.1	6.19	0.698	0.086	0.421	0.191	0.000	0.000	0.000
34.7	6.20	0.273	0.112	0.161	0.000	0.000	0.000	0.000
44.0	6.21	0.095	0.078	0.018	0.000	0.000	0.000	0.000
7.0	6.39	0.770	0.019	0.119	0.300	0.271	0.060	0.001
15.4	6.40	1.199	0.046	0.293	0.625	0.232	0.003	0.000
24.6	6.40	0.720	0.066	0.373	0.278	0.003	0.000	0.000
33.7	6.45	2.361	0.851	1.502	0.009	0.000	0.000	0.000
43.4	6.38	0.168	0.113	0.056	0.000	0.000	0.000	0.000
5.2	6.62	5.087	0.121	0.769	1.931	1.804	0.444	0.019
14.9	6.60	3.786	0.155	0.982	1.915	0.713	0.022	0.000
24.6	6.59	3.354	0.369	1.946	1.035	0.004	0.000	0.000
34.0	6.64	2.977	0.818	2.147	0.012	0.000	0.000	0.000
43.8	6.60	0.488	0.326	0.162	0.000	0.000	0.000	0.000
54.2	6.60	0.085	0.082	0.003	0.000	0.000	0.000	0.000
5.8	6.83	3.847	0.090	0.569	1.430	1.369	0.370	0.018
16.2	6.80	4.109	0.166	1.051	2.228	0.630	0.034	0.000
23.7	6.82	9.097	0.643	4.022	4.258	0.174	0.000	0.000
34.0	6.81	1.476	0.278	1.106	0.093	0.000	0.000	0.000
44.2	6.81	0.314	0.165	0.149	0.000	0.000	0.000	0.000
54.4	6.80	0.088	0.074	0.014	0.000	0.000	0.000	0.000
6.6	7.00	2.303	0.053	0.336	0.843	0.829	0.233	0.011
16.8	7.03	4.177	0.146	0.924	2.233	0.820	0.054	0.000
23.4	7.03	7.347	0.369	2.340	4.108	0.530	0.000	0.000
34.6	7.00	0.659	0.104	0.471	0.085	0.000	0.000	0.000
44.3	6.99	0.259	0.107	0.152	0.000	0.000	0.000	0.000
54.0	6.99	0.084	0.059	0.025	0.000	0.000	0.000	0.000
4.4	7.20	4.745	0.104	0.663	1.665	1.664	0.602	0.047
15.6	7.20	2.383	0.071	0.453	1.129	0.658	0.071	0.000
23.2	7.23	2.950	0.125	0.796	1.611	0.418	0.000	0.000
34.5	7.20	0.713	0.079	0.442	0.192	0.000	0.000	0.000
44.4	7.20	0.265	0.075	0.190	0.000	0.000	0.000	0.000
54.2	7.21	0.093	0.053	0.040	0.000	0.000	0.000	0.000
2.5	7.47	0.791	0.017	0.108	0.272	0.272	0.108	0.013
22.3	7.42	0.157	0.005	0.033	0.081	0.037	0.001	0.000
2.5	7.66	0.106	0.002	0.014	0.036	0.036	0.014	0.002
170.8	8.30	1.863	0.844	1.019	0.000	0.000	0.000	0.000
209.0	8.30	0.303	0.303	0.001	0.000	0.000	0.000	0.000

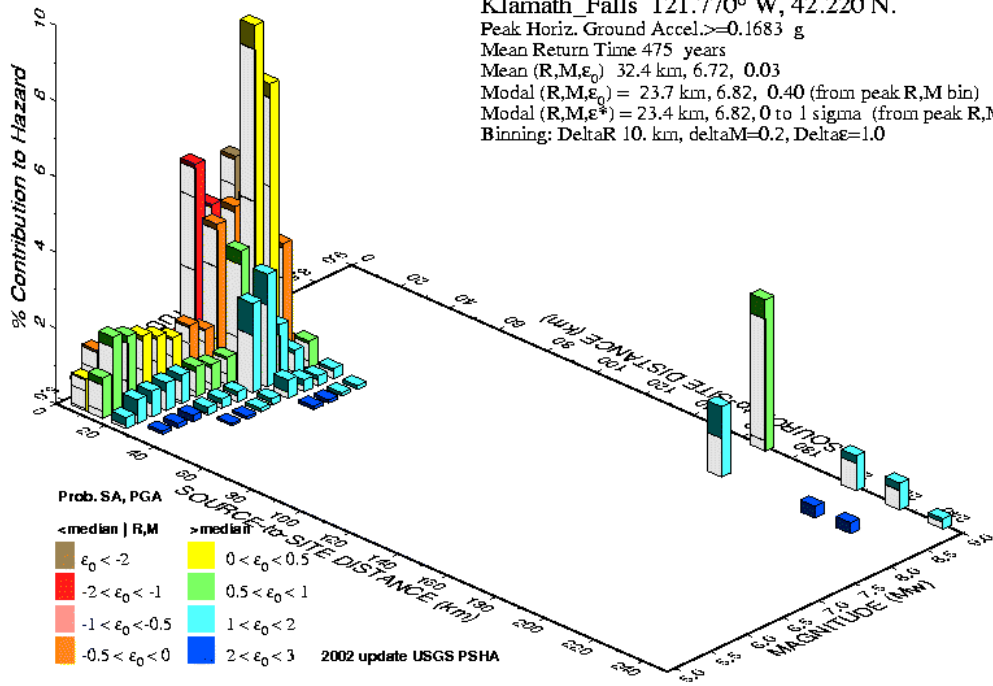
223.7	8.30	0.287	0.287	0.000	0.000	0.000	0.000	0.000
168.3	9.00	3.994	0.512	3.216	0.266	0.000	0.000	0.000
205.6	9.00	0.924	0.204	0.720	0.000	0.000	0.000	0.000
223.3	9.00	0.712	0.204	0.509	0.000	0.000	0.000	0.000
241.1	9.00	0.268	0.102	0.166	0.000	0.000	0.000	0.000

Summary statistics for above PSHA PGA deaggregation, R=distance, e=epsilon:
 Mean src-site R= 32.4 km; M= 6.72; eps0= 0.03. Mean calculated for all sources.
 Modal src-site R= 23.7 km; M= 6.82; eps0= 0.40 from peak (R,M) bin
 Gridded source distance metrics: Rseis Rrup and Rjb
 MODE R*= 23.4km; M*= 6.82; EPS.INTERVAL: 0 to 1 sigma % CONTRIB.= 4.258

Principal sources (faults, subduction, random seismicity having >10% contribution)

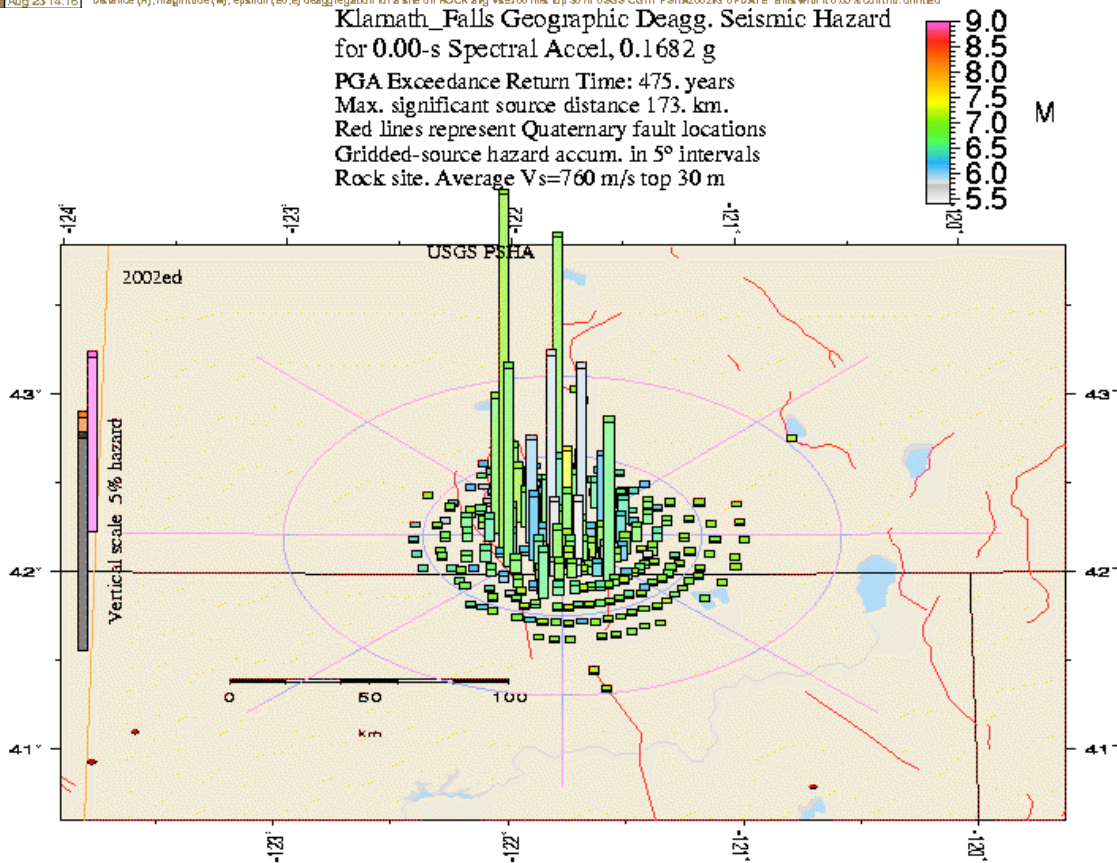
Source Category:	% contr.	R(km)	M	epsilon0 (mean values)
WUS shallow gridded	24.78	15.9	5.71	0.37
California normal/SS faults	17.55	26.9	6.84	0.60
WUS extensional faults	17.10	13.8	6.95	-0.92
CA-NV SHEAR ZONES 1-4	29.32	17.5	6.87	-0.49
Individual fault hazard details if contrib.>1%:				
Klamath graben f	1.94	2.5	7.35	-2.67
Sky Lakes FZ Ch_Mag	2.55	19.6	7.06	-0.24
Klamath graben f	1.38	18.9	7.06	-0.24
Klamath graben f	6.66	6.3	6.87	-1.76
Sky Lakes FZ	3.09	23.9	6.80	0.44
Klamath graben f	1.45	24.6	6.82	0.45
2 Cedar Mtn-Mahognany Mtn	8.21	22.9	7.01	0.15
2 Gillem-Big Crack	3.70	33.0	6.59	1.29
2 Cedar Mtn-Mahognany Mtn	4.52	25.8	6.78	0.60
2 Gillem-Big Crack	1.05	37.6	6.54	1.59
***** Southern Oregon site *****				

Prob. Seismic Hazard Deaggregation
Klamath_Falls 121.770° W, 42.220 N.
 Peak Horiz. Ground Accel. ≥ 0.1683 g
 Mean Return Time 475 years
 Mean (R,M, ϵ_0) 32.4 km, 6.72, 0.03
 Modal (R,M, ϵ_0) = 23.7 km, 6.82, 0.40 (from peak R,M bin)
 Modal (R,M, ϵ_0^*) = 23.4 km, 6.82, 0 to 1 sigma (from peak R,M, ϵ bin)
 Binning: DeltaR 10. km, deltaM=0.2, Delta ϵ =1.0



GMT Aug 23 14:16 Distance (R), magnitude (M), epsilon (ϵ_0) deaggregation for a site on ROCK avg Vs=760 m/s top 30 m USGS CGHT PSHA2002v3 UPDATE Bins with lt 0.05% contrib. omitted

Klamath_Falls Geographic Deagg. Seismic Hazard
 for 0.00-s Spectral Accel, 0.1682 g
 PGA Exceedance Return Time: 475. years
 Max. significant source distance 173. km.
 Red lines represent Quaternary fault locations
 Gridded-source hazard accum. in 5° intervals
 Rock site. Average Vs=760 m/s top 30 m



GMT 2004 Aug 23 14:16:25 Site Coord: -121.770 42.2200 (yellow disk). Max annual ExceedRate: 1730E-03 (column height prop. to ExRate). Red diamonds: historical earthquakes, Mw6

Appendix H

Deaggregation of Seismic Hazard for Klamath Falls
Return Period 975 Years (5% Probability of Exceedance in 50 Years)

Summary Tables, Plot of Relative Contributions, and Map of Geographic Hazard

*** Deaggregation of Seismic Hazard for PGA & 2 Periods of Spectral Accel. ***
 *** Data from U.S.G.S. National Seismic Hazards Mapping Project, 2002 version ***
 PSHA Deaggregation. %contributions. site: Klamath_Falls long: 121.770 W., lat:
 42.220 N.

USGS 2002-03 update files and programs. dM=0.2. Site descr:ROCK

Return period: 975 yrs. Exceedance PGA =0.2391 g.

#Pr[at least one eq with median motion>=PGA in 50 yrs]=0.02129

DIST(KM)	MAG(MW)	ALL_EPS	EPSILON>2	1<EPS<2	0<EPS<1	-1<EPS<0	-2<EPS<-1	EPS<-2
6.7	5.05	0.949	0.092	0.475	0.382	0.000	0.000	0.000
13.0	5.05	0.812	0.298	0.514	0.000	0.000	0.000	0.000
22.3	5.05	0.120	0.120	0.000	0.000	0.000	0.000	0.000
6.7	5.20	1.716	0.140	0.764	0.812	0.000	0.000	0.000
13.1	5.20	1.611	0.489	1.078	0.044	0.000	0.000	0.000
22.5	5.20	0.279	0.271	0.008	0.000	0.000	0.000	0.000
6.7	5.40	1.481	0.097	0.565	0.788	0.031	0.000	0.000
13.2	5.40	1.586	0.366	1.047	0.172	0.000	0.000	0.000
22.7	5.40	0.337	0.285	0.052	0.000	0.000	0.000	0.000
6.8	5.60	1.256	0.067	0.411	0.672	0.106	0.000	0.000
13.3	5.60	1.545	0.266	0.968	0.312	0.000	0.000	0.000
22.9	5.60	0.399	0.281	0.118	0.000	0.000	0.000	0.000
6.8	5.80	1.041	0.047	0.293	0.543	0.158	0.000	0.000
13.4	5.80	1.477	0.189	0.814	0.474	0.000	0.000	0.000
23.1	5.80	0.458	0.251	0.208	0.000	0.000	0.000	0.000
33.5	5.81	0.062	0.062	0.000	0.000	0.000	0.000	0.000
6.8	6.02	1.370	0.052	0.330	0.689	0.296	0.003	0.000
13.7	6.00	1.348	0.139	0.669	0.526	0.014	0.000	0.000
23.1	6.00	0.518	0.213	0.303	0.003	0.000	0.000	0.000
33.7	6.01	0.089	0.086	0.003	0.000	0.000	0.000	0.000
6.3	6.19	1.371	0.047	0.296	0.636	0.374	0.019	0.000
14.3	6.21	1.614	0.135	0.705	0.700	0.075	0.000	0.000
23.7	6.19	0.477	0.159	0.305	0.014	0.000	0.000	0.000
34.3	6.20	0.113	0.099	0.014	0.000	0.000	0.000	0.000
6.9	6.39	1.275	0.038	0.243	0.581	0.379	0.033	0.000
15.2	6.40	1.371	0.094	0.560	0.665	0.053	0.000	0.000
24.2	6.40	0.527	0.131	0.348	0.048	0.000	0.000	0.000
33.5	6.45	1.005	0.868	0.137	0.000	0.000	0.000	0.000
43.1	6.41	0.056	0.056	0.000	0.000	0.000	0.000	0.000
5.1	6.62	8.671	0.246	1.565	3.823	2.680	0.356	0.000
14.9	6.60	4.600	0.373	2.056	1.910	0.262	0.000	0.000
24.3	6.61	2.516	0.732	1.723	0.062	0.000	0.000	0.000
33.6	6.65	1.288	1.016	0.273	0.000	0.000	0.000	0.000
43.3	6.61	0.110	0.110	0.000	0.000	0.000	0.000	0.000
6.0	6.81	5.112	0.145	0.924	2.290	1.612	0.141	0.000
15.6	6.82	4.344	0.289	1.814	1.969	0.272	0.000	0.000
23.6	6.83	6.610	1.340	4.667	0.603	0.000	0.000	0.000
33.8	6.82	0.609	0.416	0.194	0.000	0.000	0.000	0.000
43.8	6.81	0.087	0.086	0.001	0.000	0.000	0.000	0.000
5.9	6.98	5.812	0.149	0.949	2.383	1.976	0.352	0.003
15.9	7.02	4.494	0.273	1.728	2.131	0.363	0.000	0.000
22.8	7.05	6.051	0.713	3.728	1.611	0.000	0.000	0.000
34.3	7.00	0.312	0.182	0.130	0.000	0.000	0.000	0.000
44.0	7.00	0.081	0.079	0.001	0.000	0.000	0.000	0.000
4.3	7.20	8.818	0.208	1.319	3.314	3.169	0.781	0.028
15.8	7.21	3.391	0.160	1.014	1.809	0.405	0.004	0.000
23.3	7.22	2.366	0.237	1.367	0.760	0.002	0.000	0.000
34.1	7.20	0.381	0.155	0.226	0.000	0.000	0.000	0.000
44.2	7.20	0.095	0.083	0.012	0.000	0.000	0.000	0.000
2.6	7.47	1.566	0.035	0.221	0.554	0.554	0.192	0.010
18.7	7.42	0.092	0.005	0.031	0.056	0.000	0.000	0.000
22.1	7.40	0.186	0.011	0.069	0.101	0.005	0.000	0.000
2.5	7.66	0.211	0.005	0.029	0.074	0.074	0.028	0.001
170.5	8.30	1.017	1.017	0.000	0.000	0.000	0.000	0.000
207.9	8.30	0.103	0.103	0.000	0.000	0.000	0.000	0.000
168.3	9.00	3.193	1.036	2.157	0.000	0.000	0.000	0.000
205.6	9.00	0.625	0.413	0.212	0.000	0.000	0.000	0.000
223.3	9.00	0.446	0.413	0.033	0.000	0.000	0.000	0.000
241.1	9.00	0.154	0.154	0.000	0.000	0.000	0.000	0.000

Summary statistics for above PSHA PGA deaggregation, R=distance, e=epsilon:
 Mean src-site R= 23.1 km; M= 6.73; eps0= 0.16. Mean calculated for all sources.
 Modal src-site R= 4.3 km; M= 7.20; eps0= -1.59 from peak (R,M) bin
 Gridded source distance metrics: Rseis Rrup and Rjb

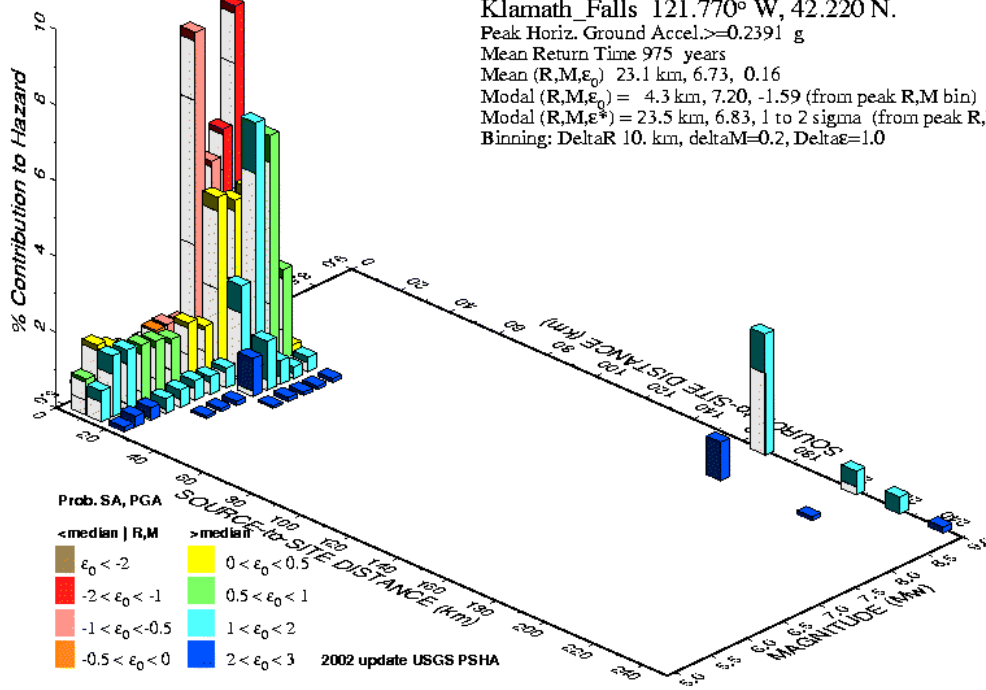
MODE R*= 23.5km; M*= 6.83; EPS.INTERVAL: 1 to 2 sigma % CONTRIB.= 4.667

Principal sources (faults, subduction, random seismicity having >10% contribution)

Source Category:	% contr.	R(km)	M	epsilon0 (mean values)
WUS shallow gridded	23.38	12.6	5.74	0.58
California normal/SS faults	11.71	25.3	6.89	1.18
WUS extensional faults	22.47	9.9	6.99	-0.69
CA-NV SHEAR ZONES 1-4	34.51	12.9	6.88	-0.22
Individual fault hazard details if contrib.>1%:				
Klamath graben f	3.81	2.6	7.35	-1.89
Sky Lakes FZ Ch_Mag	2.60	19.6	7.07	0.51
Klamath graben f	1.41	18.9	7.07	0.51
Klamath graben f	11.32	5.0	6.89	-1.22
Sky Lakes FZ	2.28	23.1	6.83	1.08
Klamath graben f	1.06	23.2	6.85	1.05
2 Cedar Mtn-Mahognany Mtn	6.71	22.9	7.03	0.90
2 Gillem-Big Crack	1.62	32.9	6.60	1.96
2 Cedar Mtn-Mahognany Mtn	3.02	24.9	6.79	1.24

***** Southern Oregon site *****

Prob. Seismic Hazard Deaggregation
 Klamath Falls 121.770° W, 42.220 N.
 Peak Horiz. Ground Accel. ≥ 0.2391 g
 Mean Return Time 975 years
 Mean (R,M, ϵ_0) 23.1 km, 6.73, 0.16
 Modal (R,M, ϵ_0) = 4.3 km, 7.20, -1.59 (from peak R,M bin)
 Modal (R,M, ϵ^*) = 23.5 km, 6.83, 1 to 2 sigma (from peak R,M, ϵ bin)
 Binning: DeltaR 10. km, deltaM=0.2, Delta ϵ =1.0



GMT Aug 23 14:33 Distance (R), magnitude (M), epsilon (ϵ_0 , ϵ) deaggregation for a site on ROCK avg V_s=760 m/s to p 30 m USGS CGHT PSHA2002v3 UPDATE Bins with lt 0.05% contrib. omitted

Geographic Seismic Hazard Plot not Available from the USGS Web Site

Appendix I

Spreadsheets for the Evaluation of Liquefaction Susceptibility
and Post-Liquefaction Undrained Residual Shear Strength

CASE NO.1; M6.2
CASE NO.1; M6.64
CASE NO.1; M8.3
CASE NO. 1; M9.0

CASE NO. 2; M6.2
CASE NO. 2; M6.64
CASE NO.2; M8.3
CASE NO.2; M9.0

References for all of the formulas and tables used are provided.

CASE NO. 1 , M6.2
1 OF 2

SPREADSHEET FOR PERFORMING SIMPLIFIED LIQUEFACTION HAZARD EVALUATIONS

Modified January 24, 2005

The Simplified Procedure of Seed and Idriss is performed using the recommendations presented by Youd et al (2001)
All equations and relationships used in this spreadsheet are referenced at the bottom of the sheet.

Moment Magnitude	6.2	
Magnitude Scaling Factor	1.63	(Eq. 24, Ref. 1)
Peak Acceleration at the Ground Surface (g)	0.26	
Embankment height (ft)	25	
Moist unit weight of fill (pcf)	125	
Saturated unit weight of native soil (pcf)	100	
Depth to the groundwater table (ft)	0	

Depth (ft)	σ'_v (psf)	Nm (bl/ft)	CN	N1 (bl/ft)	CE	CB	CR	CS	(N1)60 (bl/ft)	Fines (%)	Parameter α	Parameter β	(N1)60cs (bl/ft)
5.00	188.00	3.00	1.71	5.12	1.00	1.05	0.75	1.00	4.03	4.00	0.00	1.00	4.02
10.00	376.00	2.00	1.60	3.19	1.00	1.05	0.75	1.00	2.51	4.00	0.00	1.00	2.51
15.00	564.00	5.00	1.50	7.49	1.00	1.05	1.00	1.00	7.86	4.00	0.00	1.00	7.85
20.00	752.00	5.00	1.41	7.06	1.00	1.05	1.00	1.00	7.41	12.00	1.55	1.03	9.20
25.00	940.00	7.00	1.34	9.35	1.00	1.05	1.00	1.00	9.81	12.00	1.55	1.03	11.68
30.00	1128.00	4.00	1.27	5.07	1.00	1.05	1.00	1.00	5.32	35.00	5.00	1.20	11.38
35.00	1316.00	8.00	1.20	9.64	1.00	1.05	1.00	1.00	10.12	35.00	5.00	1.20	17.14
40.00	1504.00	10.00	1.15	11.48	1.00	1.05	1.00	1.00	12.06	35.00	5.00	1.20	19.47
45.00	1767.00	15.00	1.08	16.17	1.00	1.05	1.00	1.00	16.97	2.00	0.00	0.99	16.85
50.00	2030.00	20.00	1.02	20.31	1.00	1.05	1.00	1.00	21.32	2.00	0.00	0.99	21.17
55.00	2293.00	25.00	0.96	24.00	1.00	1.05	1.00	1.00	25.20	2.00	0.00	0.99	25.02

σ'_v	Vertical effective stress
Nm	SPT N-value measured in the field
CN	SPT N-value stress correction factor (Eq. 10, Ref. 1)
N1	SPT N-value normalized for vertical effective stress
CE, CB, CR, CS	SPT N-value corrections (Table 2, Ref. 1)
α	Parameter for fines correction to SPT N-value (Eqs. 6a-6c, Ref. 1)
β	Parameter for fines correction to SPT N-value (Eqs. 7a-7c, Ref. 1)

CASE NO. 1 , M6.2
2 OF 2

Depth (ft)	(N1)60cs (bl/ft)	CRR7.5	rd	CSR centerline	CSR free-field	CSR average	FS CSRavg	Dr (%)	K σ	K α	FS*	Ru	(su)l-os (psf)	(su)l-sh (psf)	Ncorr (blow/ft)	(su)l-avg (psf)
5.00	4.02	0.07	0.99	0.18	0.45	0.31	0.34	29.57	0.89	1.00	0.30	1.00	199.54	120.00	4	159.77
10.00	2.51	0.06	0.98	0.19	0.44	0.32	0.28	23.35	0.88	1.00	0.25	1.00	171.00	100.00	3	135.50
15.00	7.85	0.09	0.97	0.21	0.44	0.32	0.48	41.31	0.87	1.00	0.42	1.00	328.27	200.00	8	264.13
20.00	9.20	0.11	0.96	0.21	0.43	0.32	0.54	40.11	0.86	1.00	0.46	1.00	331.86	300.00	10	315.93
25.00	11.68	0.13	0.94	0.22	0.42	0.32	0.65	46.15	0.85	1.00	0.55	1.00	421.16	500.00	13	460.58
30.00	11.38	0.13	0.92	0.22	0.41	0.32	0.64	33.97	0.84	1.00	0.54	1.00	297.26	600.00	14	448.63
35.00	17.14	0.18	0.89	0.22	0.40	0.31	0.95	46.85	0.83	1.00	0.79	1.00	470.19	800.00	20	635.10
40.00	19.47	0.21	0.85	0.22	0.38	0.30	1.13	51.15	0.82	1.00	0.93	0.36	n/a	n/a	23	n/a
45.00	16.85	0.18	0.80	0.21	0.35	0.28	1.03	60.69	0.81	1.00	0.84	0.65	n/a	n/a	17	n/a
50.00	21.17	0.23	0.75	0.20	0.32	0.26	1.42	68.02	0.80	1.00	1.14	n/a	n/a	n/a	21	n/a
55.00	25.02	0.29	0.70	0.19	0.30	0.25	1.94	73.94	0.79	1.00	1.53	0.15	n/a	n/a	25	n/a

CRR7.5	Cyclic Resistance Ratio of clean sand for Moment Magnitude 7.5 earthquakes (Eq. 4, Ref. 1)
rd	stress reduction coefficient (Eq. 3, Ref. 1)
CSR	Cyclic Stress Ratio associated by the strong ground motion in the layer of interest (Eq. 1, Ref. 1)
FS	Factor of Safety against liquefaction (Eq. 23, ref. 1)
Dr	Relative Density, $Dr = (217 \cdot (N1)60)^{0.5}$
K σ	Correction for effective confining stress (Eq. 31, Ref 1)
K α	Correction for sloping ground (Figures 15, Ref. 1)
FS*	Factor of Safety against liquefaction modified to account for effective confining stress and static horizontal shear stress (Eq. 30, Ref. 1)
Ru	Excess Pore Pressure Ratio estimated from Figure 9.39 (Ref. 2)
(su)l-os	Undrained shear strength of liquefied sand (Olson and Stark procedure, Eq. 19b, Ref. 3)
(su)l-sh	Undrained shear strength of liquefied sand (Seed and Harder procedure, Ref 4, or refer to Figure 9.57, Ref. 2)
Ncorr	(N1)60 corrected for fines content as described by Seed and Harder (Ref 2 or Ref 4)

References

- 1 Youd et al (2001). Liquefaction Resistance of Soils: Summary from the 1996 NCEER and 1998 NCERR/NSF Workshops on Evaluation of Liquefaction Resistance of Soils, ASCE Journal of Geotechnical and Geoenvironmental Engineering, vol. 127, no. 10, pp. 817-833.
- 2 Kramer, S.L. (1996). *Geotechnical Earthquake Engineering*, Prentice Hall Publishers, 653 p.
- 3 Olson, S.M., and Stark, T. D. (2002). Liquefaction strength ratio from liquefaction flow failure case histories, Canadian Geotechnical Journal, vol. 39, pp. 629-647.
- 4 Seed, R.B., and Harder, L.F., Jr. (1990). "SPT-Based Analysis of Cyclic Pore Pressure Generation and Undrained Residual Strength," Proc. of the Memorial Symposium for H.Bolton Seed, Vol. 2, Bi-Tech Publishers, pp. 351-376.

CASE NO. 1 , M6.64
1 OF 2

SPREADSHEET FOR PERFORMING SIMPLIFIED LIQUEFACTION HAZARD EVALUATIONS

Modified January 24, 2005

The Simplified Procedure of Seed and Idriss is performed using the recommendations presented by Youd et al (2001)
All equations and relationships used in this spreadsheet are referenced at the bottom of the sheet.

Moment Magnitude	6.64	
Magnitude Scaling Factor	1.37	(Eq. 24, Ref. 1)
Peak Acceleration at the Ground Surface (g)	0.49	
Embankment height (ft)	25	
Moist unit weight of fill (pcf)	125	
Saturated unit weight of native soil (pcf)	100	
Depth to the groundwater table (ft)	0	

Depth (ft)	σ'_v (psf)	Nm (bl/ft)	CN	N1 (bl/ft)	CE	CB	CR	CS	(N1)60 (bl/ft)	Fines (%)	Parameter α	Parameter β	(N1)60cs (bl/ft)
5.00	188.00	3.00	1.71	5.12	1.00	1.05	0.75	1.00	4.03	4.00	0.00	1.00	4.02
10.00	376.00	2.00	1.60	3.19	1.00	1.05	0.75	1.00	2.51	4.00	0.00	1.00	2.51
15.00	564.00	5.00	1.50	7.49	1.00	1.05	1.00	1.00	7.86	4.00	0.00	1.00	7.85
20.00	752.00	5.00	1.41	7.06	1.00	1.05	1.00	1.00	7.41	12.00	1.55	1.03	9.20
25.00	940.00	7.00	1.34	9.35	1.00	1.05	1.00	1.00	9.81	12.00	1.55	1.03	11.68
30.00	1128.00	4.00	1.27	5.07	1.00	1.05	1.00	1.00	5.32	35.00	5.00	1.20	11.38
35.00	1316.00	8.00	1.20	9.64	1.00	1.05	1.00	1.00	10.12	35.00	5.00	1.20	17.14
40.00	1504.00	10.00	1.15	11.48	1.00	1.05	1.00	1.00	12.06	35.00	5.00	1.20	19.47
45.00	1767.00	15.00	1.08	16.17	1.00	1.05	1.00	1.00	16.97	2.00	0.00	0.99	16.85
50.00	2030.00	20.00	1.02	20.31	1.00	1.05	1.00	1.00	21.32	2.00	0.00	0.99	21.17
55.00	2293.00	25.00	0.96	24.00	1.00	1.05	1.00	1.00	25.20	2.00	0.00	0.99	25.02

σ'_v	Vertical effective stress
Nm	SPT N-value measured in the field
CN	SPT N-value stress correction factor (Eq. 10, Ref. 1)
N1	SPT N-value normalized for vertical effective stress
CE, CB, CR, CS	SPT N-value corrections (Table 2, Ref. 1)
α	Parameter for fines correction to SPT N-value (Eqs. 6a-6c, Ref. 1)
β	Parameter for fines correction to SPT N-value (Eqs. 7a-7c, Ref. 1)

**CASE NO. 1 , M6.64
2 OF 2**

Depth (ft)	(N1)60cs (bl/ft)	CRR7.5	rd	CSR centerline	CSR free-field	CSR average	FS CSRavg	Dr (%)	$K\sigma$	$K\alpha$	FS*	Ru	(su)l-os (psf)	(su)l-sh (psf)	Ncorr (blow/ft)	(su)l-avg (psf)
5.00	4.02	0.07	0.99	0.35	0.84	0.59	0.15	29.57	0.89	1.00	0.13	1.00	199.54	120.00	4	159.77
10.00	2.51	0.06	0.98	0.37	0.83	0.60	0.13	23.35	0.88	1.00	0.11	1.00	171.00	100.00	3	135.50
15.00	7.85	0.09	0.97	0.39	0.82	0.60	0.21	41.31	0.87	1.00	0.19	1.00	328.27	200.00	8	264.13
20.00	9.20	0.11	0.96	0.40	0.81	0.61	0.24	40.11	0.86	1.00	0.21	1.00	331.86	300.00	10	315.93
25.00	11.68	0.13	0.94	0.42	0.80	0.61	0.29	46.15	0.85	1.00	0.25	1.00	421.16	500.00	13	460.58
30.00	11.38	0.13	0.92	0.42	0.78	0.60	0.29	33.97	0.84	1.00	0.24	1.00	297.26	600.00	14	448.63
35.00	17.14	0.18	0.89	0.42	0.75	0.59	0.42	46.85	0.83	1.00	0.35	1.00	470.19	800.00	20	635.10
40.00	19.47	0.21	0.85	0.42	0.72	0.57	0.50	51.15	0.82	1.00	0.41	1.00	557.40	800.00	23	678.70
45.00	16.85	0.18	0.80	0.40	0.66	0.53	0.46	60.69	0.81	1.00	0.37	1.00	769.51	800.00	17	784.76
50.00	21.17	0.23	0.75	0.38	0.61	0.50	0.63	68.02	0.80	1.00	0.51	1.00	979.05	800.00	21	889.53
55.00	25.02	0.29	0.70	0.37	0.56	0.46	0.86	73.94	0.79	1.00	0.68	1.00	1186.44	800.00	25	993.22

CRR7.5	Cyclic Resistance Ratio of clean sand for Moment Magnitude 7.5 earthquakes (Eq. 4, Ref. 1)
rd	stress reduction coefficient (Eq. 3, Ref. 1)
CSR	Cyclic Stress Ratio associated by the strong ground motion in the layer of interest (Eq. 1, Ref. 1)
FS	Factor of Safety against liquefaction (Eq. 23, ref. 1)
Dr	Relative Density, $Dr = (217 \cdot (N1)60)^{0.5}$
$K\sigma$	Correction for effective confining stress (Eq. 31, Ref 1)
$K\alpha$	Correction for sloping ground (Figures 15, Ref. 1)
FS*	Factor of Safety against liquefaction modified to account for effective confining stress and static horizontal shear stress (Eq. 30, Ref. 1)
Ru	Excess Pore Pressure Ratio estimated from Figure 9.39 (Ref. 2)
(su)l-os	Undrained shear strength of liquefied sand (Olson and Stark procedure, Eq. 19b, Ref. 3)
(su)l-sh	Undrained shear strength of liquefied sand (Seed and Harder procedure, Ref 4, or refer to Figure 9.57, Ref. 2)
Ncorr	(N1)60 corrected for fines content as described by Seed and Harder (Ref 2 or Ref 4)

References

- 1 Youd et al (2001). Liquefaction Resistance of Soils: Summary from the 1996 NCEER and 1998 NCERR/NSF Workshops on Evaluation of Liquefaction Resistance of Soils, ASCE Journal of Geotechnical and Geoenvironmental Engineering, vol. 127, no. 10, pp. 817-833.
- 2 Kramer, S.L. (1996). Geotechnical Earthquake Engineering, Prentice Hall Publishers, 653 p.
- 3 Olson, S.M., and Stark, T. D. (2002). Liquefaction strength ratio from liquefaction flow failure case histories, Canadian Geotechnical Journal, vol. 39, pp. 629-647.
- 4 Seed, R.B., and Harder, L.F., Jr. (1990). "SPT-Based Analysis of Cyclic Pore Pressure Generation and Undrained Residual Strength," Proc. of the Memorial Symposium for H.Bolton Seed, Vol. 2, Bi-Tech Publishers, pp. 351-376.

CASE NO. 1 , M8.3
1 OF 2

SPREADSHEET FOR PERFORMING SIMPLIFIED LIQUEFACTION HAZARD EVALUATIONS

Modified January 24, 2005

The Simplified Procedure of Seed and Idriss is performed using the recommendations presented by Youd et al (2001)
All equations and relationships used in this spreadsheet are referenced at the bottom of the sheet.

Moment Magnitude	8.3	
Magnitude Scaling Factor	0.77	(Eq. 24, Ref. 1)
Peak Acceleration at the Ground Surface (g)	0.18	
Embankment height (ft)	25	
Moist unit weight of fill (pcf)	125	
Saturated unit weight of native soil (pcf)	100	
Depth to the groundwater table (ft)	0	

Depth (ft)	σ'_v (psf)	Nm (bl/ft)	CN	N1 (bl/ft)	CE	CB	CR	CS	(N1)60 (bl/ft)	Fines (%)	Parameter α	Parameter β	(N1)60cs (bl/ft)
5.00	188.00	3.00	1.71	5.12	1.00	1.05	0.75	1.00	4.03	4.00	0.00	1.00	4.02
10.00	376.00	2.00	1.60	3.19	1.00	1.05	0.75	1.00	2.51	4.00	0.00	1.00	2.51
15.00	564.00	5.00	1.50	7.49	1.00	1.05	1.00	1.00	7.86	4.00	0.00	1.00	7.85
20.00	752.00	5.00	1.41	7.06	1.00	1.05	1.00	1.00	7.41	12.00	1.55	1.03	9.20
25.00	940.00	7.00	1.34	9.35	1.00	1.05	1.00	1.00	9.81	12.00	1.55	1.03	11.68
30.00	1128.00	4.00	1.27	5.07	1.00	1.05	1.00	1.00	5.32	35.00	5.00	1.20	11.38
35.00	1316.00	8.00	1.20	9.64	1.00	1.05	1.00	1.00	10.12	35.00	5.00	1.20	17.14
40.00	1504.00	10.00	1.15	11.48	1.00	1.05	1.00	1.00	12.06	35.00	5.00	1.20	19.47
45.00	1767.00	15.00	1.08	16.17	1.00	1.05	1.00	1.00	16.97	2.00	0.00	0.99	16.85
50.00	2030.00	20.00	1.02	20.31	1.00	1.05	1.00	1.00	21.32	2.00	0.00	0.99	21.17
55.00	2293.00	25.00	0.96	24.00	1.00	1.05	1.00	1.00	25.20	2.00	0.00	0.99	25.02

σ'_v	Vertical effective stress
Nm	SPT N-value measured in the field
CN	SPT N-value stress correction factor (Eq. 10, Ref. 1)
N1	SPT N-value normalized for vertical effective stress
CE, CB, CR, CS	SPT N-value corrections (Table 2, Ref. 1)
α	Parameter for fines correction to SPT N-value (Eqs. 6a-6c, Ref. 1)
β	Parameter for fines correction to SPT N-value (Eqs. 7a-7c, Ref. 1)

**CASE NO. 1 , M8.3
2 OF 2**

Depth (ft)	(N1)60cs (bl/ft)	CRR7.5	rd	CSR centerline	CSR free-field	CSR average	FS CSRavg	Dr (%)	K σ	K α	FS*	Ru	(su)l-os (psf)	(su)l-sh (psf)	Ncorr (blow/ft)	(su)l-avg (psf)
5.00	4.02	0.07	0.99	0.13	0.31	0.22	0.23	29.57	0.89	1.00	0.21	1.00	199.54	120.00	4	159.77
10.00	2.51	0.06	0.98	0.13	0.30	0.22	0.19	23.35	0.88	1.00	0.17	1.00	171.00	100.00	3	135.50
15.00	7.85	0.09	0.97	0.14	0.30	0.22	0.33	41.31	0.87	1.00	0.29	1.00	328.27	200.00	8	264.13
20.00	9.20	0.11	0.96	0.15	0.30	0.22	0.37	40.11	0.86	1.00	0.32	1.00	331.86	300.00	10	315.93
25.00	11.68	0.13	0.94	0.15	0.29	0.22	0.44	46.15	0.85	1.00	0.38	1.00	421.16	500.00	13	460.58
30.00	11.38	0.13	0.92	0.16	0.29	0.22	0.44	33.97	0.84	1.00	0.37	1.00	297.26	600.00	14	448.63
35.00	17.14	0.18	0.89	0.16	0.28	0.22	0.65	46.85	0.83	1.00	0.54	1.00	470.19	800.00	20	635.10
40.00	19.47	0.21	0.85	0.15	0.26	0.21	0.77	51.15	0.82	1.00	0.63	1.00	557.40	800.00	23	678.70
45.00	16.85	0.18	0.80	0.15	0.24	0.20	0.71	60.69	0.81	1.00	0.57	1.00	769.51	800.00	17	784.76
50.00	21.17	0.23	0.75	0.14	0.22	0.18	0.97	68.02	0.80	1.00	0.78	1.00	979.05	800.00	21	889.53
55.00	25.02	0.29	0.70	0.13	0.21	0.17	1.33	73.94	0.79	1.00	1.05	1.00	n/a	n/a	25	n/a

CRR7.5	Cyclic Resistance Ratio of clean sand for Moment Magnitude 7.5 earthquakes (Eq. 4, Ref. 1)
rd	stress reduction coefficient (Eq. 3, Ref. 1)
CSR	Cyclic Stress Ratio associated by the strong ground motion in the layer of interest (Eq. 1, Ref. 1)
FS	Factor of Safety against liquefaction (Eq. 23, ref. 1)
Dr	Relative Density, $Dr = (217 \cdot (N1)60)^{0.5}$
K σ	Correction for effective confining stress (Eq. 31, Ref 1)
K α	Correction for sloping ground (Figures 15, Ref. 1)
FS*	Factor of Safety against liquefaction modified to account for effective confining stress and static horizontal shear stress (Eq. 30, Ref. 1)
Ru	Excess Pore Pressure Ratio estimated from Figure 9.39 (Ref. 2)
(su)l-os	Undrained shear strength of liquefied sand (Olson and Stark procedure, Eq. 19b, Ref. 3)
(su)l-sh	Undrained shear strength of liquefied sand (Seed and Harder procedure, Ref 4, or refer to Figure 9.57, Ref. 2)
Ncorr	(N1)60 corrected for fines content as described by Seed and Harder (Ref 2 or Ref 4)

References

- 1 Youd et al (2001). Liquefaction Resistance of Soils: Summary from the 1996 NCEER and 1998 NCERR/NSF Workshops on Evaluation of Liquefaction Resistance of Soils, ASCE Journal of Geotechnical and Geoenvironmental Engineering, vol. 127, no. 10, pp. 817-833.
- 2 Kramer, S.L. (1996). Geotechnical Earthquake Engineering, Prentice Hall Publishers, 653 p.
- 3 Olson, S.M., and Stark, T. D. (2002). Liquefaction strength ratio from liquefaction flow failure case histories, Canadian Geotechnical Journal, vol. 39, pp. 629-647.
- 4 Seed, R.B., and Harder, L.F., Jr. (1990). "SPT-Based Analysis of Cyclic Pore Pressure Generation and Undrained Residual Strength," Proc. of the Memorial Symposium for H.Bolton Seed, Vol. 2, Bi-Tech Publishers, pp. 351-376.

CASE NO. 1 , M9.0
1 OF 2

SPREADSHEET FOR PERFORMING SIMPLIFIED LIQUEFACTION HAZARD EVALUATIONS

Modified January 24, 2005

The Simplified Procedure of Seed and Idriss is performed using the recommendations presented by Youd et al (2001)
All equations and relationships used in this spreadsheet are referenced at the bottom of the sheet.

Moment Magnitude	9	
Magnitude Scaling Factor	0.63	(Eq. 24, Ref. 1)
Peak Acceleration at the Ground Surface (g)	0.22	
Embankment height (ft)	25	
Moist unit weight of fill (pcf)	125	
Saturated unit weight of native soil (pcf)	100	
Depth to the groundwater table (ft)	0	

Depth (ft)	$\sigma'v$ (psf)	Nm (bl/ft)	CN	N1 (bl/ft)	CE	CB	CR	CS	(N1)60 (bl/ft)	Fines (%)	Parameter α	Parameter β	(N1)60cs (bl/ft)
5.00	188.00	3.00	1.71	5.12	1.00	1.05	0.75	1.00	4.03	4.00	0.00	1.00	4.02
10.00	376.00	2.00	1.60	3.19	1.00	1.05	0.75	1.00	2.51	4.00	0.00	1.00	2.51
15.00	564.00	5.00	1.50	7.49	1.00	1.05	1.00	1.00	7.86	4.00	0.00	1.00	7.85
20.00	752.00	5.00	1.41	7.06	1.00	1.05	1.00	1.00	7.41	12.00	1.55	1.03	9.20
25.00	940.00	7.00	1.34	9.35	1.00	1.05	1.00	1.00	9.81	12.00	1.55	1.03	11.68
30.00	1128.00	4.00	1.27	5.07	1.00	1.05	1.00	1.00	5.32	35.00	5.00	1.20	11.38
35.00	1316.00	8.00	1.20	9.64	1.00	1.05	1.00	1.00	10.12	35.00	5.00	1.20	17.14
40.00	1504.00	10.00	1.15	11.48	1.00	1.05	1.00	1.00	12.06	35.00	5.00	1.20	19.47
45.00	1767.00	15.00	1.08	16.17	1.00	1.05	1.00	1.00	16.97	2.00	0.00	0.99	16.85
50.00	2030.00	20.00	1.02	20.31	1.00	1.05	1.00	1.00	21.32	2.00	0.00	0.99	21.17
55.00	2293.00	25.00	0.96	24.00	1.00	1.05	1.00	1.00	25.20	2.00	0.00	0.99	25.02

$\sigma'v$	Vertical effective stress
Nm	SPT N-value measured in the field
CN	SPT N-value stress correction factor (Eq. 10, Ref. 1)
N1	SPT N-value normalized for vertical effective stress
CE, CB, CR, CS	SPT N-value corrections (Table 2, Ref. 1)
α	Parameter for fines correction to SPT N-value (Eqs. 6a-6c, Ref. 1)
β	Parameter for fines correction to SPT N-value (Eqs. 7a-7c, Ref. 1)

**CASE NO. 1 , M9.0
2 OF 2**

Depth (ft)	(N1)60cs (bl/ft)	CRR7.5	rd	CSR centerline	CSR free-field	CSR average	FS CSRavg	Dr (%)	K σ	K α	FS*	Ru	(su)l-os (psf)	(su)l-sh (psf)	Ncorr (blow/ft)	(su)l-avg (psf)
5.00	4.02	0.07	0.99	0.15	0.38	0.27	0.15	29.57	0.89	1.00	0.14	1.00	199.54	120.00	4	159.77
10.00	2.51	0.06	0.98	0.16	0.37	0.27	0.13	23.35	0.88	1.00	0.11	1.00	171.00	100.00	3	135.50
15.00	7.85	0.09	0.97	0.17	0.37	0.27	0.22	41.31	0.87	1.00	0.19	1.00	328.27	200.00	8	264.13
20.00	9.20	0.11	0.96	0.18	0.36	0.27	0.24	40.11	0.86	1.00	0.21	1.00	331.86	300.00	10	315.93
25.00	11.68	0.13	0.94	0.19	0.36	0.27	0.30	46.15	0.85	1.00	0.25	1.00	421.16	500.00	13	460.58
30.00	11.38	0.13	0.92	0.19	0.35	0.27	0.29	33.97	0.84	1.00	0.24	1.00	297.26	600.00	14	448.63
35.00	17.14	0.18	0.89	0.19	0.34	0.26	0.43	46.85	0.83	1.00	0.36	1.00	470.19	800.00	20	635.10
40.00	19.47	0.21	0.85	0.19	0.32	0.26	0.51	51.15	0.82	1.00	0.42	1.00	557.40	800.00	23	678.70
45.00	16.85	0.18	0.80	0.18	0.30	0.24	0.47	60.69	0.81	1.00	0.38	1.00	769.51	800.00	17	784.76
50.00	21.17	0.23	0.75	0.17	0.27	0.22	0.65	68.02	0.80	1.00	0.52	1.00	979.05	800.00	21	889.53
55.00	25.02	0.29	0.70	0.16	0.25	0.21	0.88	73.94	0.79	1.00	0.70	1.00	1186.44	800.00	25	993.22

CRR7.5	Cyclic Resistance Ratio of clean sand for Moment Magnitude 7.5 earthquakes (Eq. 4, Ref. 1)
rd	stress reduction coefficient (Eq. 3, Ref. 1)
CSR	Cyclic Stress Ratio associated by the strong ground motion in the layer of interest (Eq. 1, Ref. 1)
FS	Factor of Safety against liquefaction (Eq. 23, ref. 1)
Dr	Relative Density, $Dr = (217 \cdot (N1)60)^{0.5}$
K σ	Correction for effective confining stress (Eq. 31, Ref 1)
K α	Correction for sloping ground (Figures 15, Ref. 1)
FS*	Factor of Safety against liquefaction modified to account for effective confining stress and static horizontal shear stress (Eq. 30, Ref. 1)
Ru	Excess Pore Pressure Ratio estimated from Figure 9.39 (Ref. 2)
(su)l-os	Undrained shear strength of liquefied sand (Olson and Stark procedure, Eq. 19b, Ref. 3)
(su)l-sh	Undrained shear strength of liquefied sand (Seed and Harder procedure, Ref 4, or refer to Figure 9.57, Ref. 2)
Ncorr	(N1)60 corrected for fines content as described by Seed and Harder (Ref 2 or Ref 4)

References

- 1 Youd et al (2001). Liquefaction Resistance of Soils: Summary from the 1996 NCEER and 1998 NCERR/NSF Workshops on Evaluation of Liquefaction Resistance of Soils, ASCE Journal of Geotechnical and Geoenvironmental Engineering, vol. 127, no. 10, pp. 817-833.
- 2 Kramer, S.L. (1996). Geotechnical Earthquake Engineering, Prentice Hall Publishers, 653 p.
- 3 Olson, S.M., and Stark, T. D. (2002). Liquefaction strength ratio from liquefaction flow failure case histories, Canadian Geotechnical Journal, vol. 39, pp. 629-647.
- 4 Seed, R.B., and Harder, L.F., Jr. (1990). "SPT-Based Analysis of Cyclic Pore Pressure Generation and Undrained Residual Strength," Proc. of the Memorial Symposium for H.Bolton Seed, Vol. 2, Bi-Tech Publishers, pp. 351-376.

CASE NO. 2 , M6.2
1 OF 2

SPREADSHEET FOR PERFORMING SIMPLIFIED LIQUEFACTION HAZARD EVALUATIONS

Modified January 24, 2005

The Simplified Procedure of Seed and Idriss is performed using the recommendations presented by Youd et al (2001)
All equations and relationships used in this spreadsheet are referenced at the bottom of the sheet.

Moment Magnitude	6.20	
Magnitude Scaling Factor	1.63	(Eq. 24, Ref. 1)
Peak Acceleration at the Ground Surface (g)	0.26	
Embankment height (ft)	25	
Moist unit weight of fill (pcf)	125	
Saturated unit weight of native soil (pcf)	125	
Depth to the groundwater table (ft)	0	

Depth (ft)	σ'_v (psf)	Nm (bl/ft)	CN	N1 (bl/ft)	CE	CB	CR	CS	(N1)60 (bl/ft)	Fines (%)	Parameter α	Parameter β	(N1)60cs (bl/ft)
5.00	313.00	24.00	1.63	39.14	1.00	1.05	0.75	1.00	30.82	4.00	0.00	1.00	30.76
10.00	626.00	26.00	1.47	38.18	1.00	1.05	0.75	1.00	30.07	4.00	0.00	1.00	30.01
15.00	939.00	22.00	1.34	29.38	1.00	1.05	1.00	1.00	30.85	4.00	0.00	1.00	30.79
20.00	1252.00	22.00	1.22	26.95	1.00	1.05	1.00	1.00	28.29	12.00	1.55	1.03	30.74
25.00	1565.00	19.00	1.13	21.49	1.00	1.05	1.00	1.00	22.56	12.00	1.55	1.03	24.83
30.00	1878.00	17.00	1.05	17.86	1.00	1.05	1.00	1.00	18.75	35.00	5.00	1.20	27.50
35.00	2191.00	21.00	0.98	20.59	1.00	1.05	1.00	1.00	21.62	35.00	5.00	1.20	30.95
40.00	2504.00	22.00	0.92	20.23	1.00	1.05	1.00	1.00	21.24	35.00	5.00	1.20	30.49
45.00	2817.00	20.00	0.87	17.31	1.00	1.05	1.00	1.00	18.18	2.00	0.00	0.99	18.05
50.00	3130.00	25.00	0.82	20.44	1.00	1.05	1.00	1.00	21.46	2.00	0.00	0.99	21.31
55.00	3443.00	30.00	0.77	23.24	1.00	1.05	1.00	1.00	24.41	2.00	0.00	0.99	24.23

σ'_v	Vertical effective stress
Nm	SPT N-value measured in the field
CN	SPT N-value stress correction factor (Eq. 10, Ref. 1)
N1	SPT N-value normalized for vertical effective stress
CE, CB, CR, CS	SPT N-value corrections (Table 2, Ref. 1)
α	Parameter for fines correction to SPT N-value (Eqs. 6a-6c, Ref. 1)
β	Parameter for fines correction to SPT N-value (Eqs. 7a-7c, Ref. 1)

CASE NO. 2 , M6.2
2 OF 2

Depth (ft)	(N1)60cs (bl/ft)	CRR7.5	rd	CSR centerline	CSR free-field	CSR average	FS CSRavg	Dr (%)	K σ	K α	FS*	Ru	(su)l-os (psf)	(su)l-sh (psf)	Ncorr (blow/ft)	(su)l-avg (psf)	(su)l-os free-flid
5.00	30.76	0.53	0.99	0.18	0.33	0.26	3.35	81.78	0.89	1.00	2.97	n/a	n/a	n/a	4	n/a	n/a
10.00	30.01	0.47	0.98	0.19	0.33	0.26	2.91	80.78	0.87	1.00	2.52	n/a	n/a	n/a	3	n/a	n/a
15.00	30.79	0.54	0.97	0.20	0.33	0.26	3.30	81.82	0.85	1.00	2.80	n/a	n/a	n/a	8	n/a	n/a
20.00	30.74	0.53	0.96	0.21	0.32	0.27	3.25	78.36	0.83	1.00	2.71	n/a	n/a	n/a	10	n/a	n/a
25.00	24.83	0.29	0.94	0.21	0.32	0.26	1.77	69.97	0.82	1.00	1.45	n/a	n/a	n/a	13	n/a	n/a
30.00	27.50	0.35	0.92	0.21	0.31	0.26	2.19	63.79	0.81	1.00	1.77	n/a	n/a	n/a	14	n/a	n/a
35.00	30.95	0.55	0.89	0.21	0.30	0.26	3.51	68.50	0.79	1.00	2.78	n/a	n/a	n/a	20	n/a	n/a
40.00	30.49	0.51	0.85	0.21	0.29	0.25	3.33	67.89	0.78	1.00	2.61	n/a	n/a	n/a	23	n/a	n/a
45.00	18.05	0.19	0.80	0.20	0.27	0.23	1.34	62.81	0.77	1.00	1.03	0.65	n/a	n/a	17	n/a	n/a
50.00	21.31	0.23	0.75	0.19	0.25	0.22	1.73	68.25	0.76	1.00	1.31	0.20	n/a	n/a	21	n/a	n/a
55.00	24.23	0.28	0.70	0.18	0.23	0.21	2.20	72.77	0.75	1.00	1.66	n/a	n/a	n/a	25	n/a	n/a

CRR7.5	Cyclic Resistance Ratio of clean sand for Moment Magnitude 7.5 earthquakes (Eq. 4, Ref. 1)
rd	stress reduction coefficient (Eq. 3, Ref. 1)
CSR	Cyclic Stress Ratio associated by the strong ground motion in the layer of interest (Eq. 1, Ref. 1)
FS	Factor of Safety against liquefaction (Eq. 23, ref. 1)
Dr	Relative Density, $Dr = (217 \cdot (N1)60)^{0.5}$
K σ	Correction for effective confining stress (Eq. 31, Ref 1)
K α	Correction for sloping ground (Figures 15, Ref. 1)
FS*	Factor of Safety against liquefaction modified to account for effective confining stress and static horizontal shear stress (Eq. 30, Ref. 1)
Ru	Excess Pore Pressure Ratio estimated from Figure 9.39 (Ref. 2)
(su)l-os	Undrained shear strength of liquefied sand (Olson and Stark procedure, Eq. 19b, Ref. 3)
(su)l-sh	Undrained shear strength of liquefied sand (Seed and Harder procedure, Ref 4, or refer to Figure 9.57, Ref. 2)
Ncorr	(N1)60 corrected for fines content as described by Seed and Harder (Ref 2 or Ref 4)

References

- 1 Youd et al (2001). Liquefaction Resistance of Soils: Summary from the 1996 NCEER and 1998 NCERR/NSF Workshops on Evaluation of Liquefaction Resistance of Soils, ASCE Journal of Geotechnical and Geoenvironmental Engineering, vol. 127, no. 10, pp. 817-833.
- 2 Kramer, S.L. (1996). Geotechnical Earthquake Engineering, Prentice Hall Publishers, 653 p.
- 3 Olson, S.M., and Stark, T. D. (2002). Liquefaction strength ratio from liquefaction flow failure case histories, Canadian Geotechnical Journal, vol. 39, pp. 629-647.
- 4 Seed, R.B., and Harder, L.F., Jr. (1990). "SPT-Based Analysis of Cyclic Pore Pressure Generation and Undrained Residual Strength," Proc. of the Memorial Symposium for H.Bolton Seed, Vol. 2, Bi-Tech Publishers, pp. 351-376.

CASE NO. 2 , M6.64
1 OF 2

SPREADSHEET FOR PERFORMING SIMPLIFIED LIQUEFACTION HAZARD EVALUATIONS

Modified January 24, 2005

The Simplified Procedure of Seed and Idriss is performed using the recommendations presented by Youd et al (2001)
All equations and relationships used in this spreadsheet are referenced at the bottom of the sheet.

Moment Magnitude	6.64	
Magnitude Scaling Factor	1.37	(Eq. 24, Ref. 1)
Peak Acceleration at the Ground Surface (g)	0.49	
Embankment height (ft)	25	
Moist unit weight of fill (pcf)	125	
Saturated unit weight of native soil (pcf)	125	
Depth to the groundwater table (ft)	0	

Depth (ft)	σ'_v (psf)	Nm (bl/ft)	CN	N1 (bl/ft)	CE	CB	CR	CS	(N1)60 (bl/ft)	Fines (%)	Parameter α	Parameter β	(N1)60cs (bl/ft)
5.00	313.00	24.00	1.63	39.14	1.00	1.05	0.75	1.00	30.82	4.00	0.00	1.00	30.76
10.00	626.00	26.00	1.47	38.18	1.00	1.05	0.75	1.00	30.07	4.00	0.00	1.00	30.01
15.00	939.00	22.00	1.34	29.38	1.00	1.05	1.00	1.00	30.85	4.00	0.00	1.00	30.79
20.00	1252.00	22.00	1.22	26.95	1.00	1.05	1.00	1.00	28.29	12.00	1.55	1.03	30.74
25.00	1565.00	19.00	1.13	21.49	1.00	1.05	1.00	1.00	22.56	12.00	1.55	1.03	24.83
30.00	1878.00	17.00	1.05	17.86	1.00	1.05	1.00	1.00	18.75	35.00	5.00	1.20	27.50
35.00	2191.00	21.00	0.98	20.59	1.00	1.05	1.00	1.00	21.62	35.00	5.00	1.20	30.95
40.00	2504.00	22.00	0.92	20.23	1.00	1.05	1.00	1.00	21.24	35.00	5.00	1.20	30.49
45.00	2817.00	20.00	0.87	17.31	1.00	1.05	1.00	1.00	18.18	2.00	0.00	0.99	18.05
50.00	3130.00	25.00	0.82	20.44	1.00	1.05	1.00	1.00	21.46	2.00	0.00	0.99	21.31
55.00	3443.00	30.00	0.77	23.24	1.00	1.05	1.00	1.00	24.41	2.00	0.00	0.99	24.23

σ'_v	Vertical effective stress
Nm	SPT N-value measured in the field
CN	SPT N-value stress correction factor (Eq. 10, Ref. 1)
N1	SPT N-value normalized for vertical effective stress
CE, CB, CR, CS	SPT N-value corrections (Table 2, Ref. 1)
α	Parameter for fines correction to SPT N-value (Eqs. 6a-6c, Ref. 1)
β	Parameter for fines correction to SPT N-value (Eqs. 7a-7c, Ref. 1)

**CASE NO. 2 , M6.64
2 OF 2**

Depth (ft)	(N1)60cs (bl/ft)	CRR7.5	rd	CSR centerline	CSR free-field	CSR average	FS CSRavg	Dr (%)	K σ	K α	FS*	Ru	(su)l-os (psf)	(su)l-sh (psf)	Ncorr (blow/ft)	(su)l-avg (psf)	(su)l-os free-fld
5.00	30.76	0.53	0.99	0.34	0.63	0.49	1.49	81.78	0.89	1.00	1.32	0.19	n/a	n/a	4	n/a	n/a
10.00	30.01	0.47	0.98	0.36	0.62	0.49	1.30	80.78	0.87	1.00	1.12	0.39	n/a	n/a	3	n/a	n/a
15.00	30.79	0.54	0.97	0.38	0.62	0.50	1.47	81.82	0.85	1.00	1.25	0.24	n/a	n/a	8	n/a	n/a
20.00	30.74	0.53	0.96	0.39	0.61	0.50	1.45	78.36	0.83	1.00	1.21	0.27	n/a	n/a	10	n/a	n/a
25.00	24.83	0.29	0.94	0.40	0.60	0.50	0.79	69.97	0.82	1.00	0.65	1.00	934.35	500.00	13	717.17	311.78
30.00	27.50	0.35	0.92	0.40	0.59	0.49	0.98	63.79	0.81	1.00	0.79	1.00	853.68	600.00	14	726.84	320.45
35.00	30.95	0.55	0.89	0.40	0.57	0.48	1.56	68.50	0.79	1.00	1.24	0.25	n/a	n/a	20	n/a	n/a
40.00	30.49	0.51	0.85	0.39	0.54	0.47	1.48	67.89	0.78	1.00	1.16	0.33	n/a	n/a	23	n/a	n/a
45.00	18.05	0.19	0.80	0.37	0.51	0.44	0.60	62.81	0.77	1.00	0.46	1.00	988.40	800.00	17	894.20	468.58
50.00	21.31	0.23	0.75	0.36	0.47	0.41	0.77	68.25	0.76	1.00	0.59	1.00	1194.61	800.00	21	997.30	597.78
55.00	24.23	0.28	0.70	0.34	0.44	0.39	0.98	72.77	0.75	1.00	0.74	1.00	1399.25	800.00	25	1099.63	733.50

CRR7.5	Cyclic Resistance Ratio of clean sand for Moment Magnitude 7.5 earthquakes (Eq. 4, Ref. 1)
rd	stress reduction coefficient (Eq. 3, Ref. 1)
CSR	Cyclic Stress Ratio associated by the strong ground motion in the layer of interest (Eq. 1, Ref. 1)
FS	Factor of Safety against liquefaction (Eq. 23, ref. 1)
Dr	Relative Density, $Dr = (217 \cdot (N1)60)^{0.5}$
K σ	Correction for effective confining stress (Eq. 31, Ref 1)
K α	Correction for sloping ground (Figures 15, Ref. 1)
FS*	Factor of Safety against liquefaction modified to account for effective confining stress and static horizontal shear stress (Eq. 30, Ref. 1)
Ru	Excess Pore Pressure Ratio estimated from Figure 9.39 (Ref. 2)
(su)l-os	Undrained shear strength of liquefied sand (Olson and Stark procedure, Eq. 19b, Ref. 3)
(su)l-sh	Undrained shear strength of liquefied sand (Seed and Harder procedure, Ref 4, or refer to Figure 9.57, Ref. 2)
Ncorr	(N1)60 corrected for fines content as described by Seed and Harder (Ref 2 or Ref 4)

References

- 1 Youd et al (2001). Liquefaction Resistance of Soils: Summary from the 1996 NCEER and 1998 NCERR/NSF Workshops on Evaluation of Liquefaction Resistance of Soils, ASCE Journal of Geotechnical and Geoenvironmental Engineering, vol. 127, no. 10, pp. 817-833.
- 2 Kramer, S.L. (1996). Geotechnical Earthquake Engineering, Prentice Hall Publishers, 653 p.
- 3 Olson, S.M., and Stark, T. D. (2002). Liquefaction strength ratio from liquefaction flow failure case histories, Canadian Geotechnical Journal, vol. 39, pp. 629-647.
- 4 Seed, R.B., and Harder, L.F., Jr. (1990). "SPT-Based Analysis of Cyclic Pore Pressure Generation and Undrained Residual Strength," Proc. of the Memorial Symposium for H.Bolton Seed, Vol. 2, Bi-Tech Publishers, pp. 351-376.

CASE NO. 2 , M8.3
1 OF 2

SPREADSHEET FOR PERFORMING SIMPLIFIED LIQUEFACTION HAZARD EVALUATIONS

Modified January 24, 2005

The Simplified Procedure of Seed and Idriss is performed using the recommendations presented by Youd et al (2001)
All equations and relationships used in this spreadsheet are referenced at the bottom of the sheet.

Moment Magnitude	8.0	
Magnitude Scaling Factor	0.85	(Eq. 24, Ref. 1)
Peak Acceleration at the Ground Surface (g)	0.18	
Embankment height (ft)	25	
Moist unit weight of fill (pcf)	125	
Saturated unit weight of native soil (pcf)	125	
Depth to the groundwater table (ft)	0	

Depth (ft)	σ'_v (psf)	Nm (bl/ft)	CN	N1 (bl/ft)	CE	CB	CR	CS	(N1)60 (bl/ft)	Fines (%)	Parameter α	Parameter β	(N1)60cs (bl/ft)
5.00	313.00	24.00	1.63	39.14	1.00	1.05	0.75	1.00	30.82	4.00	0.00	1.00	30.76
10.00	626.00	26.00	1.47	38.18	1.00	1.05	0.75	1.00	30.07	4.00	0.00	1.00	30.01
15.00	939.00	22.00	1.34	29.38	1.00	1.05	1.00	1.00	30.85	4.00	0.00	1.00	30.79
20.00	1252.00	22.00	1.22	26.95	1.00	1.05	1.00	1.00	28.29	12.00	1.55	1.03	30.74
25.00	1565.00	19.00	1.13	21.49	1.00	1.05	1.00	1.00	22.56	12.00	1.55	1.03	24.83
30.00	1878.00	17.00	1.05	17.86	1.00	1.05	1.00	1.00	18.75	35.00	5.00	1.20	27.50
35.00	2191.00	21.00	0.98	20.59	1.00	1.05	1.00	1.00	21.62	35.00	5.00	1.20	30.95
40.00	2504.00	22.00	0.92	20.23	1.00	1.05	1.00	1.00	21.24	35.00	5.00	1.20	30.49
45.00	2817.00	20.00	0.87	17.31	1.00	1.05	1.00	1.00	18.18	2.00	0.00	0.99	18.05
50.00	3130.00	25.00	0.82	20.44	1.00	1.05	1.00	1.00	21.46	2.00	0.00	0.99	21.31
55.00	3443.00	30.00	0.77	23.24	1.00	1.05	1.00	1.00	24.41	2.00	0.00	0.99	24.23

σ'_v	Vertical effective stress
Nm	SPT N-value measured in the field
CN	SPT N-value stress correction factor (Eq. 10, Ref. 1)
N1	SPT N-value normalized for vertical effective stress
CE, CB, CR, CS	SPT N-value corrections (Table 2, Ref. 1)
α	Parameter for fines correction to SPT N-value (Eqs. 6a-6c, Ref. 1)
β	Parameter for fines correction to SPT N-value (Eqs. 7a-7c, Ref. 1)

CASE NO. 2 , M8.3
2 OF 2

Depth (ft)	(N1)60cs (bl/ft)	CRR7.5	rd	CSR centerline	CSR free-field	CSR average	FS CSRavg	Dr (%)	K σ	K α	FS*	Ru	(su)l-os (psf)	(su)l-sh (psf)	Ncorr (blow/ft)	(su)l-avg (psf)	(su)l-os free-fld	
5.00	30.76	0.53	0.99	0.13	0.23	0.18	2.52	81.78	0.89	1.00	2.23	n/a	n/a	n/a		4	n/a	n/a
10.00	30.01	0.47	0.98	0.13	0.23	0.18	2.19	80.78	0.87	1.00	1.90	n/a	n/a	n/a		3	n/a	n/a
15.00	30.79	0.54	0.97	0.14	0.23	0.18	2.48	81.82	0.85	1.00	2.11	n/a	n/a	n/a		8	n/a	n/a
20.00	30.74	0.53	0.96	0.14	0.22	0.18	2.44	78.36	0.83	1.00	2.04	n/a	n/a	n/a		10	n/a	n/a
25.00	24.83	0.29	0.94	0.15	0.22	0.18	1.33	69.97	0.82	1.00	1.09	0.45	n/a	n/a		13	n/a	n/a
30.00	27.50	0.35	0.92	0.15	0.22	0.18	1.65	63.79	0.81	1.00	1.33	0.19	n/a	n/a		14	n/a	n/a
35.00	30.95	0.55	0.89	0.15	0.21	0.18	2.64	68.50	0.79	1.00	2.09	n/a	n/a	n/a		20	n/a	n/a
40.00	30.49	0.51	0.85	0.14	0.20	0.17	2.50	67.89	0.78	1.00	1.96	n/a	n/a	n/a		23	n/a	n/a
45.00	18.05	0.19	0.80	0.14	0.19	0.16	1.01	62.81	0.77	1.00	0.78	1.00	988.40	800.00		17	894.20	468.58
50.00	21.31	0.23	0.75	0.13	0.17	0.15	1.30	68.25	0.76	1.00	0.99	1.00	1194.61	800.00		21	997.30	597.78
55.00	24.23	0.28	0.70	0.12	0.16	0.14	1.66	72.77	0.75	1.00	1.25	0.24	n/a	n/a		25	n/a	n/a

CRR7.5	Cyclic Resistance Ratio of clean sand for Moment Magnitude 7.5 earthquakes (Eq. 4, Ref. 1)
rd	stress reduction coefficient (Eq. 3, Ref. 1)
CSR	Cyclic Stress Ratio associated by the strong ground motion in the layer of interest (Eq. 1, Ref. 1)
FS	Factor of Safety against liquefaction (Eq. 23, ref. 1)
Dr	Relative Density, $Dr = (217 \cdot (N1)60)^{0.5}$
K σ	Correction for effective confining stress (Eq. 31, Ref 1)
K α	Correction for sloping ground (Figures 15, Ref. 1)
FS*	Factor of Safety against liquefaction modified to account for effective confining stress and static horizontal shear stress (Eq. 30, Ref. 1)
Ru	Excess Pore Pressure Ratio estimated from Figure 9.39 (Ref. 2)
(su)l-os	Undrained shear strength of liquefied sand (Olson and Stark procedure, Eq. 19b, Ref. 3)
(su)l-sh	Undrained shear strength of liquefied sand (Seed and Harder procedure, Ref 4, or refer to Figure 9.57, Ref. 2)
Ncorr	(N1)60 corrected for fines content as described by Seed and Harder (Ref 2 or Ref 4)

References

- 1 Youd et al (2001). Liquefaction Resistance of Soils: Summary from the 1996 NCEER and 1998 NCERR/NSF Workshops on Evaluation of Liquefaction Resistance of Soils, ASCE Journal of Geotechnical and Geoenvironmental Engineering, vol. 127, no. 10, pp. 817-833.
- 2 Kramer, S.L. (1996). Geotechnical Earthquake Engineering, Prentice Hall Publishers, 653 p.
- 3 Olson, S.M., and Stark, T. D. (2002). Liquefaction strength ratio from liquefaction flow failure case histories, Canadian Geotechnical Journal, vol. 39, pp. 629-647.
- 4 Seed, R.B., and Harder, L.F., Jr. (1990). "SPT-Based Analysis of Cyclic Pore Pressure Generation and Undrained Residual Strength," Proc. of the Memorial Symposium for H.Bolton Seed, Vol. 2, Bi-Tech Publishers, pp. 351-376.

CASE NO. 2 , M9.0
1 OF 2

SPREADSHEET FOR PERFORMING SIMPLIFIED LIQUEFACTION HAZARD EVALUATIONS

Modified January 24, 2005

The Simplified Procedure of Seed and Idriss is performed using the recommendations presented by Youd et al (2001)
All equations and relationships used in this spreadsheet are referenced at the bottom of the sheet.

Moment Magnitude	9.0	
Magnitude Scaling Factor	0.63	(Eq. 24, Ref. 1)
Peak Acceleration at the Ground Surface (g)	0.22	
Embankment height (ft)	25	
Moist unit weight of fill (pcf)	125	
Saturated unit weight of native soil (pcf)	125	
Depth to the groundwater table (ft)	0	

Depth (ft)	σ'_v (psf)	Nm (bl/ft)	CN	N1 (bl/ft)	CE	CB	CR	CS	(N1)60 (bl/ft)	Fines (%)	Parameter α	Parameter β	(N1)60cs (bl/ft)
5.00	313.00	24.00	1.63	39.14	1.00	1.05	0.75	1.00	30.82	4.00	0.00	1.00	30.76
10.00	626.00	26.00	1.47	38.18	1.00	1.05	0.75	1.00	30.07	4.00	0.00	1.00	30.01
15.00	939.00	22.00	1.34	29.38	1.00	1.05	1.00	1.00	30.85	4.00	0.00	1.00	30.79
20.00	1252.00	22.00	1.22	26.95	1.00	1.05	1.00	1.00	28.29	12.00	1.55	1.03	30.74
25.00	1565.00	19.00	1.13	21.49	1.00	1.05	1.00	1.00	22.56	12.00	1.55	1.03	24.83
30.00	1878.00	17.00	1.05	17.86	1.00	1.05	1.00	1.00	18.75	35.00	5.00	1.20	27.50
35.00	2191.00	21.00	0.98	20.59	1.00	1.05	1.00	1.00	21.62	35.00	5.00	1.20	30.95
40.00	2504.00	22.00	0.92	20.23	1.00	1.05	1.00	1.00	21.24	35.00	5.00	1.20	30.49
45.00	2817.00	20.00	0.87	17.31	1.00	1.05	1.00	1.00	18.18	2.00	0.00	0.99	18.05
50.00	3130.00	25.00	0.82	20.44	1.00	1.05	1.00	1.00	21.46	2.00	0.00	0.99	21.31
55.00	3443.00	30.00	0.77	23.24	1.00	1.05	1.00	1.00	24.41	2.00	0.00	0.99	24.23

σ'_v	Vertical effective stress
Nm	SPT N-value measured in the field
CN	SPT N-value stress correction factor (Eq. 10, Ref. 1)
N1	SPT N-value normalized for vertical effective stress
CE, CB, CR, CS	SPT N-value corrections (Table 2, Ref. 1)
α	Parameter for fines correction to SPT N-value (Eqs. 6a-6c, Ref. 1)
β	Parameter for fines correction to SPT N-value (Eqs. 7a-7c, Ref. 1)

CASE NO. 2 , M9.0
2 OF 2

Depth (ft)	(N1)60cs (bl/ft)	CRR7.5	rd	CSR centerline	CSR free-field	CSR average	FS CSRavg	Dr (%)	K σ	K α	FS*	Ru	(su)l-os (psf)	(su)l-sh (psf)	Ncorr (blow/ft)	(su)l-avg (psf)	(su)l-os free-fld
5.00	30.76	0.53	0.99	0.15	0.28	0.22	1.53	81.78	0.89	1.00	1.35	0.18	n/a	n/a	4	n/a	n/a
10.00	30.01	0.47	0.98	0.16	0.28	0.22	1.33	80.78	0.87	1.00	1.15	0.34	n/a	n/a	3	n/a	n/a
15.00	30.79	0.54	0.97	0.17	0.28	0.22	1.50	81.82	0.85	1.00	1.27	0.22	n/a	n/a	8	n/a	n/a
20.00	30.74	0.53	0.96	0.18	0.27	0.22	1.48	78.36	0.83	1.00	1.23	0.25	n/a	n/a	10	n/a	n/a
25.00	24.83	0.29	0.94	0.18	0.27	0.22	0.81	69.97	0.82	1.00	0.66	1.00	934.35	500.00	13	717.17	311.78
30.00	27.50	0.35	0.92	0.18	0.26	0.22	1.00	63.79	0.81	1.00	0.80	1.00	853.68	600.00	14	726.84	320.45
35.00	30.95	0.55	0.89	0.18	0.25	0.22	1.60	68.50	0.79	1.00	1.27	0.22	n/a	n/a	20	n/a	n/a
40.00	30.49	0.51	0.85	0.18	0.24	0.21	1.52	67.89	0.78	1.00	1.19	0.29	n/a	n/a	23	n/a	n/a
45.00	18.05	0.19	0.80	0.17	0.23	0.20	0.61	62.81	0.77	1.00	0.47	1.00	988.40	800.00	17	894.20	468.58
50.00	21.31	0.23	0.75	0.16	0.21	0.19	0.79	68.25	0.76	1.00	0.60	1.00	1194.61	800.00	21	997.30	597.78
55.00	24.23	0.28	0.70	0.15	0.20	0.17	1.00	72.77	0.75	1.00	0.75	1.00	1399.25	800.00	25	1099.63	733.50

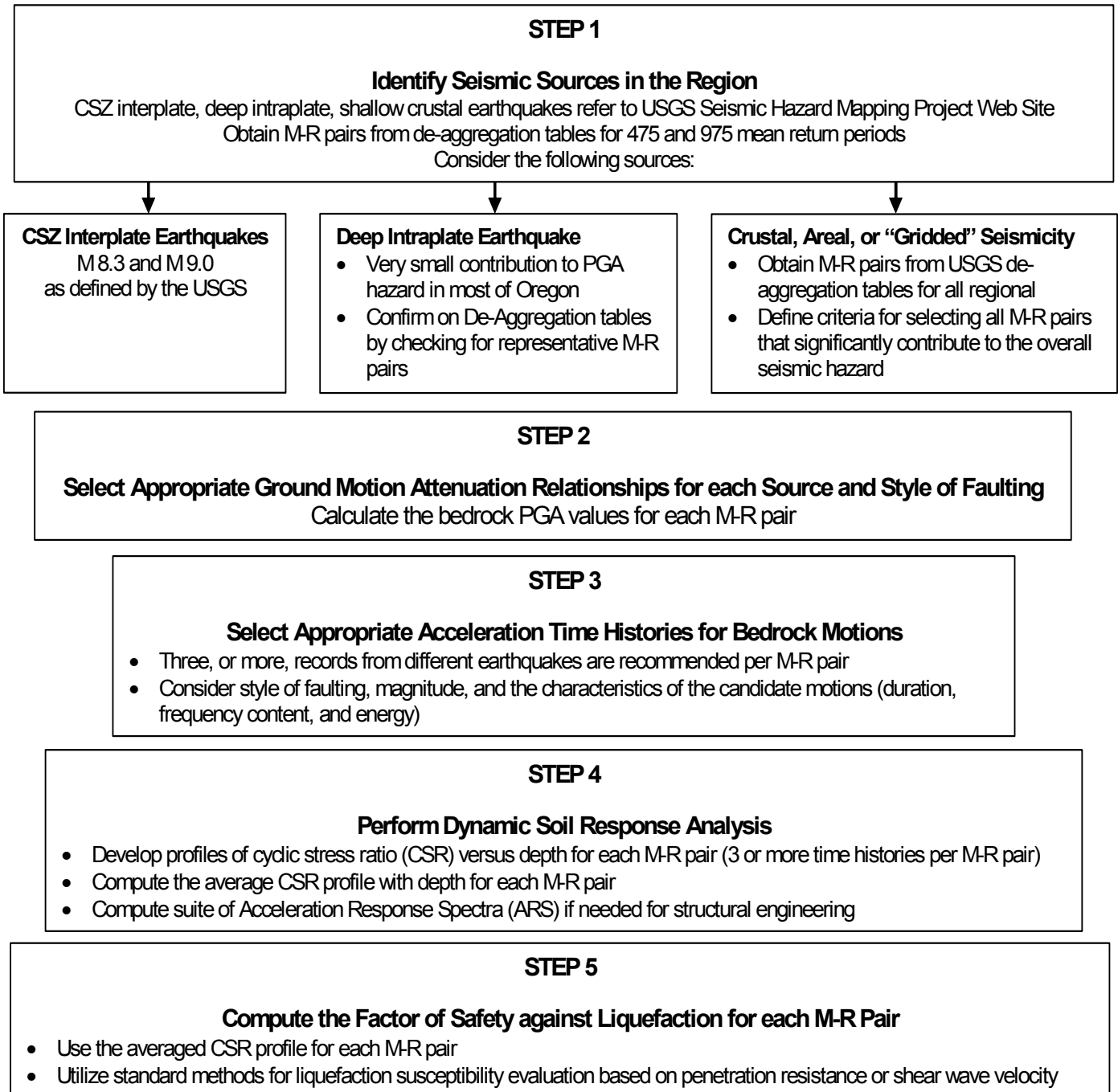
CRR7.5	Cyclic Resistance Ratio of clean sand for Moment Magnitude 7.5 earthquakes (Eq. 4, Ref. 1)
rd	stress reduction coefficient (Eq. 3, Ref. 1)
CSR	Cyclic Stress Ratio associated by the strong ground motion in the layer of interest (Eq. 1, Ref. 1)
FS	Factor of Safety against liquefaction (Eq. 23, ref. 1)
Dr	Relative Density, $Dr = (217 \cdot (N1)60)^{0.5}$
K σ	Correction for effective confining stress (Eq. 31, Ref 1)
K α	Correction for sloping ground (Figures 15, Ref. 1)
FS*	Factor of Safety against liquefaction modified to account for effective confining stress and static horizontal shear stress (Eq. 30, Ref. 1)
Ru	Excess Pore Pressure Ratio estimated from Figure 9.39 (Ref. 2)
(su)l-os	Undrained shear strength of liquefied sand (Olson and Stark procedure, Eq. 19b, Ref. 3)
(su)l-sh	Undrained shear strength of liquefied sand (Seed and Harder procedure, Ref 4, or refer to Figure 9.57, Ref. 2)
Ncorr	(N1)60 corrected for fines content as described by Seed and Harder (Ref 2 or Ref 4)

References

- 1 Youd et al (2001). Liquefaction Resistance of Soils: Summary from the 1996 NCEER and 1998 NCERR/NSF Workshops on Evaluation of Liquefaction Resistance of Soils, ASCE Journal of Geotechnical and Geoenvironmental Engineering, vol. 127, no. 10, pp. 817-833.
- 2 Kramer, S.L. (1996). Geotechnical Earthquake Engineering, Prentice Hall Publishers, 653 p.
- 3 Olson, S.M., and Stark, T. D. (2002). Liquefaction strength ratio from liquefaction flow failure case histories, Canadian Geotechnical Journal, vol. 39, pp. 629-647.
- 4 Seed, R.B., and Harder, L.F., Jr. (1990). "SPT-Based Analysis of Cyclic Pore Pressure Generation and Undrained Residual Strength," Proc. of the Memorial Symposium for H.Bolton Seed, Vol. 2, Bi-Tech Publishers, pp. 351-376.

Appendix J

FLOW CHART FOR EVALUATION OF LIQUEFACTION HAZARD AND GROUND DEFORMATION AT BRIDGE SITES



STEP 6

Establish the Post-Cyclic Loading Shear Strengths of Embankment and Foundation Soils

- This is performed for each M-R pair
- Focus on sensitive soils, weak fine-grained soils, loose to medium dense sandy soils (*potentially liquefiable soils are addressed as follows*)

If $FS_{liq} \geq 1.4$

Use drained shear strengths

If $1.4 > FS_{liq} > 1.0$

- Estimate the residual excess pore pressure
- Compute the equivalent friction angle

If $FS_{liq} \leq 1.0$

Estimate the residual undrained strength using two or more methods

STEP 7

Perform Slope Stability Analysis

- Static analysis using post-cyclic loading shear strengths for each M-R pair
- Calculate the FOS against sliding and determine the critical acceleration values for each M-R pair
- Focus trial slip surfaces on weak soil layers

STEP 8

Perform Deformation Analysis for each M-R pair

- Rigid-body, sliding block analysis (Newmark Method)
- Simplified chart solutions
- Numerical modeling

STEP 9

Evaluate Computed Deformations in Terms of Tolerable Limits

Permanent Deformations are Acceptable

- Computed displacements are less than defined limits
- Continue with structural design

Permanent Deformations are Unacceptable

- Computed displacements exceed defined limits repeat analysis incorporating the effects of remedial ground treatment
- Return to Step 4 if the soil improvement does not significantly change the anticipated dynamic response of the soil column (e.g., isolated soil improvement)
- Return to Step 3 if the ground treatment substantially alters the dynamic response of the site (e.g., extensive soil improvement in the vertical and lateral direction, extensive treatment including grouting or deep soil mixing)
- A reduced number of input time histories are acceptable for each M-R pair (bracket the problem using trends from the initial analysis)